



HAL
open science

Behavioral and electrophysiological study of spatial pattern discrimination in the rat

Pauline Kerekes

► **To cite this version:**

Pauline Kerekes. Behavioral and electrophysiological study of spatial pattern discrimination in the rat. *Neurons and Cognition [q-bio.NC]*. Université Pierre et Marie Curie - Paris VI, 2017. English. NNT : 2017PA066551 . tel-01897480

HAL Id: tel-01897480

<https://theses.hal.science/tel-01897480>

Submitted on 17 Oct 2018

HAL is a multi-disciplinary open access archive for the deposit and dissemination of scientific research documents, whether they are published or not. The documents may come from teaching and research institutions in France or abroad, or from public or private research centers.

L'archive ouverte pluridisciplinaire **HAL**, est destinée au dépôt et à la diffusion de documents scientifiques de niveau recherche, publiés ou non, émanant des établissements d'enseignement et de recherche français ou étrangers, des laboratoires publics ou privés.

Université Pierre et Marie Curie

Ecole doctorale Cerveau, Cognition, Comportement

*Unité de Neurosciences Information et Complexité / Equipe Traitement sensoriel,
neuromodulation et plasticité neuronale.*

Behavioral and electrophysiological study of spatial pattern discrimination in the rat

Par Pauline Kerekes

Thèse de doctorat de Neurosciences

Dirigée par Valérie Ego-Stengel et Daniel Shulz

Présentée et soutenue publiquement le 26/09/2017

Devant un jury composé de :

Dr. Ingrid Bureau, chargée de recherche : Examinatrice

Pr. Tansu Celikel, directeur de recherche : Rapporteur

Dr. Sylvain Crochet : Rapporteur

Dr. Valérie Ego-Stengel : Directrice de thèse

Pr. Régis Lambert : Président du jury

Dr. Daniel Shulz : Directeur de thèse

Acknowledgements

This Ph.D. work was funded by the CNRS, the Human Frontiers Science Program Organization (V.E.S), ANR Neurowhisk (V.E.S.) and Fondation pour la Recherche Médicale (P.K.).

Remerciements

J'en viens maintenant à une partie qui me tient beaucoup à coeur, les remerciements. J'ai été aidée sur le plan technique pendant cette thèse, mais j'ai aussi été entourée par une grande chaleur. Je pense que ces deux «paramètres» ont contribué à égalité dans le fait que j'ai pu avancer dans le projet.

First of all, I would like to thank Sylvain Crochet and Tansu Celikel, for having accepted to review this thesis, as well as Ingrid Bureau and Régis Lambert for being part of the examining committee.

Ensuite, j'aimerais remercier Valérie. Un jour, après t'avoir décrit à quelqu'un, il m'a dit «ah d'accord, et tu la demandes quand en mariage ?»... No panic, je n'en viendrai pas à cette extrémité. Tu m'impressionnes beaucoup, et j'imagine pour longtemps: non seulement tu as fait des études plus que brillantes, tu a été capable de débloquent en un coup de baguette magique tous les problèmes dans lesquels je me suis engluée pendant la thèse, et, comme si ça ne suffisait pas, tu excelles dans bien d'autres domaines que j'ai arrêté de compter pour préserver ma santé mentale. Quand j'ai rencontré Dan, il m'a dit «tu vas voir, Valérie est hyper-intelligente». Ma première réaction a été d'être à peu près paralysée par la peur, mais je peux dire que je n'ai pas été trompée !! Je pense que tous les gens qui te connaissent s'accorderaient sur ces lignes, et je voudrais maintenant dire quelques mots sur toi en tant que directeur de thèse. J'ai pu avancer car tu as résolu tous mes problèmes techniques et scientifiques, mais aussi parce que (tenez vous prêts, on rentre maintenant dans le surnaturel) tu as anticipé les étapes de ma thèse, et tu m'as aiguillée en fonction de ça. Souvent, je trouvais la solution à un problème donné grâce à ce que tu m'avais dit une semaine plus tôt (oui ça fait presque flipper là). Enfin, et c'est pour moi quelque chose d'important, ton empathie à toute épreuve m'a portée de nombreuses fois. Même quand il s'agissait de problèmes qui en fait n'allaient peut-être pas non plus changer la face du monde (par exemple le «trial-sur-120-que-j'ai-oublié-je-vais-mourir», spéciale dédicace à Yannick), tu prenais le temps de m'écouter déblatérer une série de détails parfois vraiment débiles. En somme, tu m'as guidée scientifiquement, accompagnée émotionnellement, et grâce à ça j'ai adoré ma thèse. J'adore être avec toi, et ne plus pouvoir venir te voir dans ton bureau va constituer un sevrage difficile. Tu m'as aussi progressivement laissé faire mes propres choix, ce qui m'a permis de m'approprier mon travail, et de m'y épanouir complètement. Je ne pouvais pas rêver d'avoir meilleur directeur de thèse, et je suis heureuse que d'autres petits poussins (comment perdre sa virilité en deux secondes ?), comme Aamir et Dorian, aient ma chance.

Je voudrais maintenant remercier très vivement Dan, que j'ai réussi à tutoyer en seulement deux ans. Au début, j'étais en freezing à peu près constant quand je te parlais, ou même quand j'entendais tes pas dans le couloir (conditionnement très réussi, bravo). Tu m'impressionnes toujours, mais je me soigne. Tu m'as soutenue et guidée tout au long de cette thèse, je n'ai pas cessé de te faire confiance, et j'ai eu raison ! Je n'ai pas eu de bourse de thèse, et je pensais que tu m'avais déjà oubliée fin août 2013 quand tu m'as appelée pour me dire que tu avais trouvé une solution ! Merci de m'avoir offert cette chance. Tu as très largement participé à mon épanouissement scientifique pendant cette thèse, et je crois que la rigueur que tu m'as enseignée m'a fait réellement aimer mon travail. Maintenant je ne freeze plus et ne veux surtout pas partir, ce qui n'est peut-être pas exactement dans tes

plans.

Je voudrais sincèrement remercier Yves Frégnac de m'avoir accueillie dans son laboratoire. J'y ai trouvé une famille scientifique pluri-disciplinaire et de haut niveau, ce qui est une vraie chance pour un travail de thèse !

Isabelle, je te colle depuis que je suis en M1, et j'espère que je te pourrai te coller toute ma vie (prends ton Xanax). Les mots ne suffisent jamais assez pour dire tout le bien que l'on pense de quelqu'un, mais je me lance quand même. Tu es un modèle scientifique et humain pour moi, et en fait souvent je me suis dit, quand j'étais faiblarde pendant ma thèse, «Isabelle n'aurait certainement pas lâché, pas abandonné». Tu m'as constamment donné de la force. Tu es quelqu'un que je ne pourrai jamais oublier, tu fais partie des personnes qui ont marqué ma vie.

J'aimerais remercier maintenant les nombreuses personnes qui m'ont donné de leur temps, appris leurs techniques, et sans qui je me serais retrouvée souvent bien incapable !!

Aurélie, j'aurais tant à te dire... Le comportement a été une très grosse partie de ma thèse, et a de fait nécessité plusieurs années de travail. Pendant tout ce temps, tu m'as accompagnée, aidée, tu as beaucoup travaillé pour ce projet. Quand j'étais un peu déprimée sous mon labyrinthe entre deux fils mal soudés (sympa l'ambiance), tu trouvais toujours les mots pour me remonter le moral tout de suite. En fait, tu ne m'as jamais laissée tomber, et tu as été quelqu'un de très important pour tout ce travail de thèse. Je ne te remercierai certainement jamais assez pour cette constance, ce travail et cette amitié. Merci aussi à Hind et Caroline, pour avoir travaillé avec nous à faire marcher le protocole ! Timothé, ton travail et ta rapidité m'ont impressionnée !

J'en profite pour remercier Valérie, Aurélien, ainsi que toutes les personnes de l'animalerie, pour s'être occupés de nos petits génies de rats, même à l'époque où ils n'avaient pas fait montre d'un QI hors norme.

Patrick et Jean-Yves, merci d'avoir supporté ma présence, à un moment donné quasi-continue, et mon débit de paroles bourdonnant dans votre atelier, et d'avoir travaillé tant de fois sur le labyrinthe ! J'ai adoré travailler avec vous, et venir vous voir à l'atelier était toujours un plaisir !! Je n'aurais pas pu construire le labyrinthe sans vous.

Guigui, merci pour ta patience, surtout lorsqu'il a fallu ramasser toutes les tranches tombées dans l'évier et calmer mon hystérie, car j'avais choisi le seul panier percé du lot... Merci aussi et surtout pour tout le travail que tu as fait, toutes ces tranches pour m'entendre dire « je ne vois toujours pas de Dil, tu penses que c'est normal ? ». Tu es génial, cher Guigui.

Merci à Paul, pour m'avoir conseillée sur les composants électroniques à acheter, et sur quelques bases en électronique qui m'ont bien servi pour le labyrinthe, ainsi que pour le deuxième projet !!

Merci à Aline et Justine pour avoir réglé nombre de mes problèmes administratifs, et je dois dire que je n'ai pas été un enfant facile pour ça ! Aline, merci pour la bienveillance (enfin ... je crois) que tu as toujours eu pour moi, Justine merci d'être un rayon de soleil dans ce labo !

J'ai aussi rencontré plusieurs personnes pendant cette thèse que je ne suis pas sur le point d'oublier...

Pierre-Louis, cher Pilou, j'ai tellement de chance de t'avoir rencontré ! Tu es un ami hors pair, et ça même Derrick l'a remarqué. Tu as une force de travail qui donne le vertige (pourtant c'est bien mon truc de faire des veillées tétrodes), et tu es un super scientifique. Je t'adore mon poto. Merci de m'avoir fait connaître ce sacré Jujy, Sandra, Séverine, Laure, Coralie, et ...

super Alex.

Ma Simo, tu es unique pour moi. Je regrette tellement les moments où tu habitais à côté du labo et où je venais te voir des heures là bas.. !! Tu es une vraie amie, une battante et une superwoman. Même lorsqu'il s'agit de manger des pizzas avec de l'ananas. Ti voglio tanto bene Simsim.

En passant par le couloir de Simo, je voudrais dire un mot pour Christine. La première fois que je suis arrivée dans le bâtiment, c'était pour faire un stage avec toi. Je sais que tu t'es arraché les cheveux quand je te ramenaient des cerveaux non pas disséqués mais déchiquetés, ou quand je t'ai rendu la première version de mon premier rapport de stage (...). Tu m'as tout expliqué, patiemment. J'ai adoré mon stage avec toi, et c'est grâce à toi que je me suis intéressée à la recherche pour la première fois.

Aamir, it's not possible to imagine my future work without you on my right side, so prepare your luggage (take just a few electrodes and survival materials such as beers), we leave next january. We shared so much during these few years, from worrying about thesis troubles to Berlin parties. You will soon be successful, your mice told me. You're such a super friend to me !!

Yannick, ou Kiki (t'as vu j'ai vraiment pas de respect), qu'auraient été toutes ces années de labeur sans ta présence (t'as vu je me rattrape) ? Merci de ne pas m'avoir soutenue quand j'ai voulu lancer la tendance mocassins-survet, ou quand j'ai dépassé les bornes de la mocheté sur snapchat. Je n'arrive pas à imaginer un endroit de travail sans t'entendre piailler et/ou geindre, alors ça veut peut-être dire que tu vas me manquer. Sale canard (signé Antoine).

Margot, qui n'a peur d'aucune folie pileuse, et ça, j'aime. Appelle-moi si tu passes aux moustaches.

Benoît, merci pour tous les moments qu'on a passés au labo. Les barres de rire le dimanche sur la terrasse restent dans ma mémoire. Tu as fait un travail énorme, et tu m'impressionnes pour ça. Tiens bon, poto, tu as largement fait le plus dur, et tu es largement capable de finir le reste.

Evan, thank you for waking me up every 15 minutes with the door, and for trying to get me sent to prison because of a fishy piece of art on my back at the airport. If not for Aamir, i would be in prison. More seriously, thank you so much for having explained to me so many things, and advised me on so many aspects of the project. To have someone like you in the team is really lucky !

Matias, thank you for precious advice on scientific subjects, and for infinite patience, especially when i'm trying to repair a matrix piezo and i'm asking every 15 sec whether it's good or not like this or like that.

Luc E, merci pour tes conseils très avisés sur le projet, et pour ton potentiel exceptionnel de lancements de sujets de conversation, en toutes circonstances. Encore plus de répartie que Yannick...

Dorian, merci pour toutes les super conversations qu'on a eu dans le bureau (en dehors d'heures de travail intense bien entendu), et pour le gâteau d'anniversaire surprise (t'as vu ça m'a touchée) !

Eugenia : tu es partie vers de nouveaux horizons (oui, il faut bien les finir, ces thèses), mais restent en tête les bons moments de thèse et de retraite de labo qu'on a pu passer ensemble !!

Sophie, la presque-Japonaise, passe le bonjour à tête de citron pour moi... En espérant te revoir bientôt dans les couloirs du labo !!

Merci à toutes les personnes de l'UNIC avec qui j'ai pu interagir, avoir des conversations très intéressantes, et qui m'ont conseillé pendant ma thèse; la liste est bien entendue non exhaustive, mais je pense à Marc, Christophe, Thierry, Cyril, Bartosz, Gilles, Domenico, Xoana, Luc F, Jonathan, Brice, Thomas, Zuzanna, Sebastian, Anthony, Alexandre (merci pour les beers on the grass, très convivial, à continuer;) !!).

Je pense aux gens que j'ai rencontrés à la fac, et qui sont maintenant de vrais amis; la fac avec les mouths, Lucie, Aurélien, et maintenant Morgane et Elin, ainsi que ma Sonia et ma Leïla. Je pense à l'avant-fac avec Morgane-Jackouillon, et bien avant l'avant-fac, avec Cecilou et ses bernard l'hermite. A mes amies de toujours (et pour toujours!) Jéro, Marie, Aurélie; je sais que le groupe des quatre est indestructible !

Merci aux grands Poutchous et aux minis, ainsi qu'à Michel et Maud. Maudine, vous êtes dans mon coeur pour toujours.

J'ai enfin une pensée très forte pour toute ma famille, en particulier mes deux parents, mes frères et sœur et mes grand-parents.

Maman, plus besoin de signer « n°1 », tu es trop importante pour moi et irremplaçable.

A Antoine, qui adoucit ma vie et la rend plus belle tous les jours.

Abstract

The rodent whisker system is a widely used model to study behavioral and neurobiological processes underlying tactile perception, in particular during the exploration of an object shape, localization or surface roughness. The general goal of this Ph.D. work was to explore the sensori-motor strategies involved in a tactile discrimination task, as well as the neuronal activity underlying such ability.

Similarly to human fingertips scanning an object, rodents are able to sweep their whiskers against surfaces in a rhythmic fashion (a process called whisking) to analyze spatial details. In most laboratory tasks, rats discriminate spatial patterns by whisking on them successively. Based on the life of these animals in the wild, we hypothesized that rodents could discriminate spatial patterns without whisking. To demonstrate this, we developed a novel task inciting the rats to touch the stimuli by running past them at such high speed that the time needed to complete a whisking cycle is not available. Rats learned to discriminate a surface with a series of vertical bars regularly spaced from a smooth surface. Both whiskers and neural activity in the primary somatosensory cortex were involved during the discrimination process. Rats could also discriminate an irregular series from the regular one. We showed that rats do not whisk on the stimuli, and that they orient their whisker arrays towards the rewarded stimulus as soon as 60ms after the first possible contact (Kerekes et al., 2017). These results demonstrate that rats can discriminate stimuli without actively whisking.

A second project of this Ph.D. work focused on the analysis of whisker deflections and thalamo-cortical neuronal responses evoked in the anesthetized rat by the stimuli passing on the whiskers mimicking the tactile condition during the task. Preliminary results show the presence of high-acceleration events occurring during whisker stimulation. These events evoked significant cortical responses, that differed according to the stimulus type (irregular or regular series). Four rats have been recorded for this study, two of them were trained on the discrimination task, and the two others were trained on a non-tactile task on the same maze. With this data, we plan to search for potential effects of learning on neuronal treatment of tactile inputs.

Both the development of the novel discrimination task and of neuronal recordings in anesthetized and awake rats will allow to tackle new questions on tactile discrimination processes, such as how spatial regularity or irregularity are encoded and how this encoding can be modulated by learning.

Keywords: tactile, neuroscience, behavior, discrimination, whiskers, learning.

Résumé

Le système vibrissal des rongeurs est un modèle très utilisé pour l'étude des processus comportementaux et neurobiologiques qui sous-tendent la perception tactile, en particulier pendant l'exploration de la forme d'un objet, sa localisation, ou la rugosité de sa surface. Le but de cette thèse a été d'explorer les stratégies sensori-motrices impliquées dans une tâche de discrimination tactile, ainsi que l'activité neuronale qui sous-tend ce processus.

De façon similaire aux doigts humains scannant un objet, les rongeurs peuvent balayer activement des surfaces avec les vibrisses de leur museau (mouvement appelé «whisking»). En laboratoire, les rats discriminent des niveaux de rugosité en faisant du whisking. D'après leurs conditions de vie naturelles, nous avons fait l'hypothèse que ces animaux peuvent discriminer des motifs spatiaux sans whisking. Pour le démontrer, nous avons développé une nouvelle tâche de discrimination dans laquelle les rats contactent des stimuli en courant à haute vitesse dans un couloir, de sorte à ce qu'il n'y a pas assez de temps pour un cycle de whisking. Les rats ont appris à discriminer des barres verticales régulièrement espacées d'une surface sans barres. Les vibrisses et le cortex somatosensoriel primaire sont impliqués dans la discrimination. Les animaux ont été également capables de discriminer les barres régulières de barres irrégulières. Nous avons montré que les rats ne font pas de whisking sur les stimuli, et qu'ils orientent leurs vibrisses du côté du stimulus récompensé environ 60ms après premier contact (Kerekes et al., 2017). Ces résultats montrent que les rats peuvent discriminer des stimuli sans faire de whisking.

Dans une deuxième partie, nous avons analysé les mouvements vibrissaux et réponses neuronales thalamo-corticales évoquées chez le rat anesthésié par le passage des stimuli utilisés pendant la tâche. Les résultats préliminaires révèlent des mouvements vibrissaux à haute accélération, encodés différemment par le cortex selon le type de stimulus (barres régulières ou irrégulières). Quatre rats ont été enregistrés pour cette étude: deux d'entre eux ont été entraînés à la tâche de discrimination, et les deux autres ont été entraînés à une tâche non-tactile sur le même labyrinthe. Grâce à ces expériences, nous allons rechercher les effets potentiels de l'apprentissage sur le traitement neuronal des informations tactiles.

Le développement combiné de la tâche comportementale et des enregistrements neuronaux sur rat anesthésié et éveillé vont nous permettre d'explorer de nouvelles questions sur la discrimination tactile, tel que le codage de la régularité de motifs spatiaux, et la modulation de ce codage par l'apprentissage.

Mots clés: tactile, neuroscience, comportement, discrimination, vibrisses, apprentissage.

Table of Contents

I. Tactile perception in the rat.....	12
I.1. «Rats inhabit a world of touches» - <i>Mitra Hartmann</i>	12
I.1.1. Underground and nocturnal life of rats in natural conditions.....	12
I.1.2. Whisker-related ethology of the rat.....	13
I.2. Organization and individual structure of the whiskers on the snout.....	16
I.2.1. Description of the whisker map on the snout.....	16
I.2.2. Structure and function of the Follicle-Sinus Complex.....	18
I.2.2.1. <i>Anatomical description of the Follicle-Sinus Complex</i>	18
I.2.2.2. <i>The mechanoreceptor types within the Follicle-Sinus Complex</i>	20
I.3. Whisker-based behavioral strategies to collect information.....	22
I.3.1. Description of active whisker movements.....	22
I.3.2. Motor control of whisker position and movement.....	26
I.3.2.1. <i>Whisker-associated muscles: the basic architecture for positioning the whiskers dynamically</i>	26
I.3.2.2. <i>A brainstem structure necessary for whisking generation</i>	27
I.3.2.3. <i>Which role for the primary motor cortex in whisker motor control?</i>	28
I.3.3. Modulation of whisker position and movement with behavior.....	33
I.3.3.1. <i>Whisker positioning is coordinated with the animal movement</i>	33
I.3.3.2. <i>Touch-induced modulation of whisker movements</i>	34
I.3.3.3. <i>Whisking in tactile detection or discrimination tasks</i>	35
I.3.3.4. <i>Tactile discrimination without whisking</i>	36
I.4. Bilateral discrimination of tactile patterns without whisking in freely-running rats.....	37
I.4.1. Kerekes P, Daret A, Shulz DE, Ego-Stengel V (2017) Bilateral discrimination of tactile patterns without whisking in freely-running rats. <i>J Neurosci</i> 37(32):7567–7579.	37
I.4.2. Additional unpublished results.....	52
I.4.2.1. <i>Increased retraction is not due to contact with the rougher stimulus</i>	52
I.4.2.2. <i>Inactivation of the primary somatosensory cortex</i>	54
I.4.2.3. <i>Reminders are needed for learning the task</i>	54
I.4.3. Discussion.....	57
I.4.3.1. <i>No whisking: which consequences for the sensori-motor closed loop?</i>	57
I.4.3.2. <i>Involvement of whiskers during discrimination</i>	58
I.4.3.3. <i>Involvement of the primary somatosensory cortex during discrimination</i>	58
I.4.3.4. <i>Towards discrimination of tactile regularity?</i>	60
II. Neuronal coding of tactile inputs by the whisker system.....	61
II.1. From the whiskers to the cortex.....	61

II.1.1. General introduction on whisker-to-cortex pathways.....	61
II.1.2. The lemniscal pathway.....	62
II.1.2.1. Somatotopy and definition of the principal whisker.....	62
II.1.2.2. Beyond the dedicated labeled line: multi-whisker integration.....	64
II.1.2.3. Two pathways through dorso-medial VPM.....	64
II.1.3. The extra-lemniscal pathway.....	67
II.1.4. The paralemniscal pathway.....	69
II.1.5. Further insights into the thalamo-cortical loops.....	70
II.1.5.1. Connections within the loops.....	70
II.1.5.2. First and Higher-Order nuclei in the thalamus.....	71
II.1.5.3. Regulation of the loop activity.....	72
II.2. Encoding object properties with the whisker system.....	73
II.2.1. Where is the object: spatial localization.....	73
II.2.1.1. Spatial localization along the rostro-caudal axis.....	73
II.2.1.2. Discrimination of stimulus distance to the snout.....	78
II.2.2. What is the object: encoding surface properties.....	80
II.2.2.1. Encoding whisker movement over the whole stimulus.....	80
II.2.2.2. Encoding acute variations in speed and acceleration.....	86
II.2.2.3. The differential resonance theory.....	88
II.3. Study of thalamo-cortical responses evoked by a smooth surface, a regular or an irregular series of bars.....	90
II.3.1. Neuronal encoding of spatial patterns.....	90
II.3.1.1. Temporal responses locked to spatial series of bars.....	90
II.3.1.2. Encoding stick/slip events.....	92
II.3.2. Materials and methods.....	93
II.3.2.1. Animals.....	93
II.3.2.2. Overview of the protocol.....	93
II.3.2.3. Implant making.....	94
II.3.2.4. Surgical implantation.....	97
II.3.2.5. Determination of neurons receptive field with the matrix.....	97
II.3.2.6. Typical recording session and hardware system to display the stimuli.....	98
II.3.2.7. Electrophysiological recordings and analysis.....	100
II.3.2.8. Whisker movement filming and tracking.....	101
II.3.3. Results.....	103
II.3.3.1. Whisker movement evoked by bar series: stick and slip events.....	103
II.3.3.2. Multi-unit responses to stick and slip events.....	109
II.3.3.3. Effect of slip amplitude and timing on multi-unit responses.....	112
II.3.4. Conclusion and discussion.....	114
II.3.4.1. Stick and slip events during bar series stimulation.....	114
II.3.4.2. Neuronal responses to stick and slip events.....	115
II.3.5. Perspectives for recording in awake behaving animals.....	117
II.3.5.1. The maze and electrophysiological acquisition.....	118

<i>II.3.5.2. Recording whisker movements</i>	119
III. General conclusion and discussion.....	120
III.1. Summary of the Ph.D. results.....	120
III.2. Perspectives: information processing in freely-behaving rodents.....	121
IV. Bibliography.....	124

Abbreviations

EIB: electrode interface board

FSC: follicle-sinus complex

GABA: gamma amino-butyric acid

G: gauge

I13, ..., I50: irregular series of bars with a maximal interval equal to 13, ..., 50mm

L: cortical layer

LPG: lateral paragigantocellularis nucleus

(w)M1: (whisker-related) primary motor cortex

NSP: neural signal processor

PFA: paraformaldehyde

PoM: postero-medial nucleus of the thalamus

Pr5: principal nucleus of the brainstem

R: surface with regular series of bars

RR (task): rough-rough (task)

RS (task): rough-smooth (task)

RTN: reticular nucleus of the thalamus

S: smooth surface

(w)S1: (whisker-related) primary somatosensory cortex

S2: secondary somatosensory cortex

Sp5: spinal nucleus of the brainstem

SD: standard deviation

TG: trigeminal ganglion

vIRt: ventral part of the intermediate band of the reticular formation

VPM: ventro-postero medial nucleus of the thalamus

VPMdm: dorso-medial part of the ventro-postero medial nucleus of the thalamus

VPMvl: ventro-lateral part of the dorso-medial ventro-postero medial nucleus of the thalamus

Foreword

Sensory inputs connect us to the environment, and shape innate behaviors as well as learned goal-directed actions. These modalities are specialized, so that each sensory modality may be particularly relevant in some contexts rather than others. Feeling how incredibly sharp a predator tooth is by palpating it might not be the best way to detect danger, whereas detecting unusual noises in the environment might be. The tactile and visual senses are both involved in the description of physical aspects of surrounding objects, while taste, sound and smell can further inform us on the materials or molecules constituting them. By analyzing inputs to the eyes or the fingertips, a complete structure of the object can be mapped. In addition, somatosensory inputs bring information on micro-patterns of surface textures. Interestingly, the flow of tactile information can be actively modified by the subject by changing the conditions of sensory perception. As changing the contrast of an image can highlight details on it, adjusting the fingertips speed can enhance differences between two surfaces patterns. Thus, the motor command can shape the tactile input, and has been shown to be critical for accurate discrimination. In rodents, long whiskers on the snout can map an object shape from macro to micro scale, as fingertips do. With a fine system of facial muscles, the animals can also sweep these whiskers on surfaces, modulating position and speed in time for maximizing accuracy. Because of remarkable abilities to perceive objects with their whiskers, the whisker system has emerged as a model to study tactile perception.

In the **first part of this thesis**, current knowledge about the behavioral importance of the whisker system is reviewed, including sensori-motor strategies that these animals use to collect tactile information around them. We then describe the discrimination task that we developed and that explores novel sensori-motor strategies of the animals.

The **second part** starts with a general review of the literature on neuronal encoding of tactile inputs, in particular during sensory discrimination of object location and texture. We present afterwards an ongoing project on the analysis of whisker deflections and neuronal responses evoked by the stimuli passing on the whiskers as during the task.

In the **Conclusion**, we place our work in the general framework of understanding tactile perception in awake animals, and discuss how future work could shed light on neuronal mechanisms of perceptual learning.

I. Tactile perception in the rat

I.1. «Rats inhabit a world of touches» - *Mitra Hartmann*

I.1.1. Underground and nocturnal life of rats in natural conditions

Populations of the wild rat, *Rattus norvegicus*, dig complex systems of burrows. These burrows are typically composed of cavities that are either nests or food caches, tunnels linking the cavities, and entry points (Figure 1). In 1962, the ethologist J.B. Calhoun published the results of a 27 month-long study on the behavior of wild rats enclosed in a semi-natural environment. The rats were free to behave and breed within the enclosed space, but they were protected by a predator-proof fence, and were supplied with food and water by the experimenters. This procedure allowed the experimenters to describe the social behavior of these animals, but also to precisely measure the dimensions of the burrows that rats dug. These measurements were carried out in 44 burrows and revealed that tunnels were dug at a median value of 194 mm under the floor surface. Their median length and width were respectively 298 mm and 83 mm. We can note here that, since a rat body diameter is around 70 mm, the tunnels were tightly fit to the size of the animals, allowing the passage of only one of them at a time. Similarly, the height of the nests was adjusted by the animal: as the rat is filling the nest floor with grass and leaves, it removes ground material from the roof, in order to keep a constant height. To construct these burrows, rats were able to move rocks with a mean weight of 66 ± 37 g, which represents ~20 % of the total rat weight. Interestingly, domestic rats raised in laboratory are able to quickly and spontaneously dig burrows with nests and tunnel segments in a semi-natural environment (Nieder et al., 1982), as wild strains do. More generally, basic behaviors such as searching for food, selecting habitats, or obeying social rules in a group seem to be conserved in laboratory rats, despite generations of domestication, as shown in the video-recorded experiment entitled « The Laboratory Rat: A Natural History », directed by the zoologist M. Berdoy and released in 2002.

Under natural conditions, rats are more active during night periods, and especially directly after sunset (Takahashi & Lore 1980). Following these results, we can infer that, since wild

rats are confined into burrows during day time and explore the outside environment mainly at night, these animals are used to live under low-light conditions. Moreover they show remarkable abilities to evolve in those complex environments, suggesting that senses other than vision, such as audition, olfaction or tactile sensation may play a critical role in their everyday life.

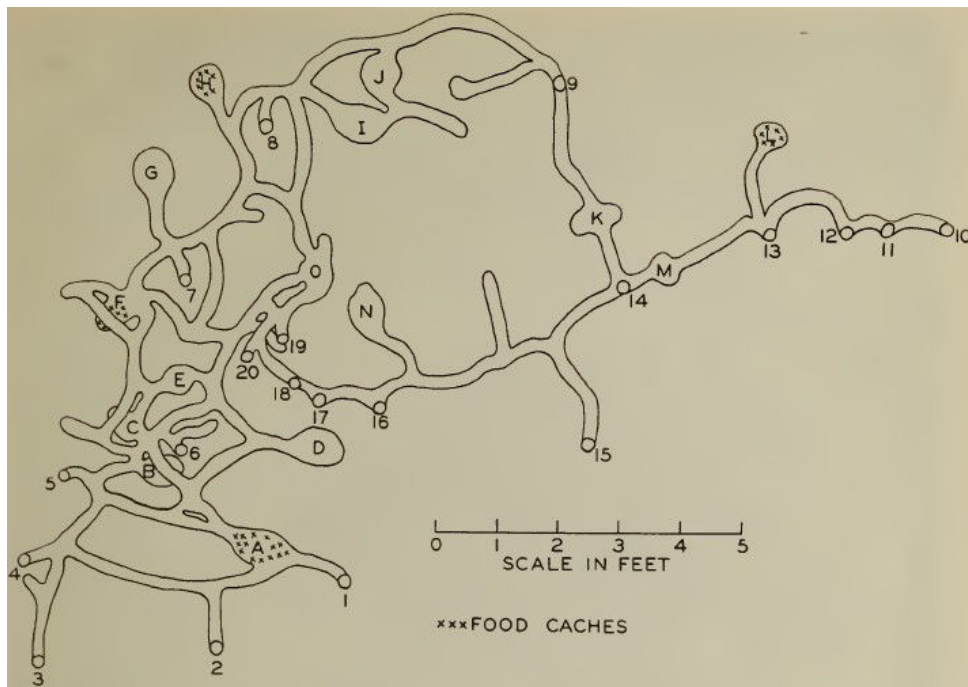


Figure 1: Detailed representation of a typical burrow.
Cavities are indicated by letters, and entries by numerals. From Calhoun (1963).

I.1.2. Whisker-related ethology of the rat

As described in I.1.1., wild rats live in underground tunnels that tightly fit their body width. In this configuration, it is very likely that the long and specialized hairs on their snout (the whiskers, Figure 2, see more details on the structure of this hair in I.2) establish frequent and sustained contacts with surrounding walls of the tunnels. Related to this proposal, it has been shown that rats prefer to spend more time close to walls in laboratory set-ups. This behavior is called thigmotaxis and can be observed in open-field arenas, where the animals remain closer to the walls of the arena rather than in its center. In addition, if cubes are

added next to the corners of the open-field, to form places surrounded by three walls (two are the open-field fences, and one more is one cube's side), rats spend significantly more time in those areas surrounded by three walls compared to places surrounded by less walls (Martinez and Morato 2011). Not only do rats prefer to stand nearby walls, but also walls, contacted by the whiskers, can be revealed as critical tactile cues to navigate an environment. Indeed, S.B. Vincent, in 1912, studied the ability of rats to navigate in a maze with alleys surrounded by vertical walls. She describes the walls as being « the source of most of the contact experiences of the vibrissae » (p. 14, in the book « The functions of the vibrissae in the behavior of the white rat », S.B. Vincent, 1912), and observed an impairment in maze navigation after cutting the whiskers. Thus, whiskers, by tracking nearby walls, allow the rats to efficiently navigate into complex environments. Whiskers are also involved in discriminating radial distances from objects to snout and fine surface textures around them. This latter aspect will be developed in II.2 and II.3. In addition to spatial navigation and object recognition, rats also use their whiskers to detect and catch preys. For instance, after cutting the whiskers, rats are less able to retain or recapture cockroaches, and these abilities are rescued once whiskers have re-grown (Favaro et al. 2011). Finally, several social behaviors can be modulated by the absence of the whiskers: the defensive boxing behavior, where rats stand on their hind legs and start hitting their opponent with the forepaws, is typically decreased after whisker removal, while biting and freezing are increased (Blanchard et al., 1977, Wolfe et al. (2011)). The degree of protraction of the whiskers also reflect the aggressiveness, with more protracted and more active whiskers associated with aggressive encounters.

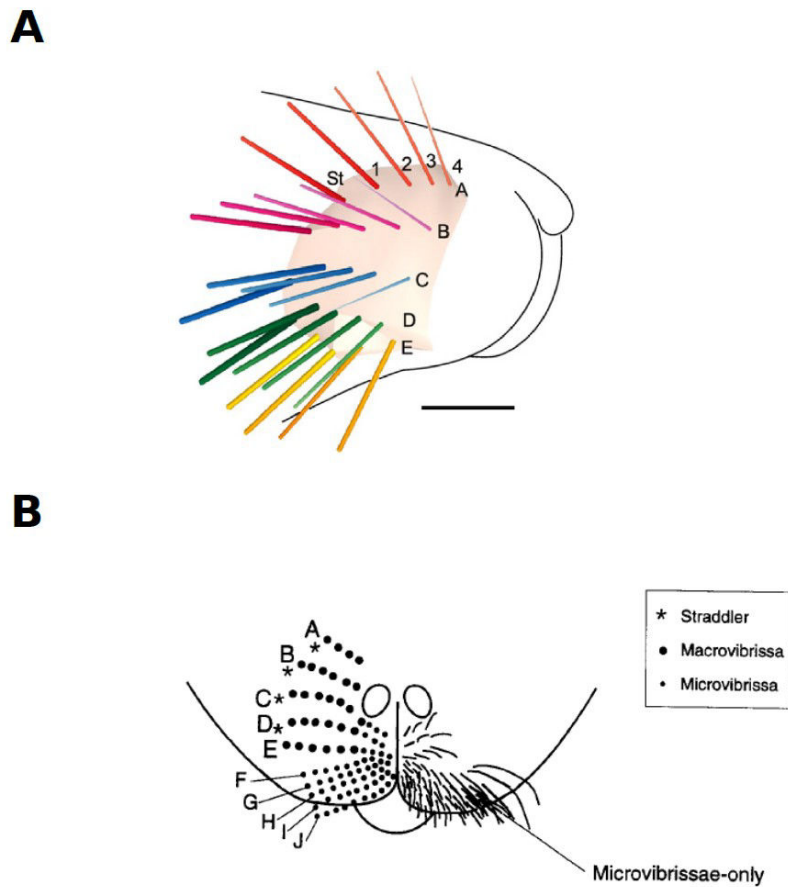


Figure 2: Macro- and micro-vibrissae on the rat's snout.

A: 3D-reconstruction of the 24 macrovibrissae of a 300g Wistar rat. Only the first 7 mm of each macrovibrissae is shown. Each color represents a different row (rows A-E). Scale bar=5mm. From Jacob et al., 2010.

B: Distribution of macrovibrissae (rows A-E) and microvibrissae (rows F-J) on the snout. From Brecht et al., 1997.

Overall, these results on the spontaneous behavior of the rat demonstrate that the whisker system has a critical role in both fulfilling basic needs for survival (navigation in space, capturing preys, interacting properly with other group members), and more sophisticated functions such as fine discrimination of objects properties and surfaces (see II.2. and II.3.).

I.2. Organization and individual structure of the whiskers on the snout

I.2.1. Description of the whisker map on the snout

The rat's vibrissae, as pelagic hairs, are cones made of dead epidermal cells that originate from epidermal follicles. They differ from common pelagic hairs by their thickness, length, and by the complex sensory innervation and motor control associated to their follicle. In addition, while pelagic hairs are displayed all over the animal's body, the vibrissae are restricted to precise locations on the rat's head (eyebrows, lips and upper-jaw). The vibrissae found in the upper-jaw part, the so-called mystacial macrovibrissae (whiskers), play a critical role in rat survival (for more details, see I.1.2). Note that there are also smaller mystacial vibrissae (Figure 2B, length < 7mm), called microvibrissae and located on the upper lip.

Whisker arc	Length (mm)	Growing speed (mm/day)
Straddlers	46-60	1.5
Arc 1	40-44	1.3
Arc 2	33-35	1.1
Arc 3	23-25	0.9
Arc 4	11-16	0.6

Table 1: Lengths and growing speeds of the macrovibrissae in the adult Wistar rat according to their position in the array. *From Ibrahim and Wright 1975. Similar measurements were obtained in other laboratories, including ours.*

Microvibrissae are known to be involved in object recognition tasks (Brecht et al. 1997) and texture discrimination (Morita et al. 2011) In this section and throughout the thesis manuscript, we will focus on the description of the tactile macrovibrissae which are the first to contact surfaces and objects. The mystacial macrovibrissae (whiskers) are arrayed in a bilaterally symmetrical, stereotypical manner on the rat's snout. This array is defined by five rows named A to E in the dorso-ventral direction, and seven arcs numbered from 1 to 7 in the caudo-rostral direction, as depicted in Figure 2A. Four additional macrovibrissae, from α to δ (dorso-ventral direction), are located in between the five rows and referred to as the straddlers (Figure 2). The length of each whisker is conserved from an animal to another, and is gradually increased from the most rostral to most caudal position in the array (Table 1).

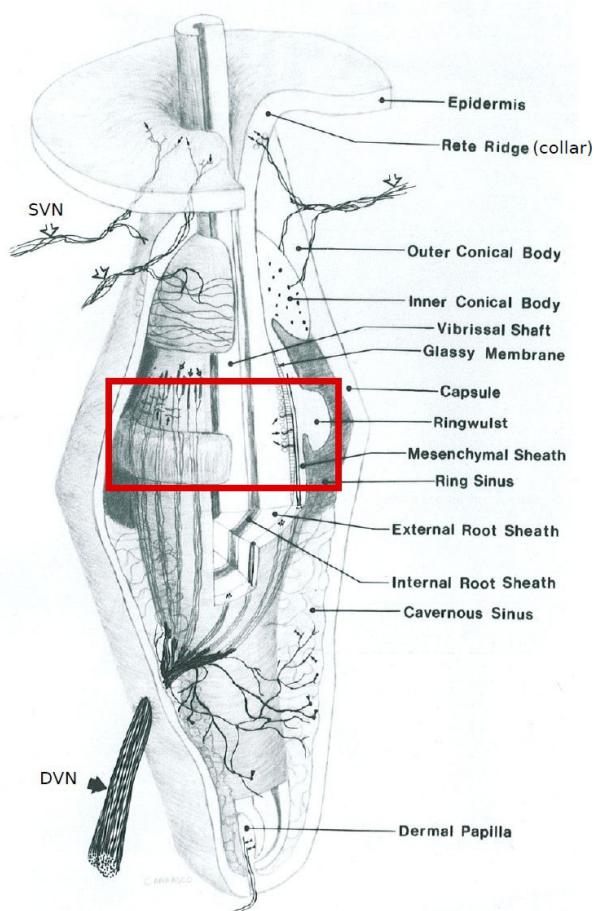
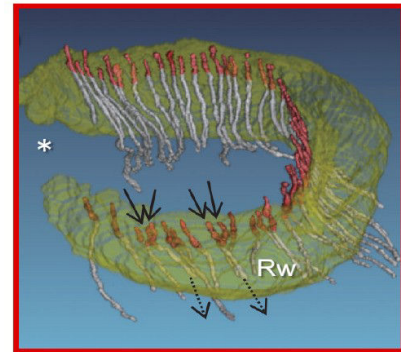
A**B**

Figure 3: Structure of the Follicle-Sinus Complex

A: Representation of the Follicle-Sinus Complex anatomy in the rat, including sensory innervation. SVN, Superficial Vibrissal Nerve; DVN, Deep Vibrissal Nerve. Sensory information is collected by several types of mechanoreceptors, located at the axonal terminals (small arrows). Adapted from Rice et al., 1986.

B: Higher magnification of the zone surrounded in red in A, the Ringwulst (Rw). Individual club-like endings (red) with their preterminal axons (white) are shown. All but 4 endings (arrows) were attached to a single axon. The exceptions converged as pairs of endings (solid arrows) into a single axon (dotted arrows). No club-like endings were observed at the open portion of the Ringwulst (large white asterisk). Adapted from Tonomura et al., 2015.

The more rostral the whisker position, the slower is its growing speed (Table 1). Growing of each whisker lasts for approximately 3-4 weeks (Ibrahim & Wright 1975). After a vibrissa has reached its maximal length, a new one begins to grow from the same follicle. When the new whisker reaches one half to three fourths of its total maximal length, the former whisker falls. Thanks to this growth cycle, each follicle position in the array never lacks a whisker shaft throughout the rodent life.

I.2.2. Structure and function of the Follicle-Sinus Complex

I.2.2.1. Anatomical description of the Follicle-Sinus Complex

The mystacial vibrissa shaft is enclosed in a multi-layer structure, the so-called Follicle-Sinus Complex (FSC), that has been precisely described in the literature (Vincent 1912, Melaragno & Montagna 1953, Melaragno & Montagna 1953, Rice et al. 1986). The FSC is oval-shaped, with a height of 1-5 mm and diameter of 0.5-2 mm (Figure 3A). The follicle corresponds to the invaginated epiderm layer, which is surrounded by a blood sinus. The blood sinus is subdivided in an upper and lower part, respectively the « ring sinus » and « cavernous sinus ». During deflection of the whisker shaft, the blood sinus is compressed on one side of the follicle and depressed on the other side, activating the mechanoreceptors located in the FSC. The outer layer of the FSC corresponds to a dense collagenous capsule, attached to the dermal papilla at the bottom of the follicle (Figure 3A), where the vibrissa actually grows. At the top, the capsule constricts around the follicle in a ring of fibrous tissue. We can note that the thickness of the capsule is changing along the follicle, with the lower part around the cavernous sinus being thicker than the upper part. The inner epidermal layer is surrounded by a mesenchymal sheath, and particularly, at the level of the ring sinus, the mesenchymal sheath gives rise to the so-called ringwulst (Figure 3A). The ringwulst is a structure of particular interest because of its dense innervation (Tonomura et al. 2015a). Notably, the ringwulst contains mechanoreceptive endings precisely arranged in a horseshoe-like manner (Figure 3B, see also part I.2.2.2).

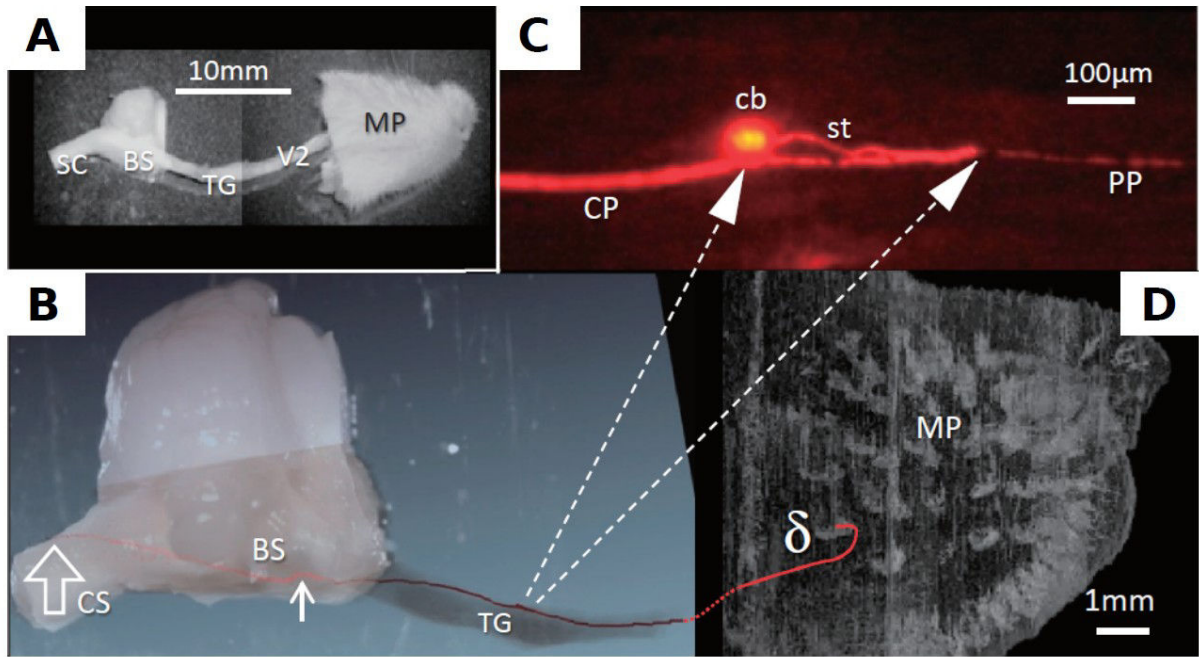


Figure 4: From the whisker follicle to the brainstem

A: Dissected rat snout including mystacial pad (MP). BS; brainstem, SC; spinal cord, TG; trigeminal ganglion, V2; maxillary nerve.

B: Reconstruction of a trigeminal ganglion (TG) neuron (red) combined with a higher magnification image of A. The cell body is in the TG. Mechanoreceptor information travels from the periphery (right) to the central targets in the brainstem (left). The first collateral is emitted at a distance of approximately 5mm from the ganglion cell body (small arrow). Open arrow; the end of the central branch of the neuron.

C: A higher magnification of the TG neuron in B. Arrows: the round cell body (cb) and the branching point of the stalk (st) into the peripheral (PP) and central (CP) branches are indicated in relation with B.

D: Reconstructed three-dimensional image of a mystacial pad evenly enlarged to match panel B. Lower magnification photos of serial 100 µm-thick sections were used. Red line; the peripheral branch of the neuron labelled in B terminated in the delta FSC.

Adapted from Tonomura et al., 2015.

1.2.2.2. The mechanoreceptor types within the Follicle-Sinus Complex

Each vibrissa FSC is innervated by two types of nerves, defined as superficial and deep (Figure 3A). The superficial vibrissal nerves innervate the upper fourth of the FSC, while the deep vibrissal nerves connect the remaining area. Both nerve types overlap in the inner conical body (Figure 3A). The deep nerves, contrary to the superficial ones, are mainly myelinated. In addition, one deep nerve innervates only one FSC, whereas several superficial nerves innervate one FSC, and several FSCs can be connected by the same superficial nerve (Rice et al. 1986, Fundin et al. 1994). Deep and superficial nerves of all FSCs in a given row merge together, and the five row-specific bundles of nerves join in the infraorbital nerve. The infraorbital nerve is one of the three branches of the maxillary nerve. The dendritic projections forming this pathway belong to pseudo-unipolar neurons with somas in the trigeminal ganglion. Approximately 300 ganglion neurons innervate each follicle. The entire cell arborization from vibrissal FSC to trigeminal ganglion (TG) and up to the brainstem can be entirely visualized using the injection of a tracer (neurobiotin) in individual TG cells (Figure 4, (Tonomura et al. 2015b)). On Figure 4B-D, the red labelling reveals projections from a single TG neuron to both the vibrissal FSC it innervates and to central structures in the brainstem, overall spanning 20 mm. The different mechanoreceptor types (i.e. the types of axonal endings) are associated to either the superficial or the deep nerve fibers according to their location within the FSC. Axonal endings have been mainly observed in the following regions of the FSC (Figure 3A) in the rat (Rice et al. 1986): the collar of the FSC (Merkel endings), at the level of the ring sinus (Merkel, lanceolate and club endings), the inner conical body (lanceolate, Ruffini and free-nerve endings), the cavernous sinus (lanceolate and Ruffini endings), and the ringwulst (Figure 3B, club-like endings).

Both the density and the spatial location of the mechanoreceptors within the FSC may reflect their functional role in tactile signals transmission. For instance, the density of the inner conical body innervation differs according to the species, and further seems to be correlated with the ability of the species to « whisk ». In whisking animals like the rat, the inner conical body is much more densely innervated compared with non-whisking animals, such as the cat and the rabbit, and it has been proposed that this structure could play a role in proprioception during whisking movements (Rice et al. 1986). Note that apart from

transmitting information during active whisking, most mechanoreceptors can be activated by passive deflections of the whiskers contacting objects. The spatial arrangement of the axonal endings probably influences their functional properties: Merkel receptors that are sensitive to pressure are likely to be pushed against the ring sinus while the whisker is deflected, thus potentially carrying an information on the direction and duration of movement. Interestingly, club-like endings are arranged in a « croissant » shape around the ringwulst (Figure 3B), with an opening (i.e. with no receptors within the opening) oriented towards the dorso-medial side (Tonomura et al. 2015b). This suggests that this subset of receptors could be tuned to detect particular orientations of the vibrissa movement and play a role in discrimination of deflection orientation (Tonomura et al. 2015). A work in preparation by Furuta and colleagues (cited in Tonomura et al., 2015) goes along with this hypothesis, demonstrating that some of the mechanoreceptors of the FSC display a particular orientation tuning for vibrissal movement. The diversity of mechanoreceptor types and morphologies as well as the anatomical pathways followed by the nerves to convey information from the periphery to the central nervous system have been described in the literature (Dörfl 1985, Rice et al. 1986, Rice et al. 1993, Ebara et al. 2002). However, relatively little is known about the relationship between the type of mechanoreceptor (given by its morphology), and the associated electrophysiological responses in neurons of the TG because of the technical difficulties. Recently, Tonomura and colleagues developed a method to identify the mechanoreceptor type associated to the individual TG cells they record from. Briefly, the authors were injecting Neurobiotin in TG cell bodies through an intracellular recording pipette. Neurobiotin travelled through the axonal projection to the FSC, revealing the morphology of each axonal ending (Tonomura et al. 2015b). In parallel, the authors recorded the TG cell responses to whisker stimulation, and reported the evoked activity level according to the type of mechanoreceptor involved in the pathway. Particularly, neurons with club-like endings displayed the highest firing rates in response to whisker stimulation. This method opens new possibilities to explore in detail the link between the structure of axon terminals and the physiological responses of the TG neurons.

In the following section, we describe how rats use their whiskers to obtain information about their environment, particularly by actively moving them to contact objects.

I.3. Whisker-based behavioral strategies to collect information

I.3.1. Description of active whisker movements

As mentioned previously, rodents can move their whiskers in different directions, thus spanning a large volume around their snout. Several behavioral strategies, such as stabilizing the whiskers position to discriminate aperture widths (Krupa et al. 2001), have been described, however whisking is the most studied, probably because it can easily be observed. Whisking refers to a particular behavior of some rodents, such as rats and mice, during which the whiskers are actively moved back and forth to explore the proximal environment (Carvell & Simons 1990, Kleinfeld & Deschênes 2011, Zuo et al. 2011, Voigts et al. 2015). During whisking, the macrovibrissae are oscillating at frequencies ranging from 5 to 25Hz in the rat (Figure 5A, lower panel). Similar oscillations have been observed in mice, with a median frequency around 20Hz (Figure 5A, upper panel), which is higher than the median frequency recorded in rats (8Hz) over the same experimental conditions (Jin et al. 2004). In rats, one cycle typically lasts 120 ms, and two thirds of this cycle correspond to a protracted state. In both rats and mice, the retraction phase is faster than the protraction phase (Gao et al. 2001, Jin et al. 2004). When rats are freely exploring an environment, whisking cycles are mainly characterized by large amplitude sweeps, with a frequency ranging from 5 to 15 Hz. This behavior is referred to as «exploratory whisking» (Berg & Kleinfeld 2003; (Kleinfeld et al. 2006). However if the animals begin to explore a particular object, they typically display the so-called "foveal whisking" (Berg & Kleinfeld 2003), with frequencies ranging from 15 to 25 Hz, and a decreased amplitude of the vibrissa movement compared to the exploratory whisking pattern. In addition, the whisking set-point, which can be defined as the angle around which whisking is centered (Kleinfeld et al. 2006), is more rostral than during the exploratory whisking: the whiskers are more protracted towards the object. Typical whisking velocity spans 300-2000°/s, with maximal values up to 3000°/s (Knutsen et al. 2005). While rats whisk on objects, the temporal sequence of contacts is dependent on head position, head velocity, whisker angle and the degree of asynchrony among adjacent whiskers.

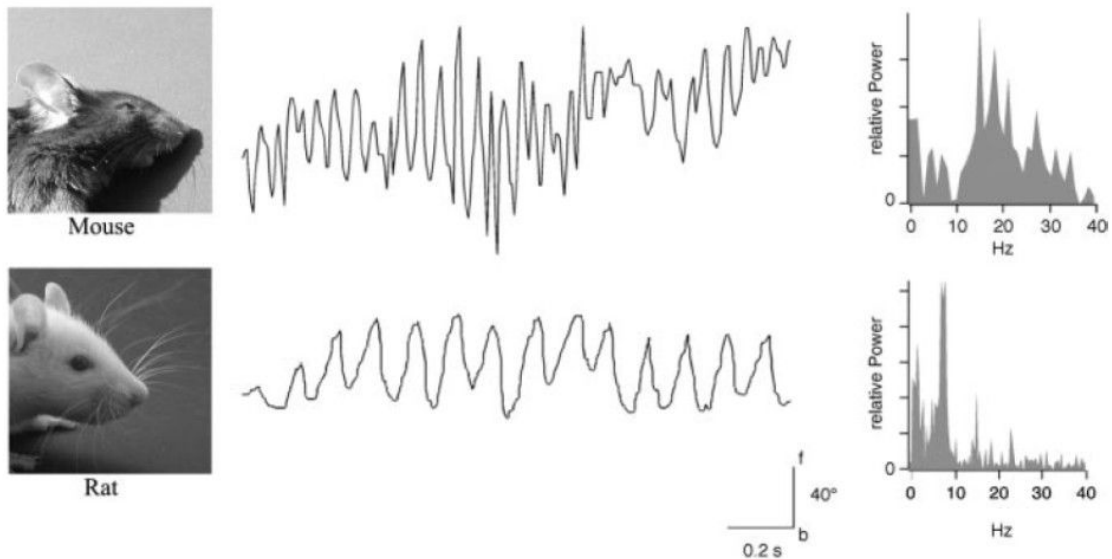
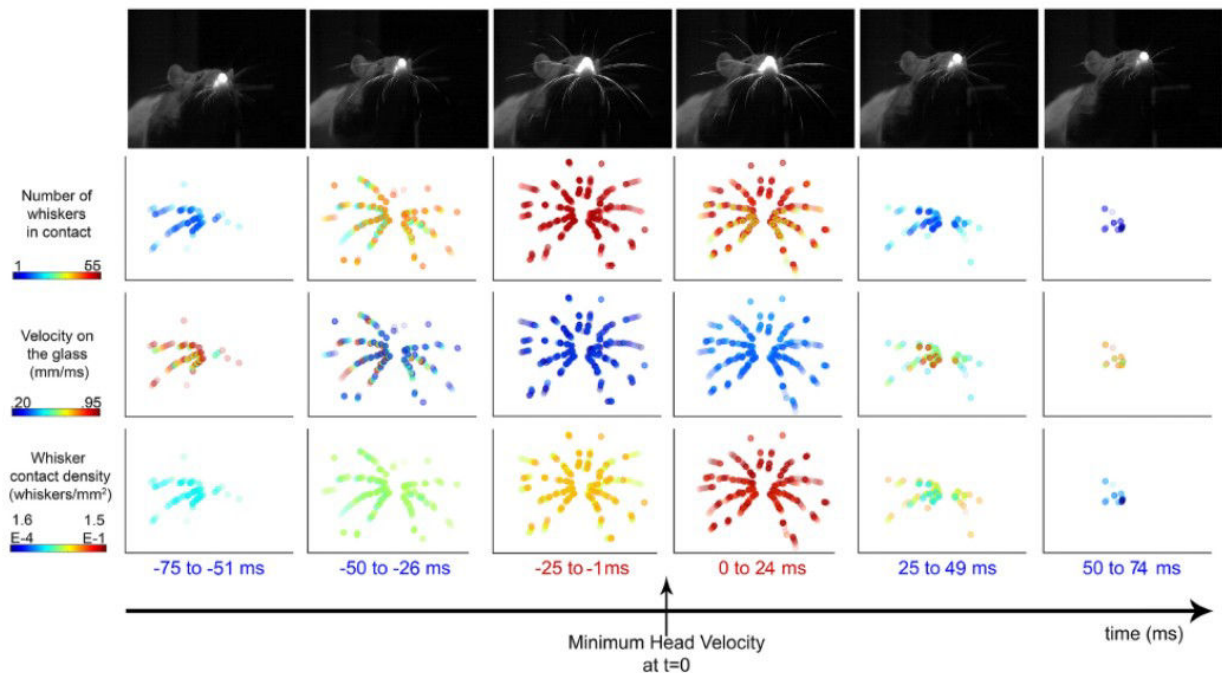
A**B**

Figure 5: Whisking spatio-temporal properties

A: Example traces of whisking trajectories (middle panel, *f*: forwards, *b*: backwards) and whisking power spectra (right panel) in the mouse and in the rat. From Jin et al., 2004.

B: An example whisk illustrates the number, velocity, and density of whiskers during exploration of a vertical glass surface around the time of minimum head velocity. A laser sheet projected in front of the glass allows detection of each whisker contact. Top row: Each image of the rat is from a single video frame taken near the middle of the time windows indicated at the bottom of the figure. Rows 2–4: In each panel, the dots indicate whisker-surface contact locations superimposed for all frames during the specified time window. Row 2: The color of each dot represents the number of whiskers in contact with the surface in the corresponding frame. Row 3: The color of each dot represents the velocity of the whisker at that contact point location. Row 4: The color of each dot represents the density of whiskers in contact with the surface in that frame. From Hobbs et al., 2015.

Despite the high variability in those temporal sequences, some general rules emerge: when the head velocity is minimal, the number of whiskers in contact with the object is maximal, and the speed of the whiskers is decreasing to establish a sustained (25-60 ms) contact with the object (Figure 5B, Hobbs et al. 2015). Also, whiskers that first contact the objects have been observed to keep touching longer (Sachdev et al. 2001), and those whiskers are more often located in arc 2 (Hobbs et al. 2015; Sachdev et al. 2001). The switch between exploratory to foveal whisking illustrates the ability of the whisker system to change the motor output according to the incoming tactile signal. For instance, when a whisker touches an object that can be of interest, the animal can interrupt ongoing movements and orient its whiskers towards the object before starting foveal whisking. The whisker system is therefore considered as an interesting model to study the relationship between the sensori- and motor- structures in the brain, and more precisely closed-loop processes (Ahissar & Assa 2016). The sensori-motor interaction is termed as "closed-loop" when the tactile input is triggering, as a feedback mechanism, an adjustment of the subsequent motor command. This way, the motor command is impacting the incoming tactile signal, and this tactile signal is reshaping the motor command, closing the loop. Note that this dynamic adaptation of the whisker position exists whether the animal is whisking or not.

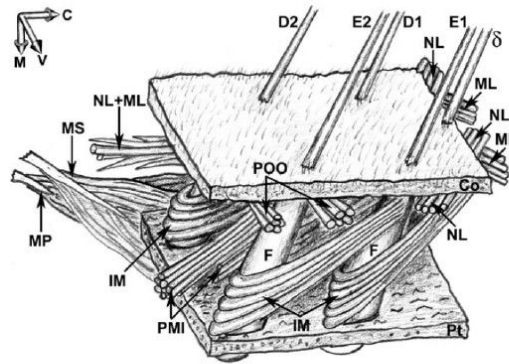
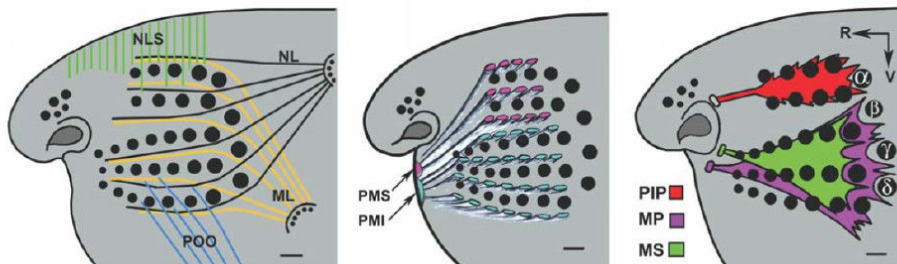
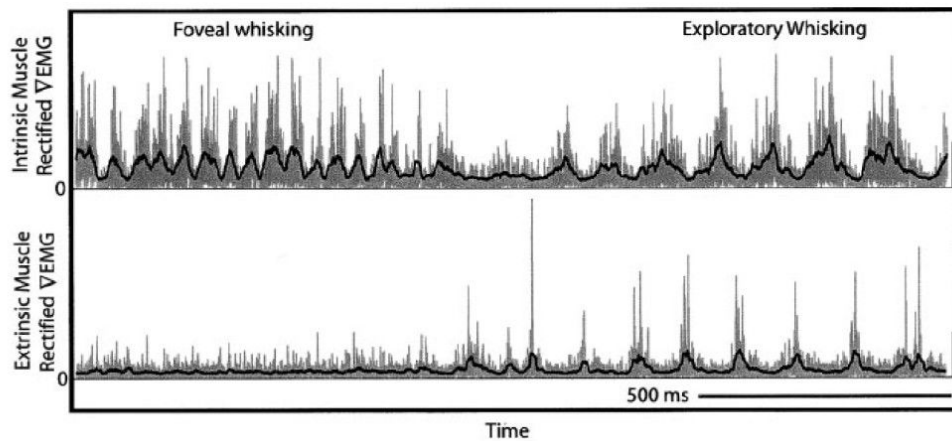
A**B****C**

Figure 6: Muscles of the whisker pad

A: Schematic drawing of part of four whiskers and their corresponding FSCs and associated muscles in the rat mystacial pad.

B: Representation of the muscles location in the whisker pad. Left, superficial muscles. Middle, deep protracting muscles. Right, deep retracting muscles.

Abbreviations for A and B: C, caudal; Co, corium; d, the ventralmost straddler; D1, D2, E1, E2, vibrissae; F, follicles; IM, intrinsic muscles; M, medial; ML, M. maxillolabialis; MP and MS, Partes maxillares profunda and superficialis, respectively, of the M. nasolabialis profundus; NL, M. nasolabialis; PMI, Pars media inferior of the M. nasolabialis profundus; POO, Pars orbicularis oris of the M. buccinatorius; Pt, plate; V, ventral. From Haidarliu et al., 2010.

C: EMG of the intrinsic (upper panel) and extrinsic (lower panel) muscles; the black line is the smoothed data. From Berg and Kleinfeld, 2003.

1.3.2. Motor control of whisker position and movement

1.3.2.1. Whisker-associated muscles: the basic architecture for positioning the whiskers dynamically

In mice and rats, the muscles of the mystacial subdivide into two categories, extrinsic and intrinsic muscles (Dörfl 1982; Haidarliu et al. 2010). These muscles are innervated by projections forming the facial nerve and belonging to motoneurons in the facial lateral nucleus. Extrinsic muscles are attached to the skull or the nasal cartilage (Figure 6B) and reach the epiderm ("corium" in Figure 6A) or deep dermal layers ("plate" in Figure 6A) surrounding the vibrissa FSC, whereas intrinsic muscles are tightly linked to the follicle: each of these muscles links two adjacent FSCs together, with the deep part of the rostral FSC linked to the superficial part of its caudal neighbor (Figure 6A). The extrinsic muscles can be divided in several types according to their anchor sites, their spreading to the whisker pad and their depth below the epidermal surface (Figure 6B). Given the insertion site in the pad and the spatial orientation of each muscle, Haidarliu and colleagues (2010) could extrapolate the effect of a muscular contraction on the movement of the whiskers. For instance, the *Pars maxillaris profunda* of the *Nasolabialis Profundus* ("MP" on Figure 6B, right panel), is attached to the nasal cartilage and inserted into the plate (Figure 6A), and thus its contraction will lead to a rostral pulling of the plate. The deep part of the FSC is attached to the plate, and will therefore be moved in the rostral direction: the whisker is retracting. They found that some extrinsic muscles could retract the whisker shaft (*Nasolabialis*, *Maxillolabialis*, and three deep sub-parts of the *Nasolabialis Profundus*, Figure 6A-B), while others could on the contrary protract the whisker shaft (two sub-parts of the *Nasolabialis Profundus*). Given the attachment of the intrinsic muscles (Figure 6A), their contraction results in a protraction of the whisker shaft. The action in antiphase of intrinsic and retracting extrinsic muscles gives rise to active protraction and retraction phases of the whisker shaft during exploratory whisking (Figure 6C; Berg & Kleinfeld 2003). More precisely, it seems the whisking protraction is initiated by the contraction of some of the *Nasolabialis Profundus* sub-units, then continued and amplified by the action of the intrinsic muscles (Hill et al. 2008). The retraction can subsequently occur with the cessation of protractive muscles

activity and the increase in extrinsic retractive muscles such as the *Nasolabialis* and the *Maxillolabialis*. In addition, Berg & Kleinfeld (2003) showed that during foveal whisking, solely the intrinsic muscles remain rhythmically active (Figure 6C), and thus the retraction process seems to be passive. Another hypothesis could be that the foveal retraction is active but involves other muscle types than the superficial ones recorded in that study, for instance deeper sub-parts of the *Nasolabialis Profundus*. In addition to retractive muscles, the origin of some extrinsic muscles is located either ventrally (*Nasolabialis superficialis*, Figure 6B, left panel) or dorsally (*Pars orbicularis oris* of the *Buccinatorius*, Figure 6B, left panel) to the whisker pad, and thus their contraction leads to bulging of the pad and dorso-ventral movements of the whisker shaft. This can be useful to precisely position a given whisker in 3D, for example in a gap-crossing or pole-touching task. Note that all muscles of the whisker pad are likely to contribute too, even those which seem dominantly involved in whisking. This result can be linked with the observation that whiskers often bend upward or downward (Huet et al. 2015).

1.3.2.2. A brainstem structure necessary for whisking generation

Moore and collaborators (2013) recently described a population of neurons in the brainstem able to drive rhythmic whisking movements of the vibrissae (Figure 7). This population is located in the ventral part of the intermediate band of the reticular formation (vIRt), near two structures known to be involved in breathing, the Pre-Bötzinger and the Bötzing complex. The authors, along with another study (Takato et al. 2013), showed that the vIRt and the facial nucleus are anatomically directly connected. In addition, the activation of the vIRt led to an initial protraction of the whiskers followed by rhythmic cycles of protraction and retraction. On the contrary, lesions of this area resulted in a cessation of whisking movements on the ipsi-lateral side of the snout, whereas the contra-lateral side was not affected. This last experiment shows that the vIRt is necessary for whisking generation. In addition, the authors demonstrated the existence of anatomical connections from the Pre-Bötzing complex to the vIRt. This suggests that, in addition to triggering inspiration during breathing, the Pre-Bötzing complex could also directly activate the vIRt and thus protraction of the whiskers. This mechanism is reflected in the phase-locking between

inspiration and whisking protraction observed in awake rats.

Together, these results demonstrate the existence of a central pattern generator of whisking, as suggested earlier (Gao et al. 2001), located in the brainstem (Figure 7 summarizes the involved circuits).

1.3.2.3. Which role for the primary motor cortex in whisker motor control?

The primary motor cortex can trigger whisking

The primary motor area (M1) was first described as a cortical region that, when electrically stimulated with tens to hundreds of micro-amperes, evokes movements of parts of the body (Hall & Lindholm 1974). This motor area can be divided in smaller regions that evoke movements in distinct body parts (Donoghue & Wise 1982); (Hall & Lindholm 1974), such that all these regions form a complete representation of the rat's body motion. Further, longer electrical stimulation of M1 in monkeys have shown that specific regions are dedicated to complex series of ethologically-relevant movements (Graziano & Aflalo 2007). For instance, rather than activating a restrained set of muscles in the body, the stimulation of some regions could elicit closing the hand, moving the arm to bring the hand to the mouth and opening the mouth, or moving limbs as if the monkey was about to jump.

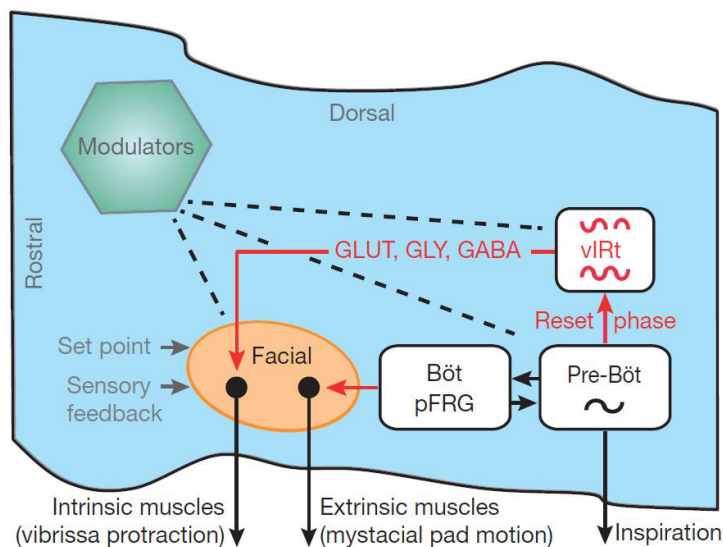


Figure 7: Generation of whisking patterns in the brainstem

Model of the medullary circuitry that generates whisking in coordination with breathing. Dashed lines indicate diffuse synaptic input from modulatory brain nuclei. GLUT, glutamate; GLY, glycine; GABA, c-aminobutyric acid. From Moore et al., 2013.

In the rat, the particular stimulation of a medial region in M1 (wM1) elicited movements of the whiskers on the snout (Brecht et al. 2004a). Electrical stimulation of single wM1 neurons at 50 Hz evoke a backward (retractive) movement of several whiskers, followed by cycles of forward and backward movements similar to whisking patterns (Figure 8A; Brecht et al. 2004b), although their amplitude was smaller than those reported during natural whisking. These results have been obtained with intracellular stimulations in deeper layers of wM1, but same trends were observed with extracellular stimulation in those layers (Brecht et al. 2004b), and increasing current intensity during the stimulation leads to an increase in evoked movement amplitude (Cramer & Keller 2006) at 50 Hz. Interestingly, the direction of the first evoked movement (backward or forward) was dependent on the frequency of stimulation (Brecht et al. 2004). Indeed, 50 and 100 Hz stimulation, resulting in the emission of spikes at respectively 50 and 100 Hz, first evoked backward movement, whereas 10 Hz stimulation first evoked forward movement (Figure 8B). This result has been confirmed by a work from Ebbesen and collaborators (2017), which showed that 100 Hz electrical microstimulation of wM1 deeper layers results in whisker retraction. This highlights the fact that wM1 neurons can initiate both protraction and retraction. Recently, Matyas et al. (2010) pointed out two zones in M1, one corresponding to the area that is activated right after sensory stimulation (Ferezou et al. 2006), and another one, more medial to the first area. When stimulated, the first area triggers a protraction of the whisker (and is named $M1_{\text{Protract}}$) and the second one triggers retraction ($M1_{\text{Retract}}$). The authors notably showed that if the glutamatergic transmission from $M1_{\text{Retract}}$ to the primary somatosensory cortex (S1) is suppressed, $M1_{\text{Retract}}$ stimulation results in a protraction of the whisker. They inferred from these data a role of S1 for retracting the whisker during whisking, and also that M1 is essentially protractive (Figure 8D). In conclusion, the retractive or protractive effect of wM1 depends on the frequency of the electrical stimulation in deeper layers, and on the location of this stimulation along the medio-lateral axis (stimulating more $M1_{\text{Protract}}$ or $M1_{\text{Retract}}$, see Figure 8C-D). The sensori-motor control of whisking illustrates the closed-loop model: the tactile input is conducted from the vibrissa to the sensory cortex, then reaches the motor cortex that can modulate the motor output applied on the whisker shaft.

Though wM1 activation is sufficient to trigger whisking cycles, its necessity for generating

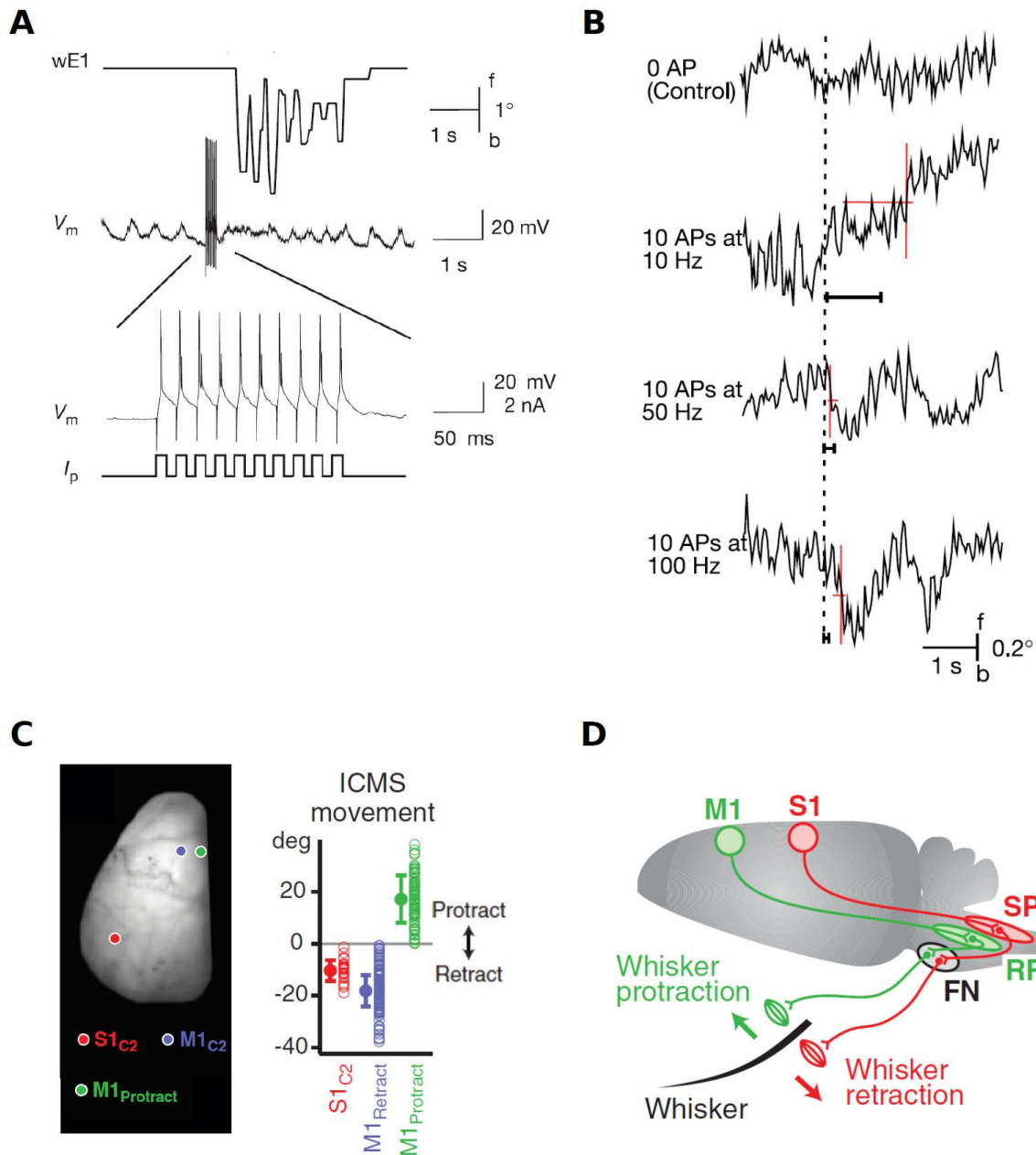


Figure 8: The primary motor cortex can trigger whisking

A: Top trace, position of whisker E1 (wE1) in an intracellular stimulation trial (10APs at 50 Hz). Bottom traces, membrane potential recordings and current injection steps. f , forward movement; b , backward movement. From Brecht et al., 2004.

B: Average movements of whisker C2 in 15 stimulation trials with initiation of 10 APs at 10, 50 or 100 Hz. Vertical red lines indicate the 50% amplitude time point and the amplitude measured; horizontal red lines indicate the 20–80% rise times. From Brecht et al., 2004.

C: Left, location of C2 barrel in $S1$ ($S1_{C2}$), $M1_{Retract}$ ($M1_{C2}$), and $M1_{Protract}$. Right, the amplitude of the whisker movement elicited by the stimulation of $S1_{C2}$, $M1_{Retract}$ or $M1_{Protract}$. From Matyas et al., 2010.

D: Schematic drawing of two parallel whisker motor pathways from the cortex to the motor neurons located in the facial nucleus (FN). From Matyas et al., 2010.

these rhythmic movements is still debated. Removal of the whole neocortex (Semba & Komisaruk 1984), specific lesions of the wM1 (Gao et al. 2003), and reversible wM1 inactivation using lidocaine (Ebbesen et al. 2017), did not prevent rats from whisking. However, recently, optogenetic activation of GABA expressing neurons in wM1 led to a significant decrease in the probability of initiating whisking (Sreenivasan et al. 2016). Thus, wM1 is at least strongly involved in this process. This implies that several pathways may control in parallel whisking initiation. Further, lidocaine application on wM1 resulted in an increase in the number of whisking cycles (Ebbesen et al. 2017), whereas optogenetic stimulation of GABA-expressing neurons in wM1 reduced whisking cycles (Sreenivasan et al. 2016). These two results appear contradictory, but the methods used for cortical inactivation differ, which may partly explain the observed differences. Indeed, optogenetic stimulations were applied with 1 s-long pulses of light (Sreenivasan et al. 2016), whereas lidocaine inactivated wM1 continuously for 10-40min (Ebbesen et al. 2017). It is possible that longer wM1 inactivation recruits more efficiently parallel compensatory pathways to initiate whisking.

The primary motor cortex can modulate frequency and amplitude of whisking oscillations

Interestingly, larger amplitudes of whisking movement are obtained when a train of electrical stimulations of wM1 is delivered at 11Hz (Figure 9, left panel; (Lang et al. 2006), a value included in the whisking frequency range (5-15 Hz). This particular tuning curve is not observed if the facial nerve, and not wM1, is stimulated (Figure 9, right panel). This is suggesting, along with the fact that single motor unit activity is correlated with the movement amplitude (Friedman et al. 2012), that wM1 could play a role in setting the amplitude of the whisker shaft movement. During unilateral inactivation, differences in amplitude and velocity of the whiskers between the ipsi- and the contra-lateral sides of the snout were reported (Gao et al. 2003), adding another evidence that wM1 activity has a role in adjusting kinematic parameters of the vibrissa movement.

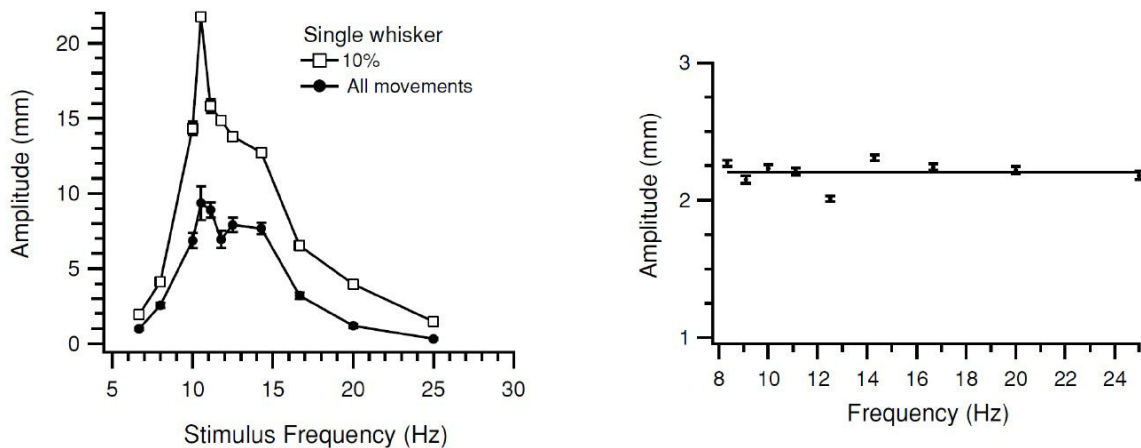


Figure 9: Movement amplitude as a function of wM1 stimulation frequency

Left, plot of average movement amplitude as a function of wM1 stimulation frequency for a single whisker. Averages were taken from all movements (filled circles), and the top 10% (open squares) at each frequency.

Right, plot of average movement amplitude as a function of the facial nerve stimulation frequency for a single whisker.

From Lang et al., 2006.

Pathways from the primary motor cortex to whisker motoneurons.

The anatomical connections from wM1 to the lateral facial nucleus, which contains the whisker-related motoneurons, are multiple. First, wM1 is anatomically connected to the vIRt in the brainstem (Matyas et al. 2010), a necessary structure for generating whisking movements (Moore et al. 2013), see I.3.2.2. for more details). Second, there is an anatomical (Takatoh et al. 2013) and functional (Cramer et al. 2007) connection from wM1 to a serotonergic nucleus of the brainstem, the lateral paragigantocellularis nucleus (LPG). Following the stimulation of wM1, neurons from the LPG responded by an increase in firing rate, positively correlated with the whisking frequency displayed by the animal. Moreover, the authors demonstrated *in vitro* that serotonin elicits rhythmic firing of the motoneurons found in the lateral facial nucleus. Along with the fact that LPG neurons project to whisker muscles (Takatoh et al. 2013), these results show that LPG in the brainstem could be a functional relay between wM1 and the snout muscles to modulate the whisking pattern. In addition to these pathways through the brainstem, a direct anatomical connection from the wM1 to the lateral facial nucleus has also been uncovered (Grinevich et al. 2005). Other

important cerebral structures involved in whisker-related sensori-motor processes are connected by M1 (for review, see Bosman et al. 2011), particularly the striatum (Reig & Silberberg 2016), the superior colliculus (Miyashita & Mori 1995), and the cerebellum (Proville et al. 2014).

Overall, the picture that emerges is that of multiple control pathways converging onto the FN neurons that govern muscles contraction in the whisker pad. While the literature has focused on large stereotypical oscillatory whisking movements for its ease of observation, it is however clear that whiskers can be controlled in very subtle ways at multiple timescales.

I.3.3. Modulation of whisker position and movement with behavior

I.3.3.1. Whisker positioning is coordinated with the animal movement

As eyes turn in coordination with the head rotation to seek for a particular field of view, the whiskers are tightly coordinated with the rat's body movements. Again, this has been predominantly studied during whisking periods.

Towal & Hartmann (2006) reported that the whisker arrays on both sides of the snout became asymmetrical and asynchronous before a movement of the head. Typically, the whiskers were more retracted on the side the rat was about to turn the head. This so-called « head-turning asymmetry » (Figure 10, first and second panels) is described in goal-directed (Towal & Hartmann 2006)(Schroeder & Ritt 2016)(Sofroniew et al. 2014) and spontaneous

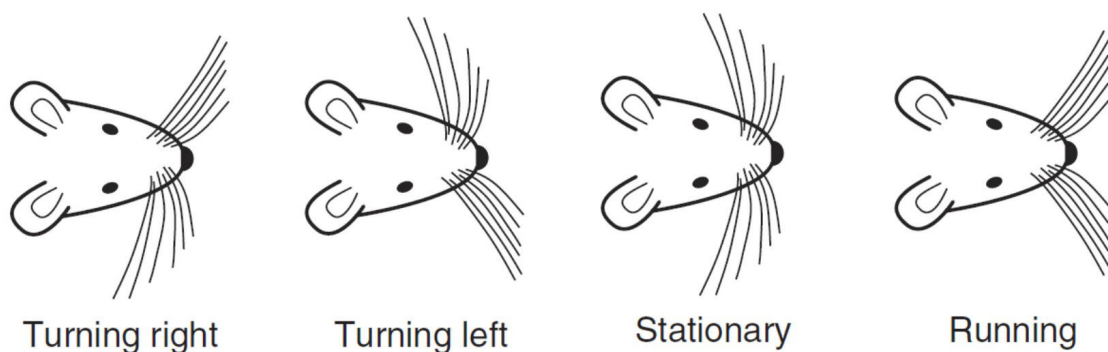


Figure 10: Whisking modulation according to behavioral contexts

From Sofroniew & Svoboda (2015).

exploratory (Mitchinson et al. 2007) behaviors of rats and mice. This modulation of the whisking pattern has been proposed to reflect a stimulus-driven attentional process (Mitchinson & Prescott 2013).

The whiskers are also coupled with locomotion, and notably when the animals are running at high speed in the dark, the whisking set-point is protracted (Figure 10, right panels), i.e. the whiskers are more protracted in front of the animal (Arkley et al. 2014), and unpublished work from Yves Boubenec in the laboratory). This behavior is described as a «look ahead» strategy. Interestingly, animals that can see in front of them show an opposite relationship between whisk amplitude and running speed to functionally blind animals, increasing rather than reducing amplitude as they move faster.

1.3.3.2. Touch-induced modulation of whisker movements

Although deafferentation experiments (Gao et al. 2001) indicate that the sensory inputs are not necessary to generate whisking in rodents, there are some behavioral evidence that touch can induce a modulation of the whisking pattern. As the rat whiskers are touching an expected object (when the animals are for instance trained to contact a sensor), the amplitude of movements of the whisker array on the side of contact becomes larger than the non-contacted side (Sachdev et al. 2003). On the contrary, if the animals encounter an unexpected object, the protraction on the side of contact is immediately ceasing and the space between whiskers in arcs of the mystacial array is reduced, probably to increase the number of whiskers in contact with the object (Grant et al. 2009). To be more accurate while scanning a surface or an object, rats may have to increase the number of contacting whiskers, but can also increase the contact duration per whisker and per whisk cycle by touching twice the object with small amplitude and high-velocity movements, performing the so-called « touch-induced pumps » (Deutsch et al. 2012). Given the low latency for generating touch-induced pumps after the first contact (~18ms), these events are thought to be processed through the brainstem loop (Nguyen & Kleinfeld 2005). During spatial localization tasks also, touch can induce a change in the amplitude of subsequent cycles. Indeed, if mice are trained to localize a platform in front of them, they precisely set their protraction to the distance at which they expect this platform during cycles following contact (Voigts et al. 2015).

Taken together, these behavioral data support the hypothesis that whisker movements are tightly regulated by a closed-loop mechanism between the sensory and motor structures.

1.3.3.3. Whisking in tactile detection or discrimination tasks

If humans are asked to assess roughness of a surface, they spontaneously sweep their fingertips onto it (Johnson & Hsiao 1992). Similarly, rodents whisk on surfaces to scan them with their vibrissae and discriminate between them (Chen et al. 2015); (von Heimendahl et al. 2007). With this method, rats are notably able to discriminate groove series with spaces of 1 mm vs 1.06 mm (Carvell & Simons 1995). If the surface asperities to discriminate are smaller, rats tend to sweep their whiskers with a higher speed and higher amplitude (Carvell & Simons 1995). Indeed, in the particular study of Carvell & Simons (1995), rats had to discriminate either between a surface with grooves and a smooth surface (RS task), or between two grooved surfaces with different spatial frequencies (RR task). The differences in motifs were thus smaller in the RR task. Protraction speed was reported to be at 580 °/s during the RR task, and significantly decreased to 500 °/s during the RS task. Amplitude of the whisking sweeps was also significantly modified, decreasing from 21° (RR task) to 18° (RS task). In addition, the velocity and amplitude of whisking have been reported to be adjusted throughout learning of discrimination between objects differing in shape and surface textures (Harvey et al. 2001). These results highlight the importance of contact speed for discriminating surface roughness or object shape, and that this parameter is adjusted to achieve good performance during learning. Like in humans (Gamzu & Ahissar 2001), good performers at the discrimination task tend to spend more time palpating the surfaces (Carvell & Simons 1995). Interestingly, if some whiskers are lacking in the mystacial array, rats spend more time palpating the surfaces, increasing the duration of contact per whisker compared to the condition with the intact whisker array (Zuo et al. 2011). This shows that the total contact duration, defined as the sum of contact duration on every whisker, may be an important parameter for discrimination since the animals compensate a decreased number of whiskers by an increase of contact duration per whisker.

To conclude, rats spontaneously use whisking to discriminate between surfaces or objects, and adjust through learning the whisking speed, amplitude, and frequency to improve the information content of the incoming signal.

1.3.3.4. Tactile discrimination without whisking

In laboratory tasks such as discrimination of aperture width (Krupa et al. 2001), or detection and discrimination of oscillating stimuli (Mayrhofer et al. 2013)(Miyashita & Feldman 2013), rats and mice do not whisk while solving the task. Furthermore, some evidence shows that in these conditions whisking could impair tactile detection abilities (Mayrhofer et al. 2013). Although these recent articles tackle several important aspects of rats discrimination abilities, whether freely-moving rodents are able to discriminate surface properties simultaneously, bilaterally, and without whisking has not been explored yet (Table 2). To answer this question, we developed a novel discrimination task (Kerekes et al., 2017) with the following constrains: 1) simultaneity and bilaterality of the stimulation, meaning that the two discriminanda are applied at the same time on both sides of the snout, and 2) the task has to be performed in freely-running animals. The freely-running condition implies that rats do not stop on the stimuli, and we therefore hypothesized that they would not use whisking to solve the task.

	Freely-moving	Discrimination type	Bilateral	Simultaneous
Krupa et al., 2001	Yes	Spatial location	Yes	Yes
Mayrhofer et al., 2012	No	Temporal patterns	Yes	Yes
Miyashita and Feldman, 2013	Yes	Spatial location	Yes	No
Kerekes et al., 2017	Yes	Spatial patterns	Yes	Yes

Table 2: Tactile discrimination tasks performed by rats without whisking.

The recent study from Mayrhofer and collaborators (2013) shows that rats and mice can discriminate vibrotactile stimuli of different frequencies bilaterally, simultaneously, and without whisking (Table 2). However, our goals differ on several points from this study, and thus our work tackles novel aspects of rodents behavior during tactile discrimination. First of all, Mayrhofer and collaborators use a controlled temporal stimulus, whereas we use a spatial stimulus that allows non-constrained movements of the whiskers to happen. Second,

their animals are immobile and head-fixed, whereas in our conditions rats run while discriminating. Third, they apply the stimulation on one whisker in the array, whereas the task we developed involves contacts with multiple whiskers. This is of particular importance since we know that cortical and thalamic neurons can code for global direction of groups of whiskers (Ego-Stengel et al. 2012)(Jacob et al. 2008).

In addition, the fact that rats discriminate surfaces while running and by contacting stimuli simultaneously on both sides of the snout could be a situation encountered by these animals in the wild. Indeed, rats live in tunnels that tightly fit their body size (Calhoun, 1963). The spread of the rat's macrovibrissae is larger than its body width, and the right and left arrays of the snout macrovibrissae may therefore contact the walls of the tunnels while the animal is walking or running inside.

Thus, our study is the first to explore the discrimination abilities of rats while they run and contact stimuli on both sides, as it occurs in natural conditions.

I.4. Bilateral discrimination of tactile patterns without whisking in freely-running rats

I.4.1. Kerekes P, Daret A, Shulz DE, Ego-Stengel V (2017) Bilateral discrimination of tactile patterns without whisking in freely-running rats. *J Neurosci* 37(32):7567–7579.

This Week in The Journal

Two Coding Schemes in Gustatory Cortex

Max L. Fletcher, M. Cameron Ogg, Lianyi Lu, Robert J. Ogg, and John D. Boughter, Jr.

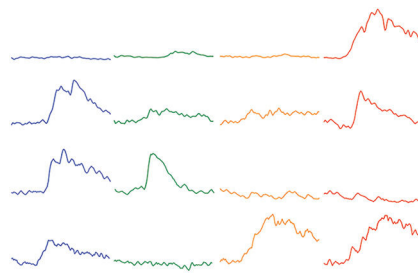
(see pages 7595–7605)

A longstanding controversy in neuroscience regards how tastes are represented in the nervous system. Some researchers have argued for a labeled-line scheme, in which taste-receptor cells and all downstream neurons are dedicated to representing a specific taste category (sweet, salty, etc.). Others, however, have argued that taste is represented by a combinatorial code, in which most cells respond to multiple taste categories, and the representation of taste depends on the activation of specific subsets of these cells. As with most scientific controversies, the truth is likely to be between these two extremes. Indeed, most studies have found that throughout the gustatory pathway, some neurons are narrowly tuned, responding best to a single taste category, while other neurons are more broadly tuned, responding to multiple categories. A notable exception is a study in which calcium imaging in the gustatory insular cortex revealed discrete clusters (“hot spots”) of neurons that responded to single taste categories, but found no evidence of neurons responsive to multiple tastes (Chen et al. 2011 *Science* 333: 1262). This study provided strong support for the labeled-line hypothesis of gustatory coding.

Fletcher et al. now bring new life to the combinatorial code hypothesis. They used a recently developed calcium sensor (GCaMP6s), which is more sensitive than that used by Chen et al., to record responses of neurons in mouse gustatory cortex, including a broad region between hot spots where Chen et al. found no taste-responsive neurons. Consistent with the previous work, Fletcher et al. found many neurons that responded selectively to sweet, salty, and bitter tastes. Unlike the previous study, however, they also found neurons that responded to sour taste, and they found no evidence of spatial cluster-

ing of neurons having similar response properties. Most importantly, they found that ~45% of recorded neurons responded to multiple tastes.

These results support the hypothesis that the CNS uses both labeled-line and combinatorial codes to represent taste qualities. To bolster this conclusion, responses to a broader range of tastants—different bitter- or sweet-tasting compounds, for example—should be examined. Future work should also investigate the extent to which the two coding schemes interact and whether they serve the same or different functions.



Example traces from four neurons in mouse gustatory cortex that responded to more than one of the primary tastes: sweet (blue), salty (green), sour (yellow), and/or bitter (red). See Fletcher et al. for details.

Texture Discrimination via Passive Whisker Stimulation

Pauline Kerekes, Aurélie Daret, Daniel E. Shulz, and Valérie Ego-Stengel

(see pages 7567–7579)

Rodents use their whiskers for many things, including navigation, judging distances, and discerning object shape and texture. Rats continually explore their environment by rhythmically sweeping their whiskers (whisking). Thus, whisking is a type of active sensing, analogous to humans running their fingers over an object. Information obtained by whisking is thought to be processed in the primary somatosensory (barrel) cortex.

Although active whisking is unnecessary for navigation in rats, whether it is needed for fine texture discrimination has been unclear. Moreover, the necessity of barrel cortex in passive whisker-dependent sensation has been debated. To address these questions, Kerekes et al. trained rats to run through a maze in which the direction of reward was indicated by the presence or pattern of vertical bars on the corridor walls. Because rats were motivated to run quickly to obtain the reward, their whiskers contacted the tactile cue for only a brief period—less time than is needed to complete a whisking cycle.

Learning this task proved difficult for rats. The authors initially had to repeat the cue at multiple locations along the passage and then remove the cues one by one before rats could reliably use a single cue to determine the correct turn. Nonetheless, rats eventually learned to discriminate the presence of bars versus a smooth surface and subsequently, to discriminate regularly and irregularly spaced bars that were presented simultaneously on opposite sides of the snout. Performance of the task was impaired by trimming the whiskers or by inhibiting barrel cortex, indicating that both structures were involved in the task. Remarkably, however, rats eventually learned to navigate the maze even without whisker-derived cues, despite the researchers' attempts to remove any olfactory, visual, or auditory cues.

These results demonstrate that rats can use whiskers to discriminate textures even without actively whisking, and that this ability depends on barrel cortex activity. The authors suggest that the rats can also discriminate tactile cues with the skin of their snout and trunk when whiskers are removed. Future work can build on these results to investigate neural mechanisms underlying passive versus active tactile sensing.

This Week in The Journal was written by  Teresa Esch, Ph.D.

Bilateral Discrimination of Tactile Patterns without Whisking in Freely Running Rats

 Pauline Kerekes, Aurélie Daret, Daniel E. Shulz,* and Valérie Ego-Stengel*

Unité de Neurosciences, Information et Complexité, Centre National de la Recherche Scientifique, FRE 3693, 91198 Gif-sur-Yvette, France

A majority of whisker discrimination tasks in rodents are performed on head-fixed animals to facilitate tracking or control of the sensory inputs. However, head fixation critically restrains the behavior and thus the incoming stimuli compared with those occurring in natural conditions. In this study, we investigated whether freely behaving rats can discriminate fine tactile patterns while running, in particular when stimuli are presented simultaneously on both sides of the snout. We developed a two-alternative forced-choice task in an automated modified T-maze. Stimuli were either a surface with no bars (smooth) or with vertical bars spaced irregularly or regularly. While running at full speed, rats encountered simultaneously the two discriminanda placed on the two sides of the central aisle. Rats learned to recognize regular bars versus a smooth surface in 8 weeks. They solved the task while running at an average speed of 1 m/s, so that the contact with the stimulus lasted < 1 typical whisking cycle, precluding the use of active whisking. Whisker-tracking analysis revealed an asymmetry in the position of the whiskers: they oriented toward the rewarded stimulus during successful trials as early as 60 ms after the first possible contact. We showed that the whiskers and activity in the primary somatosensory cortex are involved during the discrimination process. Finally, we identified irregular patterns of bars that the rats can discriminate from the regular one. This novel task shows that freely moving rodents can make simultaneous bilateral tactile discrimination without whisking.

Key words: freely running behavior; somatosensory cortex; tactile discrimination; whiskers

Significance Statement

The whisker system of rodents is a widely used model to study tactile processing. Rats show remarkable abilities in discriminating surfaces by actively moving their whiskers (whisking) against stimuli, typically sampling them several times. This motor strategy affects considerably the way that tactile information is acquired and thus the way that neuronal networks process the information. However, when rats run at high speed, they protract their whiskers in front of the snout without large movements. Here, we investigated whether rats are able to discriminate regular and irregular patterns of vertical bars while running without whisking. We found that the animals can perform a bilateral simultaneous discrimination without whisking and that this involves both whiskers and barrel cortex activity.

Introduction

The rodent whisker system has been a widely used model to study behavioral and neurobiological processes underlying the analysis

of surface properties (for review, see Jadhav and Feldman, 2010). In particular, the whisker system allows focusing on the sensorimotor strategy used by the animals during discrimination: can we observe particular features in the motor command when an animal explores a stimulus that would optimize the acquisition of tactile information? For instance, in humans, to feel whether a surface is smooth or rough, the subjects may sweep their fingertips against it, whereas to determine whether an object is vibrating, they may apply immobile fingertips onto it (for review, see Johnson and Hsiao, 1992).

Rodents are able to sweep their whiskers in a rhythmic fashion (whisking) to scan surfaces (Carvell and Simons, 1990; von Heimendahl et al., 2007). Whisking allows sampling the stimuli several times and adjusting parameters such as speed and ampli-

Received Feb. 24, 2017; revised May 22, 2017; accepted June 17, 2017.

Author contributions: P.K., D.E.S., and V.E.-S. designed research; P.K., A.D., and V.E.-S. performed research; P.K. analyzed data; P.K., D.E.S., and V.E.-S. wrote the paper.

This work was supported by the Centre National de la Recherche Scientifique, the Human Frontier Science Program Organization (Grant CDA 00044-2010), and the Agence Nationale Recherche (NeuroWhisk). We thank Patrick Parra and Jean-Yves Tiercelin for mechanical design and construction of the maze; Paul Galloux for advice and help concerning the electronics of the maze; Caroline Correia and Hind Baba Aïssa for training rats and the development of the behavioral protocol; and Zuzanna Piwkowska, Thomas Deneux, Evan Harrell, Brice Bathellier, Luc Estebanez, and Isabelle Férézou for advice during the behavioral training and discussions concerning the interpretation of the results.

The authors declare no competing financial interests.

*D.E.S. and V.E.-S. contributed equally to this work.

Correspondence should be addressed to either Daniel E. Shulz or Valérie Ego-Stengel, Unité de Neurosciences, Information et Complexité (UNIC), Centre National de la Recherche Scientifique, FRE 3693, 91198 Gif-sur-Yvette, France. E-mail: daniel.shulz@unic.cnrs-gif.fr or valerie.stengel@unic.cnrs-gif.fr.

DOI:10.1523/JNEUROSCI.0528-17.2017

Copyright © 2017 the authors 0270-6474/17/377567-13\$15.00/0

tude of the movement to improve the information content of the signal (Zuo et al., 2011). Indeed, rats spontaneously use whisking in discrimination tasks involving sandpaper (von Heimendahl et al., 2007) or microgrooved surfaces (Carvell and Simons, 1990). However, rats are also able to analyze aperture size (Krupa et al., 2001) and perform temporal frequency discrimination (Mayrhofer et al., 2013; Miyashita and Feldman, 2013) without overtly moving their whiskers, in a way that has been previously described as a passive reception mode of the tactile inputs (Kleinfeld et al., 2006). Moreover, it has been shown that whisker movements can significantly decrease the performance of head-fixed rats in a vibration detection task (Mayrhofer et al., 2013). These results suggest that whisking might not be required for discrimination of stimuli, but rather appears in laboratory tasks to be a consequence of the experimental conditions. In particular, animals that are head-fixed or restrained on a platform may whisk merely to contact the stimuli. We therefore decided to test whether rats are able to discriminate surface properties without whisking by placing the stimuli in the middle of a long alley so that rats would tend to run past the stimuli rather than stop on them. At full speed, the contact should occur within a duration of less than a typical whisking cycle.

In studies using freely behaving rats, the animals discriminate two stimuli by sampling them with both sides of the snout successively (Carvell and Simons, 1990; von Heimendahl et al., 2007; Morita et al., 2011; Zuo et al., 2011). It is still unknown whether, under these unrestrained conditions, rats could differentiate two stimuli received simultaneously, one on each side. We took advantage of the running alley configuration to test whether animals are capable of bilateral discrimination.

The primary somatosensory cortex (S1) is involved in many whisking-based tasks such as roughness discrimination (Guic-Robles et al., 1992) and object localization (O'Connor et al., 2010), but its necessity in tasks without whisking is still debated. Indeed, S1 is required for detecting oscillations of panels applied onto immobile whiskers (Miyashita and Feldman, 2013), but not for detecting frequency changes of air puff pulses (Hutson and Masterton, 1986), although this is still controversial (Sachidanandam et al., 2013). To test the effects of S1 silencing in tactile discrimination, we designed a cranial implant for chronic application of the GABAergic agonist muscimol.

For this study, we developed a novel, two-alternative forced choice task inciting the rats to discriminate stimuli by running past them at high speed, sampling each stimulus with whiskers on one side of the snout and only once. Rats learned to discriminate a surface with a series of vertical bars regularly spaced versus a smooth surface. They could also discriminate an irregular series from the regular one. The stimulus sampling occurred in <100 ms and the animals oriented their whisker arrays toward the rewarded stimulus as soon as 60 ms after the first possible contact. Both whiskers and S1 activity were involved during the discrimination process.

Materials and Methods

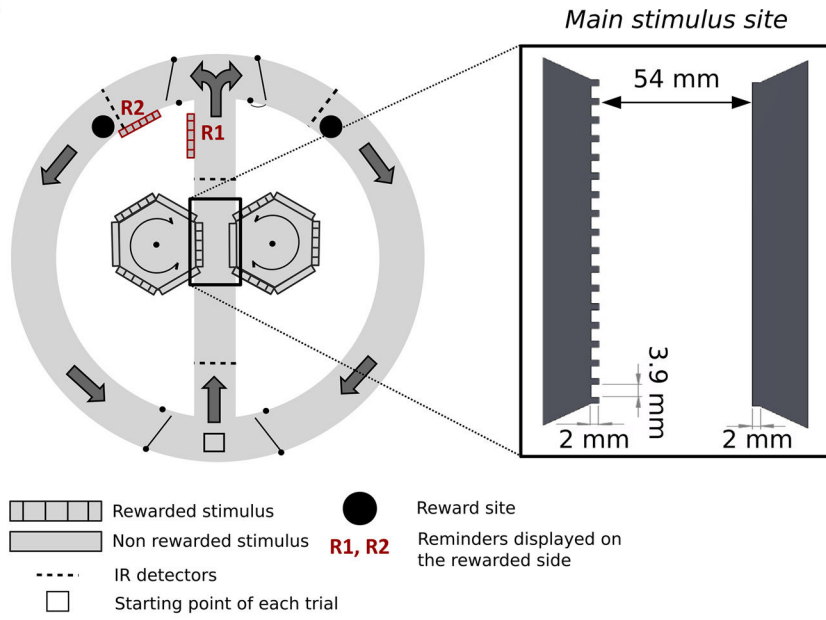
Animals. All experimental and surgical procedures were approved by the French Ethical Committee (project #526.01). In total, 10 male adult Long-Evans rats were used. Two animals were used exclusively for acute electrophysiology experiments and eight animals were trained on the discrimination task. The training began when the animals were 6 weeks old and weighed 250–350 g. The rats were housed individually in cages of length 60 cm and width 44 cm with a 25-cm-long tunnel to enrich their environment and were food deprived to 80–85% of their normal weight during the whole learning course. The 100% weight reference was deter-

mined with two control rats that were housed in the same conditions and fed *ad libitum*.

Behavioral apparatus. Freely moving animals had to discriminate between pairs of 10.2 cm long surfaces, with either 18 vertical bars spaced irregularly, 18 vertical bars spaced regularly, or no vertical bars (smooth). The stimuli were designed using the SolidWorks software and 3D printed (Easy Up 120 printer; A4 Technologie) using black ABS plastic material. For the regular series of bars, the interval between the bars was 3.9 mm wide and the bars were 2 mm thick and 2 mm wide (see Fig. 1A1). The two surfaces were facing each other in the central alley of the maze. The stimuli holders were 25-cm-wide rotating hexagons with a stimulus on each of the six sides. We always used three different copies of the same stimulus to avoid learning specific details of one particular surface. The stimuli combinations were pseudorandomly distributed across trials. The maze (Fig. 1A1) was automated with a custom-made program implemented on an Arduino Mega2560 board with servo motors to move the doors, stepper motors to rotate the stimuli holder, two pellet dispensers (Campden Instruments 80209) controlled by TTL inputs and four infrared (IR) sensors (Adafruit product ID 2167). The sensor signals were used to trigger the different trial events: open/close the doors, change the stimuli, deliver the rewards, and provide a measure of the running speed in the central alley. At the beginning of learning, we used copies of the rewarded stimulus mounted on servo motors as reminders (R1 and R2). The reward was two 45 mg pellets (Bilaney F0021) per successful trial and was triggered by the IR sensor placed 2 cm in front of the reward cup. Auditory masking noise (white noise) was presented with a loudspeaker located 50 cm away from the maze. We cleaned the maze after each session with a 30% ethanol solution to mask olfactory cues and checked after learning that the animals were not using olfactory cues from the stimuli themselves. All training took place in the dark to avoid visual cues. The position of the rewarded stimulus, the choice, and the speed of the animal in the central alley were automatically recorded through the Arduino interface for each trial.

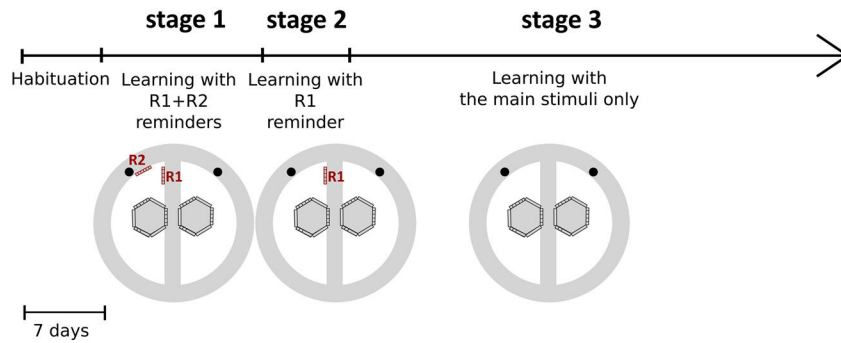
Behavioral protocol. The goal of the learning protocol was to have the rats discriminate between the surface with the regular series of bars and another surface, the smooth one first, while running at high speed. During the first week, the animals were habituated to be handled and taken to the experimental room in the dark with the white noise and maze motor noise. The animals were separated in individual cages on the third day and food restriction began on the sixth day. On day 7, rats were placed in each arm of the maze with all doors closed, first during 2 min in the light, then during 2 min in the dark. They received one pellet in the dispenser cup each time they crossed the IR sensor to make them associate this site with the reward. The day after, we began the learning of the association between the regular bars surface and the reward. This learning course was divided into three stages with one 25-min-long session per day. During the first stage, in addition to the main stimuli in the central alley, we used reminders of the rewarded stimulus (Harvey et al., 2012) before the choice point and just before the reward site (R1 and R2, respectively; Fig. 1A2). The rats had to turn to the side corresponding to the regular bars surface to get a reward and were forced to continue forward in the maze because the doors closed automatically just after they went through. The animals had to perform at least 80% correct trials during three consecutive sessions to enter the next stage. During the second stage (Fig. 1A2), only the reminder before the choice point was presented (in addition to the main stimuli). The same criterion as for stage 1 was used to consider this stage completed. Throughout the third and last stage (Fig. 1A2), the reminders at the choice site were displayed during the first five trials and removed for the rest of the session. The rats had then to learn the task with the main stimulus site only. For this stage, the performance throughout learning was quantified on all trials except the first five ones. The criterion to complete the third stage was to reach a mean performance at $\geq 70\%$ and a $SD \leq 4.2\%$ on 6 consecutive sessions. This threshold for the SD value was determined by calculating the mean SD on seven blocks of six sessions on two rats trained in a preliminary experiment. More precisely, these rats were initially trained with an empty space facing the regular series and the smooth surface was introduced during stage 3 only. These two animals are not included in the results of Figure 2

A1

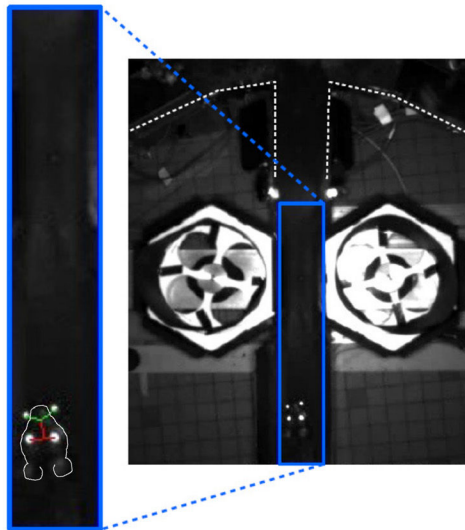


A2

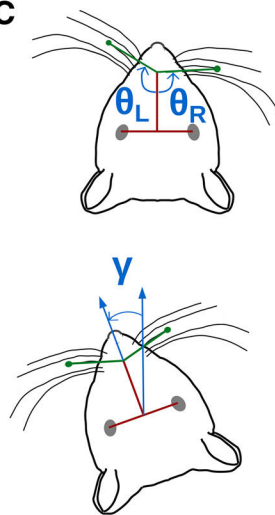
Behavioral protocol



B



C



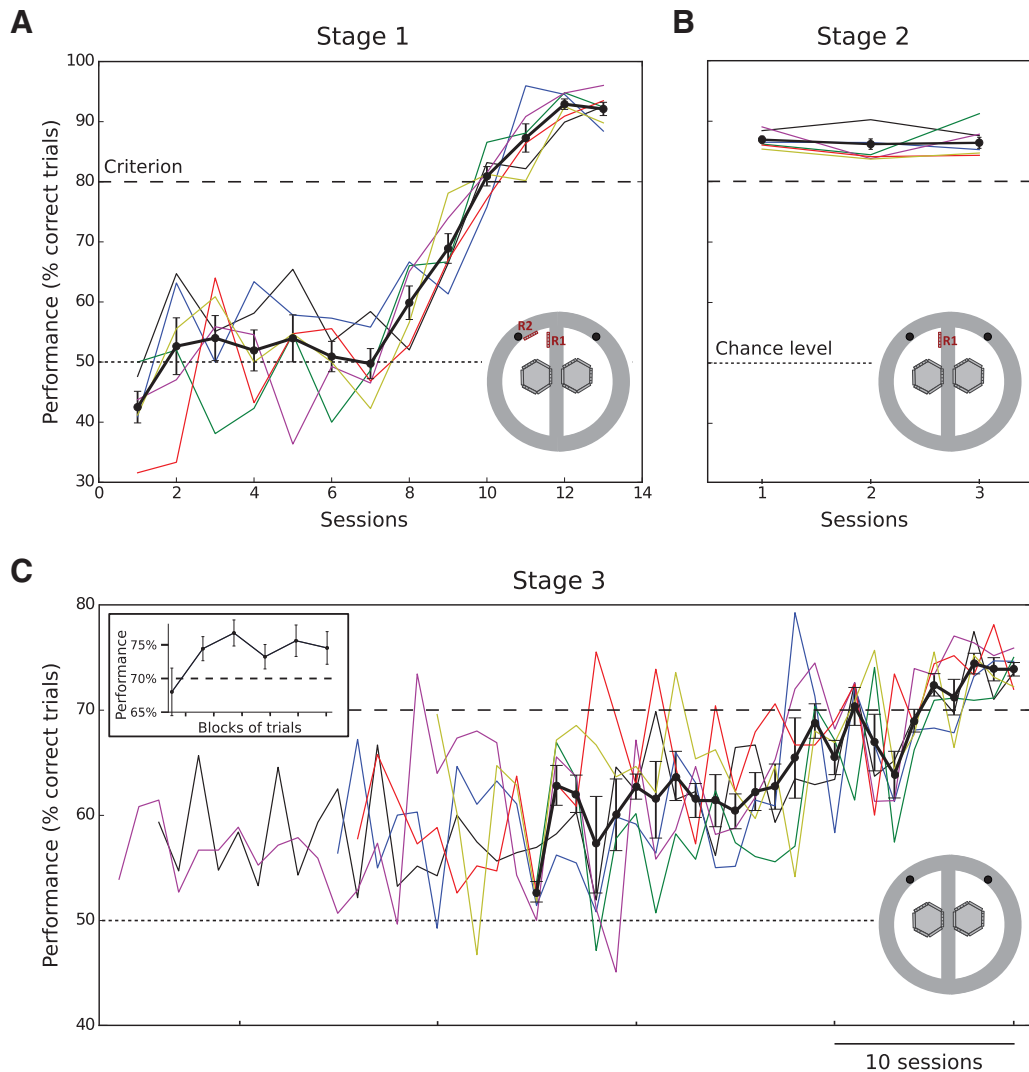


Figure 2. Discrimination between a smooth surface and a surface with regularly spaced vertical bars in 8 weeks. **A**, Learning curves for stage 1 with two reminders of the rewarded stimulus. The animals had to achieve at least 80% of correct trials during three consecutive sessions to enter the following stage. **B**, Learning curves with one reminder at the choice position (same criterion as for stage 1). **C**, Learning curves for stage 3, with only the main stimuli present in the central alley. The criterion to complete learning was to maintain a mean performance of 70% with a maximal SD of 4.2% on 6 consecutive sessions. All curves have been aligned on the final session of learning for each rat (range 25–46 sessions). The inset details the performance within a session, calculated by splitting each session into 6 blocks of trials of equal length and averaged over the last 6 sessions of stage 3 ($n = 6$ rats). In this figure and the following, the thick dark line indicates the mean performance \pm SEM and color traces show individual results.

←

Figure 1. Behavioral maze and learning protocol for investigating whisker-based discrimination in the freely moving rat. **A1**, Schematic representation of the automated maze. For each trial, the rats had to run in the central alley through the main stimulus site (black rectangle, enlarged on the right). A smooth surface and a surface with a regular series of bars were displayed on the right and left sides randomly. At the end of the alley, the animals had to turn to the side on which the regular series of bars was presented to receive a reward. **A2**, After a period of habituation, task learning was divided into several stages. In stage 1, two reminders of the rewarded stimulus were displayed on the rewarded side: one at the end of the alley near the choice point (R1) and the other next to the reward site (R2). During stage 2, reminder R1 was displayed only. During stage 3, only stimuli at the main site were present. **B**, Top view of a rat running in the alley before contacting the stimuli. The blue rectangle encloses the tracking area. The corresponding enlargement shows tracking of the head direction using IR light reflection on the eyes (red lines) and tracking of the angle values of the right and left whiskers carrying reflection material (green lines). **C**, Variables measured during tracking. Top, Absolute angle of the right and left whiskers (respectively, θ_R and θ_L) relative to the head axis. When the whiskers are oriented toward the right side, $\theta_R < \theta_L$ and the ratio is < 1 . Bottom, Head direction (γ) relative to the central alley (vertical on the video frames as in **B**).

and were only used for control experiments (whisker cutting and cortical inactivation; see Fig. 4). Their performance in control sessions, once learning was completed, was indistinguishable from the main group of rats.

Discrimination of the regular and irregular bar series. These experiments were performed on rats that had already learned the regular versus smooth discrimination. Our next goal was to assess whether these rats could report a difference between a regular and an irregular series of bars. We designed five types of irregular series, all containing 18 bars, that could be perceived as intermediate stimuli between the smooth surface and the regular series (Fig. 3A). One irregular series was designed by picking the location of the bars at random on the surface (Poisson-like series, containing intervals of 0.5 mm to at most 13 mm between 2 bars). The four remaining irregular series included one forced interval between two bars of 30, 40, 48, or 50 mm placed randomly and smaller intervals between the remaining bars. We hypothesized that this wide smooth interval would be a feature similar to the smooth stimulus and consequently that, the wider this interval, the more easily the rats could discriminate the irregular series from the regular series. Between two consecutive tests involving an irregular series, the rats were trained on the regular versus smooth paradigm for at least 4 d. For each type of irregular

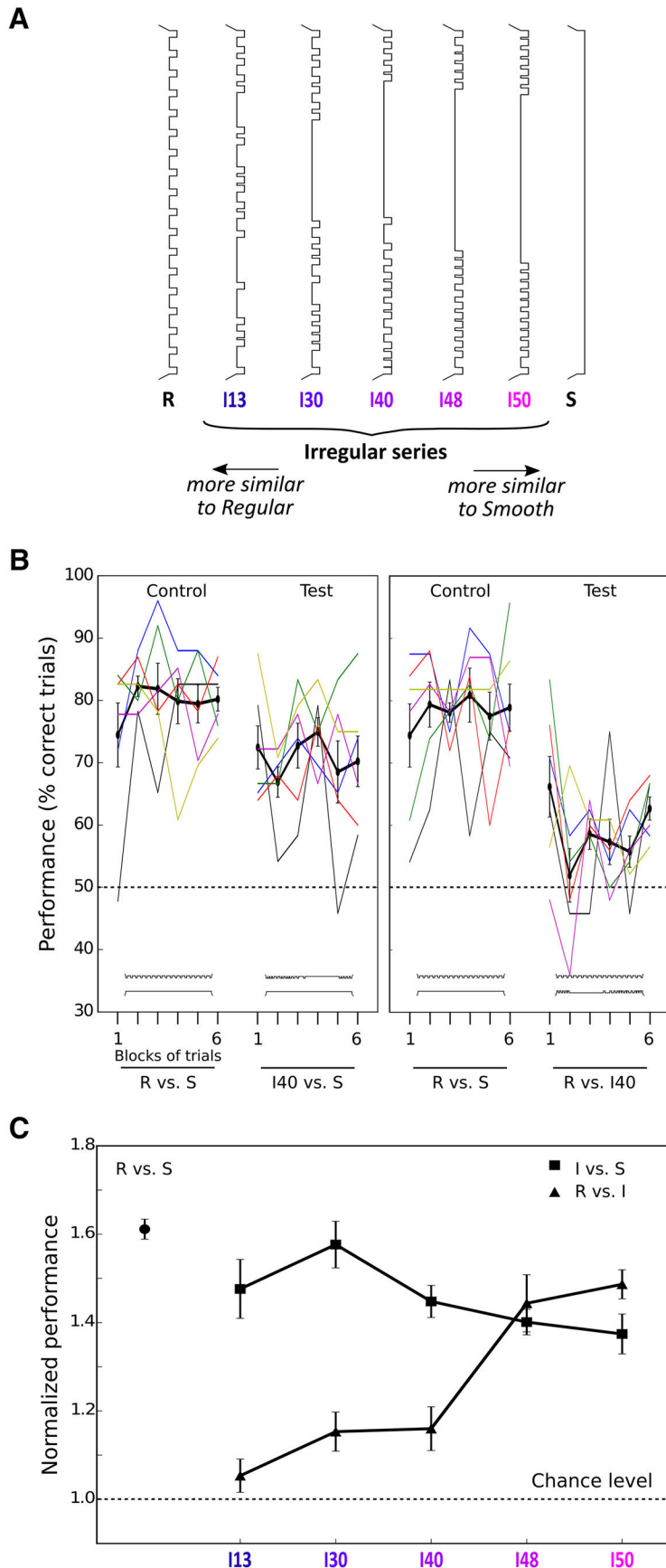


Figure 3. Discrimination of surfaces with irregularly spaced bars from the smooth and regular stimuli. **A**, Profiles of the irregular series arranged by increasing width of the largest interval between bars. **B**, Replacement of either the regular or the smooth

series, we performed two tests, always in the same order: (1) irregular versus smooth with the irregular stimulus being rewarded and (2) regular versus irregular with the regular stimulus being rewarded.

Whisker cutting. We anesthetized the rats with isoflurane (3%) for 2–5 min and cut all large facial whiskers (rows A–E, arcs 1–7, and the four straddler whiskers) on both sides of the snout with a small pair of scissors. The fur on the face and the microvibrissae were not cut. The animals ($n = 7$) were tested at least 1 h after the end of the anesthesia.

Surgical procedures. We tested the effects of muscimol application on neuronal activity in the barrel cortex and on behavioral performance in the discrimination task. The animals were anesthetized with isoflurane (1.5–3% in 0.2 L/min O_2 and 0.8 L/min N_2O ; Medical Supplies and Services). Their temperature was monitored with a rectal probe and maintained at 37°C with a heating blanket. The respiration was monitored throughout the experiment by means of a piezoelectric sensor placed between the chest and the platform on which the animal rested. After the animal was mounted in a stereotaxic frame, different craniotomies were drilled according to the type of experiment. We performed acute electrophysiological recordings of the neuronal activity during S1 muscimol application ($n = 2$ naive rats) and chronic implantations for muscimol applications during sessions of the behavioral task ($n = 3$ trained rats). For acute experiments, we made craniotomies over S1 (0–2 mm posterior, 4–6 mm lateral from bregma; Paxinos and Watson, 2009) and the hippocampus (2.6–5.6 mm posterior, 2.4–5.4 mm lateral from bregma) on the left side. The two craniotomies joined with a third one between (1.7–4.7 mm posterior, 4–6 mm lateral from bregma) to apply muscimol. We used 3D-printed implants with one hole to apply the muscimol on top of the S1 cortex and guiding structures to hold tetrode microdrives. For chronic implantations of trained animals, bilateral craniotomies were made over S1 (0.4–4 mm posterior, 4–6 mm lateral from bregma). These experiments were performed using 3D-printed implants with holes to apply the muscimol on top of the S1 cortex bilaterally. For both chronic and acute implantations, the dura was removed in the craniotomies and the implant was cemented on the skull. Two screws were inserted in the bone to better interlock the implant and the skull with dental cement for chronic experiments and one ground screw was added for acute recordings. At the end of

←

stimulus by the irregular I40 stimulus ($n = 6$ rats). In both panels, the pretest session (day before replacement) and the test session (day of replacement) are shown, split into six blocks of trials of equal length (20–28 trials depending on the animal). **C**, Performance divided by chance level after replacement of either the regular (square symbols) or the smooth (triangles) stimuli by each of the irregular series (I13, I30, I40, I48, and I50). The regular versus smooth performance in this figure was calculated as the mean performance during all pretest sessions.

chronic implantations, 0.1 ml of saline was added in each reservoir of the implant to protect the craniotomies from getting dried out and a cap of silicon sealant (Kwik-Cast; World Precision Instrument) was used to close the two reservoirs. One hundred microliters of Metacam (meloxicam, 2 mg/ml) were injected under the skin in the neck for pain management. Drops of betadine were applied on the skin around the implant to prevent infection.

Cortical inactivation with muscimol. Muscimol hydrobromide powder (Sigma-Aldrich, 18174–72-6) was diluted in PBS and applied to the surface of the cortex (Higley and Contreras, 2006). For acute experiments, we deposited 0.2 ml of muscimol solution (0.5 mg/ml) in the reservoir using a syringe. For chronic experiments, we anesthetized the animal with isoflurane (1.5–3%) to rinse the craniotomies and apply the same muscimol solution. The animals ($n = 3$) were tested on the behavioral task 70 min after muscimol application, thus ~60 min after the anesthesia ended. After each muscimol session, the animal was anesthetized again for 20 min to rinse the craniotomies and to apply 0.1 ml of saline solution in each reservoir. In control sessions, we followed the same protocol with saline instead of muscimol.

Electrophysiological recording and whisker stimulation. Neural activity was recorded extracellularly using tetrodes (20 μm NiCr wire insulated with Teflon; Kanthal Palm Coast). The 3D-printed implants were designed to hold microdrives that guided the tetrodes into the brain (250 μm displacement per screw turn). Before the implantation, tetrodes were gold plated to decrease their impedance level to 250 k Ω and to increase the signal/noise ratio. For whisker stimulation, we used a stimulator composed of 25 independent piezoelectric actuators adapted to the five rows and the five caudal arcs of the whisker pad (Jacob et al., 2010). Whiskers were trimmed to a length of 10 mm and inserted 3 mm into short polypropylene tubes glued on the actuators. The actuators were driven with RC-filtered (time constant = 2 ms) voltage pulses of 30 ms duration (10 ms rise, 10 ms hold, 10 ms fall time) to produce displacements of 0.93° along the rostrocaudal axis. For our experiments, we used sparse noise stimulation applied on the 24 whiskers. Every sequence of stimulation included the deflection of each of the 24 whiskers in both rostral and caudal directions in a random order at 20 Hz.

Global whisker movement tracking. To track the global movement of the whiskers during behavioral sessions, we glued square IR reflectors (2.25–3 mm², 1–2 mg) on the C1 or C2 whisker on both sides of the snout at a distance of 8–10 mm from the follicle. The part of the whisker extending past the reflector was cut so that the whisker could not touch the stimuli. Similar physical loading was tested in a previous study aiming at precise quantification of the kinematics of an individual whisker during contact and was found to not alter the whisker movements (Bermejo et al., 1998). In our conditions, we also verified that possible brushing of the immediately anterior whisker on the reflector did not affect the tracked whisker movement. Importantly, there was no change in performance in the tactile discrimination task after gluing of the reflectors (mean performance \pm SD just before: $79.3 \pm 2.5\%$ vs just after: $76.5 \pm 6.6\%$, paired t test $p = 0.6$, $n = 3$ rats). Note that all sessions described in Figures 2, 3, 4, and 5 were performed with intact whiskers (except in the whisker-cutting sessions) and without markers. Videos were acquired with an IR camera with LED illumination (OptiTrack V100; R2; Blackrock Microsystems) and the NeuroMotive software (Blackrock Microsystems; Fig. 1B). The frames were captured at 100 Hz with a resolution of 640×480 pixels. The rat eyes were naturally reflecting the IR beams of the camera (Fig. 1B, blue enlargement). This frame rate and bird's eye view of the setup allowed us to follow the rat head and the global position of the whisker arrays in time, including the detection of whisking (5–12 Hz). Note that it would not have been sufficient to track individual whiskers precisely in time and space. The tracking was implemented in a custom-made Python program using the OpenCV module for image processing and the `minEnclosingCircle` function to extract the coordinates of the eyes and whisker markers. We analyzed the head direction $\gamma(t)$, the angle of the labeled whiskers $\theta_R, \theta_L(t)$ with the head axis (Fig. 1C), and the speed of the animal before and during stimulus contact. We estimated the time of first possible contact with the stimulus based on the maximal protraction of whiskers relative to the nose (39 ± 2.3 mm mean \pm SEM; Morita et al., 2011).

A few video recordings were performed during the muscimol and whisker-cutting sessions without reflector markers. Three such sessions were tracked manually by clicking on the rat snout and the midpoint between the eyes on ~30 frames per discrimination trial while the rat was running past the stimuli. For each trial, we extracted the minimal distance from the snout to the stimuli (precision 1 pixel = 1.5 mm), the maximal head angle (precision around 4°), and the minimal distance from the midpoint between the eyes to the stimuli (precision 1 pixel). We estimated that, when this last measure was <15 mm, there was a possibility that the head fur was touching the stimuli.

Statistics. Statistical errors are SEM unless indicated otherwise. A binomial test was used to compare behavioral performance to chance level after the following manipulations: whisker cutting, cortical inactivation, and stimuli replacement. All statistical tests were built-in functions from the `scipy.stats` module of Python.

Results

Discrimination of a smooth surface versus a regular series of bars

We trained six rats to discriminate between two surfaces placed on the right and left sides randomly while running in an alley (Fig. 1A). One surface displayed a regular series of vertical bars and the other one was smooth. The animals had to turn to the side corresponding to the regular stimulus at the end of the alley to obtain a reward. In preliminary tests, we found that the rats had difficulties to learn the task if only the stimuli in the center of the alley were present. Therefore, we added reminders of the rewarded stimulus along the way from the main stimulus site to the reward site (Harvey et al., 2012). During the first learning stage, two reminders were displayed (Fig. 1A, R1 and R2). The six rats reached the 80% criterion in 13 sessions (~1560 trials; Fig. 2A). During this stage, the number of trials increased from 20.2 ± 3.7 to 129 ± 18 trials per session (mean \pm SD). The running speed in the central alley increased to 118.7 ± 7.2 cm/s (mean \pm SD), confirming that the rats ran at full speed when passing the central stimuli. In the second learning stage, the reminders next to the reward sites (R2) were removed. The high level of performance already during the first session of stage 2 ($86.9 \pm 3.6\%$, mean \pm SD) indicated that the rats could immediately solve the task without the R2 reminders (Fig. 2B). Figure 2C displays the learning curves of the six rats during the last stage of the protocol, when only the main stimuli in the central alley were present. Although there was a large variability from one session to the next, the animals took on average 35.7 ± 8 sessions (mean \pm SD) to reach the 70% correct trials level and stabilize their performance (Fig. 2C). The inset in Figure 2C shows the temporal profile of the performance within a session at the end of learning. Typically, the performance started at ~70% during the first trials, increased, and then stabilized or decreased slightly throughout the session. After learning the whole protocol, the mean running speed was still very high at 117.9 ± 7.6 cm/s (mean \pm SD, calculated over 20 sessions after learning, $n = 5$ rats). Overall, we conclude from these data that rats can learn to discriminate a smooth surface from one displaying regular vertical bars while freely running at full speed in an alley. The total training course (stages 1–3) lasted for 8.4 ± 1.6 weeks (mean \pm SD).

Discrimination of regular versus irregular series of bars

One initial goal of our study was to assess whether rats can discriminate surfaces displaying regular versus irregular patterns of bars. We designed several irregular patterns, all containing 18 vertical bars as the regular series but differing by the locations of these bars. Each series was identified by the widest interval it contained: 13, 30, 40, 48, or 50 mm (I13–I50; Fig. 3A; see Mate-

rials and Methods). First, we tested whether, after having learned the regular versus smooth discrimination task, the rats could perceive the sudden replacement of the regular surface by an irregular surface. If this was the case, then we would expect a drop in performance after the replacement. Indeed, Figure 3B, left, shows the results of a standard regular versus smooth discrimination session, followed on the next day by a test session in which the regular series was replaced by the irregular I40 series. In the control session, the performance was ~75% during the first block and then tended to increase, as was typical of regular versus smooth sessions (Fig. 2C, inset). During the test session, the performance started almost at the same level, but then never increased. This altered performance in the I40 versus smooth session (paired *t* test compared with regular vs smooth, $p < 0.05$, $n = 6$) indicates that the animals detected a change in the surface displaying a bar pattern, which led them to choose the side corresponding to the nonrewarded smooth surface more often than in control sessions.

We then investigated whether the rats could discriminate directly the regular series versus the I40 series. In those sessions, the performance of three rats of six was significantly above chance (paired *t* test, $p < 3 \times 10^{-3}$; Fig. 3B, right). In fact, in the first block of trials, the rats made the right choice in 65% of the trials, confirming that they discriminated the two surfaces. We hypothesized that the long smooth interval present on the I40 surface was the main feature that led the rats to treat the I40 surface as a smooth one when performing correctly in these sessions. Conversely, the 18 bars present on the I40 surface led the rats to treat it as equivalent to the regular surface in the I40 versus smooth session. The mean performance was significantly higher during the I40 versus smooth discrimination than during the regular versus I40 one (paired *t* test, $p < 7 \times 10^{-3}$, $n = 6$), suggesting that the rats perceived the I40 as more similar to the regular than the smooth surface.

More generally, we repeated these tests with other irregular patterns of bars and observed that the regular versus irregular task performance increased with the size of the maximal interval within the irregular series. Conversely, the irregular versus smooth task performance decreased when the size of the maximal interval increased (Fig. 3C). Particularly, the I48 versus smooth and the regular versus I48 tasks resulted in a similar level of performance. This indicates that, from a perceptual point of view, the I48 may be equally close to the smooth as to the regular surface. Overall, we conclude that surfaces with irregular series of bars are perceived as intermediate stimuli between the smooth and the regular surfaces depending on the size of the widest smooth interval present.

Rats use their whiskers to solve surface discrimination

To assess the role of the whiskers during the regular versus smooth discrimination task, we trimmed all the macrovibrissae on both sides of the snout and measured the resulting effect on performance. After cutting the whiskers, the performance dropped significantly compared with the previous control session (Fig. 4A,B, paired *t* test, $p < 10^{-4}$). More precisely, the performance was at chance level during the first third of the session (Fig. 4A, binomial test, $p > 0.1$, $n = 6$ rats) and then increased, although not to the same level as before cutting. A second test session confirmed the drop in performance after whisker trimming (Fig. 4A, right). The decrease in performance indicates that the rats learned to solve the task using their macrovibrissae. The partial recovery afterward further indicates that they can find an alternative strategy rather quickly during the first session after

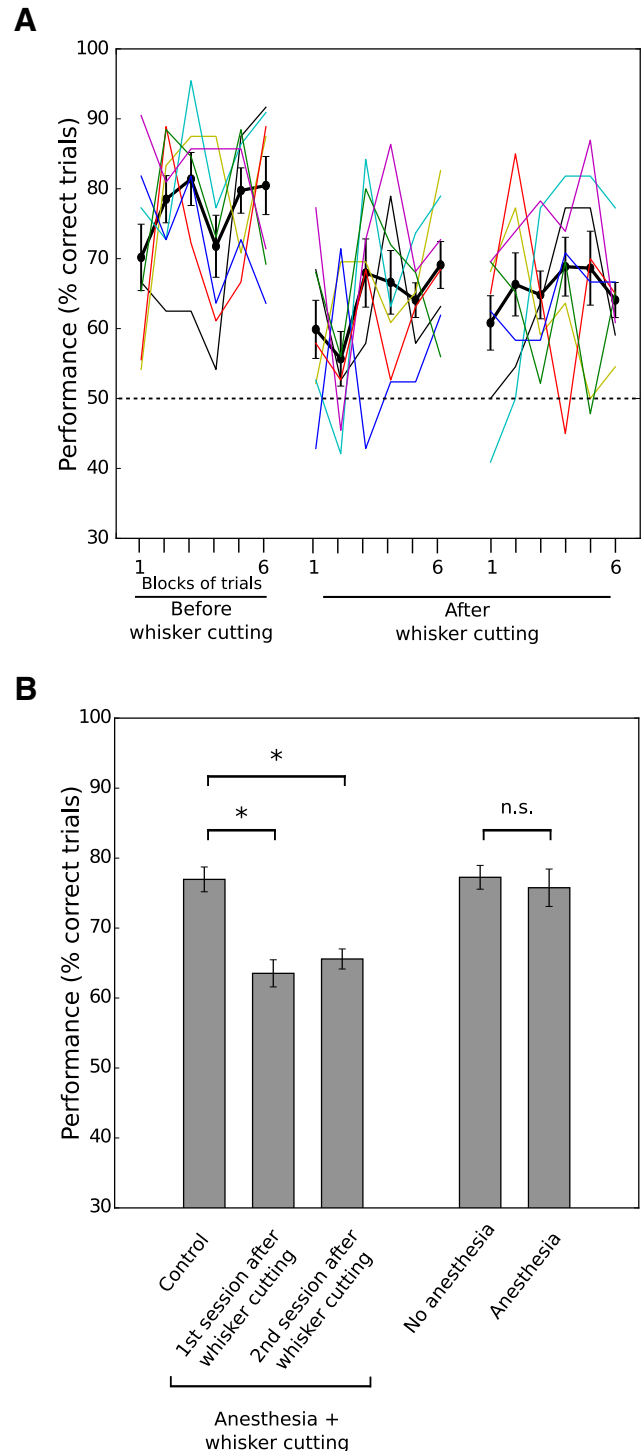


Figure 4. Whisker cutting impairs discrimination. **A**, Performance for the session before and two sessions after whisker cutting ($n = 7$ rats). Each session (regular vs smooth) has been split into six blocks of trials. **B**, Performance averaged over all trials of the sessions before and after whisker cutting ($n = 7$ rats) and before and after anesthesia only ($n = 3$ rats). * $p < 0.05$, paired *t*-test.

whisker removal. We also investigated whether the initial reduction in performance could be a consequence of the brief anesthesia used for whisker cutting. Three control animals were anesthetized using the same procedure but without cutting the whiskers. They showed no drop in performance (Fig. 4B, paired *t* test, $p > 0.05$), excluding the possibility that anesthesia was causing the reduction in performance after whisker trimming.

Interestingly, the rats could still navigate the maze after cutting the whiskers, even though nontactile cues were tightly controlled (see Materials and Methods). There was no change in the mean time to complete a trial (11.1 ± 1 s vs 11.8 ± 1.2 s before and after cutting, paired *t* test, $p = 0.1$, $n = 7$ rats). The long training on the maze up to the whisker cutting, taking 4 months or more, combined with remaining tactile information from the rest of the body, including the paws, were enough for the animals to navigate very rapidly. We hypothesized further that the partial recovery of discrimination performance during sessions without macrovibrissae could depend on tactile cues from the microvibrissae, the head, or the trunk. To test this possibility, we analyzed two sessions recorded by videography just after whisker cutting. We measured the minimal distance between the rat snout and the stimuli by manual tracking. We found that it was >8 mm in at least 95% of the trials. This indicates that it is unlikely that the rats used their microvibrissae to discriminate the stimuli. Touching of the stimuli with the head fur remained possible in $\sim 15\%$ of the trials (20/116 and 19/142 trials for the two rats; see Materials and Methods). We conclude that rats use their whiskers to solve the task in normal conditions, although they can learn another strategy if needed, which could involve the skin on the head posterior to the whisker pad as well as on the rest of the body.

Neural activity in the barrel cortex is involved in solving the task

To test the involvement of the somatosensory cortex during the regular versus smooth discrimination, we used the GABA-A agonist muscimol to inactivate the S1 cortex while the animals were performing the task ($n = 3$). First, we determined the temporal window within which the cortex, but not the subcortical regions, could be inactivated when applying muscimol on the cortical surface. We recorded neuronal activity extracellularly using tetrodes in the barrel cortex and, as a control, in the hippocampus before and after a topic application of muscimol on S1 in rats anesthetized with isoflurane (acute experiments, $n = 2$ animals). We found that $200 \mu\text{l}$ of muscimol at 0.5 mg/ml inactivated the S1 cortex after 40–50 min for a period of at least 3 h. Indeed, multiunit activity in response to deflection of a whisker decreased dramatically after muscimol application (Fig. 5A; 2 recordings followed up to 3 h were still at 0 sp/stim). On the contrary, the hippocampus was still active after 3 h: spontaneous activity was equal to 33 spikes/s (sp/s) 10–20 min before muscimol application and to 14 sp/s 170–180 min after. Based on these results and on the literature (Higley and Contreras, 2006), rats already trained on the regular versus smooth protocol were fitted with custom-made implants containing two reservoirs, one over each S1 cortex, initially filled with saline (see Materials and Methods). The behavioral tests were done at least 48 h after the surgery. During bilateral inactivation of the S1 cortex with muscimol, the mean performance of the regular versus smooth discrimination task significantly decreased from $73.3 \pm 1.4\%$ (control) to $58.8 \pm 2.3\%$ (mean \pm SD; Fig. 5B,C). By looking at the time course within the session, we found that the percentage of correct trials remained at chance level during the first half and then increased back during the second half (Fig. 5B). One day after the muscimol test, we applied saline ($n = 2$) or no solution ($n = 1$) and found that the performance was immediately back to the control level (Fig. 5B,C, paired *t* test, $p > 0.05$). The running speed and the number of trials per session were not different between muscimol and control conditions (paired *t* test, $p > 0.05$) and there was no sign of ataxia (Sturgeon et al., 1979), suggesting that the general

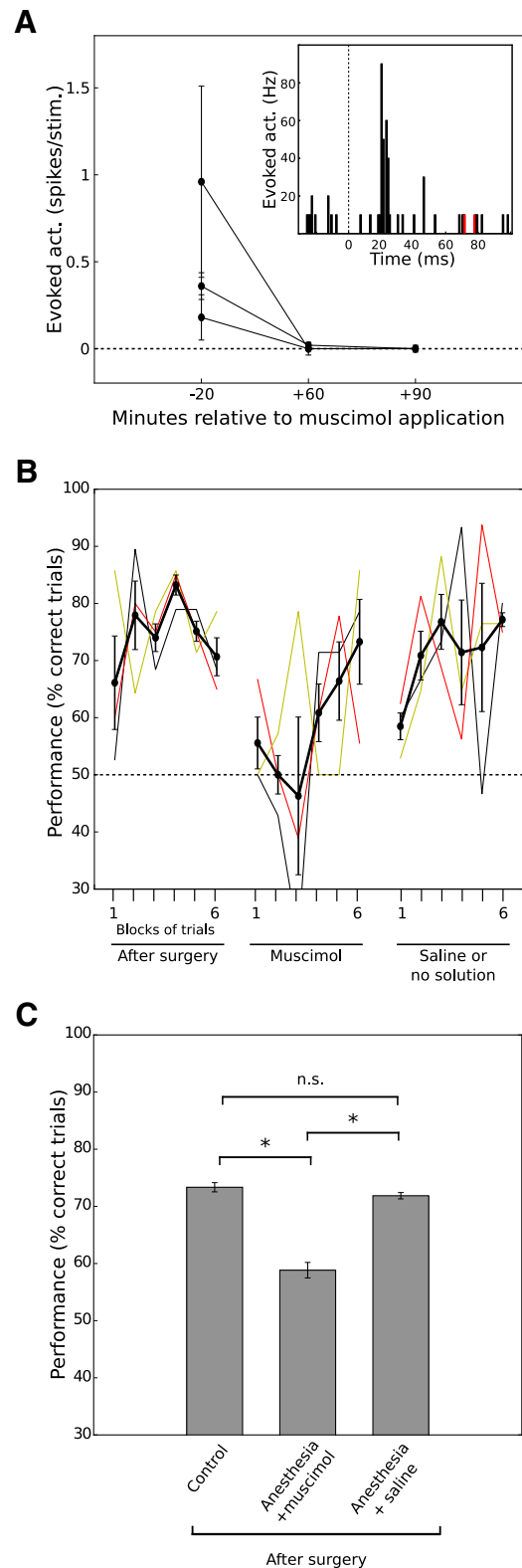


Figure 5. Cortical inactivation impairs discrimination. **A**, Multiunit activity in response to stimulation of a functionally identified whisker as a function of time around the application of muscimol on the barrel cortex surface ($n = 3$ recordings in 2 rats). Inset, Peristimulus time histogram of the activity recorded on one tetrode while stimulating whisker D2 20 min before (black) and 60 min after (red) muscimol application. Activity 90 min after was null. **B**, Performance during a control session, during muscimol application, and during saline application (two rats) or no solution (one rat). Each session (regular vs smooth) has been split into six blocks of trials. **C**, Performance averaged over all trials of the sessions before and after muscimol or saline cortical application ($n = 3$ rats). * $p < 0.05$, paired *t*-test.

behavior of the rat was not affected by the muscimol application. We analyzed one video recording by manual tracking of the head. Results were similar to those obtained after whisker cutting, with no evidence for microvibrissae touch and limited involvement of the head skin (see above). Overall, these results indicate a role for the somatosensory cortex in the discrimination of tactile patterns, with partial recovery in time that could be mediated by distant body parts.

Running speed in the central alley

To estimate whether the rats could be sampling the stimuli several times by whisking on them, we first measured the running speed in the central alley of the maze based on the two IR detectors placed before and after the main stimulus site (Fig. 1A). As already stated, after learning, the mean running speed was 117.9 ± 7.6 cm/s (mean \pm SD). Given that the stimulus was 102 mm long, we infer that the mean contact duration between the whiskers and the stimuli is ~ 86 ms, which is less than a typical whisking cycle at 10 Hz. This result strongly suggests that the rats do not whisk on the stimuli.

The running speed measure also allowed us to investigate its possible effect on performance. Indeed, it has been shown that the duration of whisker contact is a critical parameter for discrimination (Zuo et al., 2011) and also that the scanning speed modulates the amplitude of vibrissae micromotions (Ritt et al., 2008). We found that the running speed was significantly higher for successful compared with failed trials, although the size of the effect was quite small (respectively, 118.8 ± 7.8 cm/s and 115 ± 9.1 cm/s, Wilcoxon test, $p < 9 \times 10^{-7}$, mean \pm SD calculated over 20 sessions or ~ 2400 trials after learning, $n = 5$ rats). This result suggests that there may be an optimal speed for tactile scanning of the stimuli.

Whiskers retract slowly at the estimated time of first contact

To gain more insight into a possible strategy of the animals regarding the positioning and dynamics of the whisker arrays during the task, we placed IR reflectors on the C1 or C2 whiskers to track the angle on the left side (θ_L) and on the right side (θ_R) of the snout while the rats were approaching and contacting the stimuli (Fig. 1B, $n = 15$ regular vs smooth sessions on 3 rats). Addition of such a lightweight marker (1–2 mg) was reported to not alter whisker kinematics (Bermejo et al., 1998). Analysis of these video recordings provided further evidence on the absence of whisking during contact with the stimuli. Figure 6A shows the left and right whisker angle as a function of time during a typical discrimination trial. The time course was slow, with no evidence for oscillatory movements. In contrast, we were able to find an example of spontaneous whisking with clear oscillations at ~ 10 Hz (Fig. 6B). Power spectrum calculation confirmed that there was very little signal in the 5–12 Hz whisking-frequency band during the discrimination periods (Fig. 6C; Jenks et al., 2010). We conclude from these results that rats did not discriminate the stimuli by whisking on them.

Next, we investigated whether the rats were approaching the stimuli with random whisker angle and speed or if these variables were actively controlled before and/or during the discrimination. The eyes reflected IR beams (Fig. 1B), so we could obtain the head angle (γ) relative to the central alley axis and the whisker angles relative to the head axis (Fig. 1C). In this configuration, a protracted state for the whiskers is defined by an angle $>90^\circ$. Figure 7A shows the angular trajectory of the right whisker as a function of the position of the rat eyes in the central alley for the 665 trials of one animal (five sessions). The red horizontal line indicates the

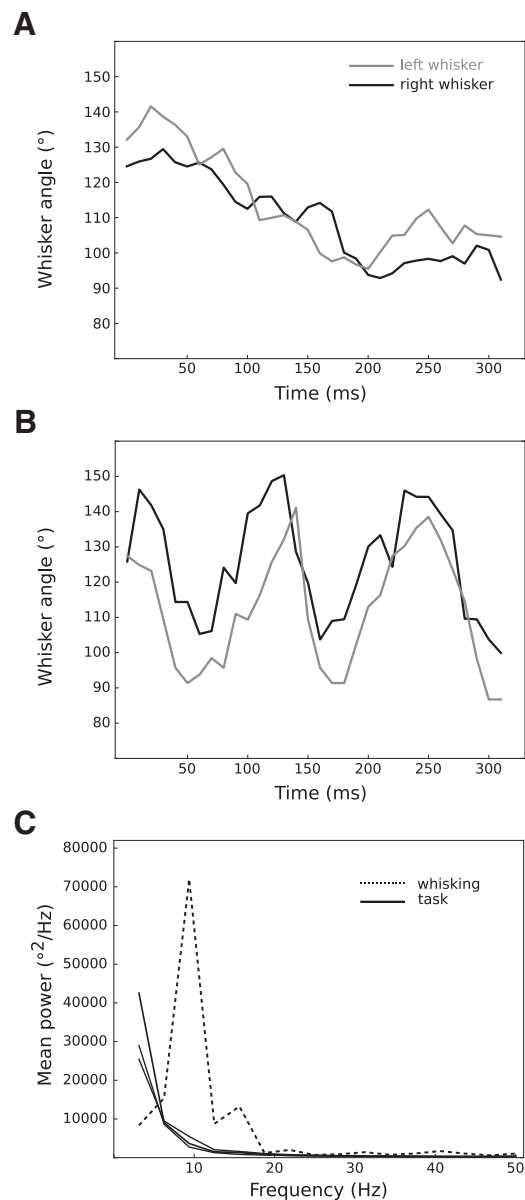


Figure 6. Discrimination of stimuli was performed without whisking. **A**, Left and right whisker angle as a function of time for an example discrimination trial in the central alley. **B**, Left and right whisker angle as a function of time during a spontaneous bout of whisking in a reward arm. **C**, Power spectrum of the whisker angle ($n = 336$ trials, 3 rats) and power spectrum of the traces of **B** showing a peak in the whisking frequency range.

physical position of the stimulus in the alley and the black arrow the estimated position where the rat would first be able to contact the stimulus if it had its whiskers maximally protracted. Two consecutive points on each colored curve are separated by 10 ms. We observed that the whisker followed a reproducible trajectory from trial to trial. It was initially protracted when approaching the stimulus, with an angle of $121 \pm 7.9^\circ$ (mean \pm SD) 90 ms before the first possible contact, and then retracted to $99.2 \pm 8.1^\circ$ (mean \pm SD) 170 ms after the first possible contact (Fig. 7A). It is important to note that the markers were placed on the tip of whiskers cut 8–10 mm from the skin of the snout so that the markers could not touch the stimuli. This implies that the measured movement of the marker was not due to the physical contact onto the stimulus, but rather to the movement of the whisker itself. Therefore, the whisker angle values that we measured re-

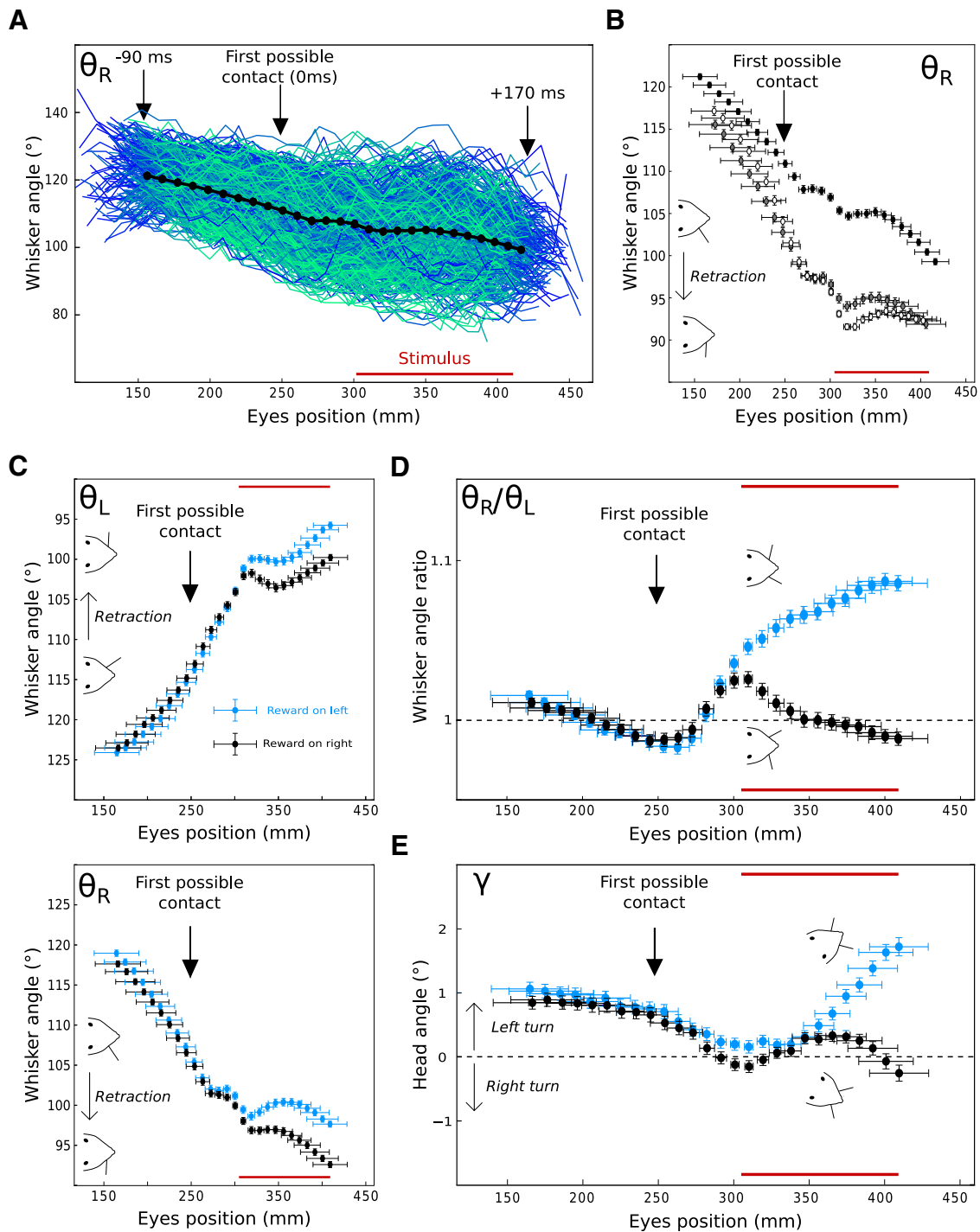


Figure 7. Whisker angle and head direction during stimulus discrimination. **A**, Individual trial trajectories of the right whisker angle as a function of the rat position (measured as the eyes position) in the central alley for five regular versus smooth sessions in the same animal ($n = 665$ trials). The color indicates time within sessions (green: beginning; blue: end). Each point corresponds to the measure on one video frame; 27 frames were analyzed for each trial. Interval between two points was 10 ms. The thick black line indicates the mean trajectory. The red horizontal line indicates the physical position of the stimulus along the alley and the vertical arrow indicates the first possible contact between the whiskers and the stimulus if the whiskers were fully protracted. **B**, Mean (\pm SEM) right whisker angular trajectories for each of three rats as a function of the rat position in the central alley. The horizontal error bars represent the SD of the eye position distribution. For panels **B–E**, only successful trials were kept. **C**, Left (top) and right (bottom) whisker angle values as a function of the rat position in the central alley ($n = 3$ rats). In each panel, the angle values have been separated in two groups depending on whether the rewarded stimulus was on the right (black trace) or on the left (blue trace). **D**, **E**, Whisker angle ratio (right/left) and head direction plotted as a function of the rat position in the central alley ($n = 3$ rats). Angle ratios have been divided by their baseline value before averaging across animals.

port the general protraction state of each vibrissal array. Similar whisker trajectories were observed for the three rats (Fig. 7B), confirming that the animals developed a particular motor strategy to explore the stimuli.

Orientation of the whiskers and head direction during the task

Given the reproducibility of the whisker angular trajectory while the animals were engaged in the discrimination, we wondered

whether we could observe a relation between the stimulus encountered and the ongoing whisker movement. The animals might adjust their touch dynamically depending on whether they recognize the rewarded or an unrewarded stimulus. We found that, during successful trials, the whisker protraction level on both sides of the snout was modulated by the side of the rewarded stimulus. More precisely, the right whisker retracted more when the rewarded stimulus was placed on the right (Fig. 7C, top, black trace) than when it was placed on the left (blue trace). Conversely, the left whisker retracted more when the rewarded stimulus was placed left (Fig. 7C, bottom). Therefore, during successful trials, the whisker position was actively modulated as a consequence of the position of the rewarded stimulus. To quantify whisker asymmetry, we calculated the ratio between the right and left whisker angles (θ_R/θ_L). An increase in this ratio indicates that the whiskers are orienting to the left side (Fig. 1C). The results are shown in Figure 7D. After the first possible contact, the mean ratio value increased when the rewarded stimulus was on the left side and decreased when the rewarded stimulus was on the right side. Therefore, during successful trials, the whisker arrays were adjusted by the animal and oriented toward the rewarded stimulus. The mean ratio value was significantly higher for left-rewarded trials compared with right-rewarded trials as soon as 60 ms after the first possible contact (Wilcoxon rank-sum test, $p < 1.9 \times 10^{-3}$; Fig. 7D), indicating that this dynamic adjustment was taking place already well before the end of contact with the stimulus. We verified that the excess retraction on the rewarded stimulus was not due to friction on the rewarded surface, always rougher than the nonrewarded smooth surface, by analyzing failed trials. In those instances, the whisker arrays did not orient toward the regular bars surface after the initial contact. If anything, there was a tendency for transient excess retraction on the smooth surface. This observation leads us to conclude that, in successful trials, the orientation of the whisker array toward the rewarded stimulus is not a mechanical effect, but rather an active process. In addition, we observed that the animal started to turn its head toward the rewarded stimulus side ~ 130 ms after the first possible contact (Wilcoxon rank-sum test, $p < 4.2 \times 10^{-3}$; Fig. 7E). We conclude from these data that rats running at high speed in a narrow alley can discriminate patterned stimuli placed on the sides within single sweeps and that they anticipate the turn indicating their choice by first orienting their whiskers and then orienting their head toward the rewarded side.

Discussion

We developed a new two-alternative forced choice task that involves fast (<100 ms) and simultaneous discrimination of surfaces with or without vertical regularly spaced bars. The rats learned to distinguish these surfaces in 8 weeks and could further distinguish patterns of vertical bars differing in their spatial arrangement. Learning of the task involved the use of the whiskers and neural activity in S1. Nonetheless, alternative strategies to solve the task were rapidly developed when the whiskers were cut or when S1 was inactivated. Rats performed the discrimination while running at full speed without whisking, but with precise and systematic control of the whisker arrays. During successful trials of the task, the whiskers were actively positioned in an asymmetric manner around the snout and oriented toward the rewarded stimulus. This whisker asymmetry was followed by a turn of the head toward the rewarded stimulus 70 ms later as the rat was leaving the stimuli site.

Reminders of the rewarded stimulus guide learning

The idea of stimulus reminders placed between the discrimination site and the reward site to guide and accelerate learning was inspired from a recent visual discrimination task study (Harvey et al., 2012). The goal was to shorten the delay between the last contact with the rewarded stimulus and the reward and thus to facilitate the association between them. In our study, all the rats quickly learned the task with two reminders (stage 1; Fig. 2A). Interestingly, the removal of the reminder at the choice site reduced the performance to chance level, indicating that the rats were basing their discrimination largely on these stimuli when present. Indeed, further learning in the task was slow. One way to speed up learning in future experiments could be to transition slowly between stages 2 and 3 by keeping the reminders at the choice site during $\sim 80\%$ of the session and decrease this proportion gradually once learning becomes measurable.

Rats can discriminate regular from irregular bar series

When we introduced surfaces with irregular series of bars, the rats showed immediately a very high performance in discriminating the I13 surface from the smooth surface, with no significant decrease compared with the regular versus smooth discrimination level. Two hypotheses could be raised: either they do not perceive the difference between the regular and irregular surfaces or they quickly associate them. Given that the direct regular versus irregular combination dropped performance down to chance level, one could infer that the animals are not able to perceive the difference between the two series. However, many reports in the literature already highlighted the abilities of rats to discriminate fine differences between two surfaces (Carvell and Simons, 1990, 1995; von Heimendahl et al., 2007; Morita et al., 2011). In particular, rats can discriminate spaces between grooves that differ by $125 \mu\text{m}$ (Carvell and Simons, 1995), suggesting that they could learn to perceive the difference between the bar series in our study. Therefore, we think that the animals learned to associate only the presence of the bars with the reward, not the fact that these bars were displayed regularly. This contingent generalization is likely a consequence of the task design based on two-alternative choices. Nonetheless, by varying the size of the maximal smooth interval in the irregular series from 13 to 50 mm, we revealed that the irregular surface could be distinguished from the regular surface during acute comparisons. In particular, when a long smooth interval was present, the regular versus irregular discrimination became similar to the regular versus smooth discrimination. We conclude that the animals are able to base their discrimination on the pattern of the bars on the surface and that the precise location of the bars governs the difficulty of the discrimination.

Whisker cutting impairs task performance

To ensure that the discrimination task involves the whiskers, we cut all macrovibrissae ($n = 7$ rats). We found that the performance of the animals immediately decreased to chance level, confirming the involvement of the whiskers. However, maze navigation was not altered and the performance increased back within one session, suggesting that the animals may find quickly an alternative strategy. This recovery could be based on tactile inputs conveyed by receptors other than those of the macrovibrissae. We were controlling the visual, auditory, and olfactory conditions by training animals in total darkness, constant masking noise, and wiping stimuli with ethanol 30% so that we could exclude the use of nontactile cues. We thus speculate that the rats learned to use the skin of their head or trunk. Indeed, it was shown previously that rats are able to discriminate surfaces

using their microvibrissae (Brecht et al., 1997; Kuruppath et al., 2014) or even the skin of their snouts (Morita et al., 2011). However, we tracked the animal head manually on the video recordings of sessions for two rats after whisker cutting and found that the rats never stopped on the stimuli. Instead, in at least 95% of the trials, the rats ran rather parallel to the stimuli without approaching the nose and hence the microvibrissae. We conclude that intact rats readily discriminate stimuli placed on their path using their whiskers. In addition, they can develop a new strategy if their whiskers are removed, probably based on tactile inputs from the skin either on the posterior part of the head or on the trunk.

Cortical inactivation reduces behavioral performance

We tested the effects of cortical inactivation by applying muscimol on the surface of the barrel cortex during the behavioral session using a custom-made bilateral implant. Performance decreased to chance level immediately at the start of the session even though, as for whisker-cutting experiments, maze navigation was normal and no ataxia could be detected (Sturgeon et al., 1979). Cortical inactivation was in fact even more effective than whisker cutting: in the first half of the sessions, the performance was lower after muscimol than after whisker cutting for each of the three rats tested in both (mean value 50.8% vs 60.6%), and the recovery took longer to occur (cf. average performance in middle session, Figs. 5B, 4A). This is not necessarily surprising because muscimol could have spread outside of the barrel cortex region, invading part of the trunk region juxtaposed next to it. This result strengthens the idea that the rats could use the skin of their trunk as an alternative strategy to using their whiskers.

Whisker contact on surfaces is tightly controlled throughout the discrimination

Whisking is a sampling strategy often displayed by rodents performing roughness discrimination and it can be adjusted quickly and accurately during tasks (Harvey et al., 2001; Voigts et al., 2015). Whisking has two main consequences that could be beneficial to surface perception: it allows the whiskers to contact the discriminanda several times before making a choice and it sets a particular speed of the whiskers on the scanned surface. We designed the task such that multiple sampling would not be favored because it would lengthen trials and thus prevent receiving rewards frequently. Indeed, in our protocol, the rats could be trained to perform the task at high running speed without stopping and coming back after first encountering the stimuli so that the whiskers contacted the surfaces only once during each trial. To confirm that this single contact event did not involve whisking, we first estimated its duration. The running speed of the animal was ~ 1 m/s. This value is at the higher end of the range of speeds observed on freely moving animals exploring surfaces, between 0.2 to 0.6 m/s (Carvell and Simons, 1990; Ritt et al., 2008; Grant et al., 2009) up to 1.2 m/s (Hobbs et al., 2015). The resulting whisker–stimulus contact duration, estimated at 86 ms, was too short to allow a whisking cycle. Second, we calculated the power spectrum of whisker movements and found no evidence for a peak in the whisking frequency band, but rather a gradual decrease in power as a function of frequency (Fig. 6). This is in contrast to a study by Jenks et al. (2010), who reported the presence of whisking in approximately one-third of trials while rats ran in a central alley. However, their animals were not trained to detect or discriminate stimuli and thus probably did not adopt a specific strategy regarding their whiskers. This is supported by the observation that, in contrast to our study, these animals did not

approach the stimuli with a specific whisker angle (Jenks et al., 2010).

We conclude that rats are able to discriminate surfaces without whisking, passing their whiskers on the stimuli only once in a continuous sweep while running in an alley. We propose that the main behavioral advantage of whisking may be to impose a whisker-on-stimulus contact speed in an optimal range to ensure an efficient transformation of the surface profile into mechanoreceptor activation patterns (Boubenec et al., 2014). The fast active movement of whisking would not be necessary anymore when the animal is running at an adequate speed along surfaces, as in our study. This hypothesis is compatible with other studies arguing for active control of the contact speed, including the recent report that whisker speed is kept constant under wind perturbations (Saraf-Sinik et al., 2015). In addition, it does not preclude a role of whisking for multiple sampling in more complex object recognition tasks.

Finally, we observed that the rats controlled precisely the position of their whiskers before contacting the stimuli and further oriented them as early as 60 ms after the first possible contact. This whisker movement was followed by a turn of the head toward the same side while the rat was leaving the stimuli. These results agree and extend the head-turning asymmetry process previously described in goal-directed (Towal and Hartmann 2006; Schroeder et al., 2016) and spontaneous exploratory (Mitchinson et al., 2007) behaviors of rats and mice, reflecting a stimulus-driven attentional process (Mitchinson et al., 2013).

References

- Bermejo R, Houben D, Zeigler HP (1998) Optoelectronic monitoring of individual whisker movements in rats. *J Neurosci Methods* 83:89–96. [CrossRef Medline](#)
- Boubenec Y, Clavier LN, Shulz DE, Debrégeas G (2014) An amplitude modulation/demodulation scheme for whisker-based texture perception. *J Neurosci* 34:10832–10843. [CrossRef Medline](#)
- Brecht M, Preilowski B, Merzenich MM (1997) Functional architecture of the mystacial vibrissae. *Behav Brain Res* 84:81–97. [CrossRef Medline](#)
- Carvell GE, Simons DJ (1990) Biometric analyses of vibrissal tactile discrimination in the rat. *J Neurosci* 10:2638–2648. [Medline](#)
- Carvell GE, Simons DJ (1995) Task- and subject-related differences in sensorimotor behavior during active touch. *Somatosens Mot Res* 12:1–9. [CrossRef Medline](#)
- Grant RA, Mitchinson B, Fox CW, Prescott TJ (2009) Active touch sensing in the rat: anticipatory and regulatory control of whisker movements during surface exploration. *J Neurophysiol* 101:862–874. [Medline](#)
- Guic-Robles E, Jenkins WM, Bravo H (1992) Vibrissal roughness discrimination is barrelcortex-dependent. *Behav Brain Res* 48:145–152. [CrossRef Medline](#)
- Harvey CD, Coen P, Tank DW (2012) Choice-specific sequences in parietal cortex during a virtual-navigation decision task. *Nature* 484:62–68. [CrossRef Medline](#)
- Harvey MA, Sachdev RN, Zeigler HP (2001) Cortical barrel field ablation and unconditioned whisking kinematics. *Somatosens Mot Res* 18:223–227. [CrossRef Medline](#)
- Higley MJ, Contreras D (2006) Balanced excitation and inhibition determine spike timing during frequency adaptation. *J Neurosci* 26:448–457. [CrossRef Medline](#)
- Hobbs JA, Towal RB, Hartmann MJ (2015) Spatiotemporal patterns of contact across the rat vibrissal array during exploratory behavior. *Front Behav Neurosci* 9:356. [CrossRef Medline](#)
- Hutson KA, Masterton RB (1986) The sensory contribution of a single vibrissa's cortical barrel. *J Neurophysiol* 56:1196–1223. [Medline](#)
- Jacob V, Estebanez L, Le Cam J, Tiercelin JY, Parra P, Parésys G, Shulz DE (2010) The Matrix: a new tool for probing the whisker-to-barrel system with natural stimuli. *J Neurosci Methods* 189:65–74. [CrossRef Medline](#)
- Jadhav SP, Feldman DE (2010) Texture coding in the whisker system. *Curr Opin Neurobiol* 20:313–318. [CrossRef Medline](#)
- Jenks RA, Vaziri A, Bolori AR, Stanley GB (2010) Self-motion and the

- shaping of sensory signals. *J Neurophysiol* 103:2195–2207. [CrossRef Medline](#)
- Johnson KO, Hsiao SS (1992) Neural mechanisms of tactual form and texture perception. *Annu Rev Neurosci* 15:227–250. [CrossRef Medline](#)
- Kleinfeld D, Ahissar E, Diamond ME (2006) Active sensation: insights from the rodent vibrissa sensorimotor system. *Curr Opin Neurobiol* 16:435–444. [CrossRef Medline](#)
- Krupa DJ, Matell MS, Brisben AJ, Oliveira LM, Nicoletis MA (2001) Behavioral properties of the trigeminal somatosensory system in rats performing whisker-dependent tactile discriminations. *J Neurosci* 21:5752–5763. [Medline](#)
- Kuruppath P, Gugig E, Azouz R (2014) Microvibrissae-based texture discrimination. *J Neurosci* 34:5115–5120. [CrossRef Medline](#)
- Mayrhofer JM, Skreb V, von der Behrens W, Musall S, Weber B, Haiss F (2013) Novel two-alternative forced choice paradigm for bilateral vibrotactile whisker frequency discrimination in head-fixed mice and rats. *J Neurophysiol* 109:273–284. [CrossRef Medline](#)
- Mitchinson B, Prescott TJ (2013) Whisker movements reveal spatial attention: a unified computational model of active sensing control in the rat. *PLoS Comput Biol* 9:e1003236. [CrossRef Medline](#)
- Mitchinson B, Martin CJ, Grant RA, Prescott TJ (2007) Feedback control in active sensing: rat exploratory whisking is modulated by environmental contact. *Proc Biol Sci* 274:1035–1041. [CrossRef Medline](#)
- Miyashita T, Feldman DE (2013) Behavioral detection of passive whisker stimuli requires somatosensory cortex. *Cereb Cortex* 23:1655–1662. [CrossRef Medline](#)
- Morita T, Kang H, Wolfe J, Jadhav SP, Feldman DE (2011) Psychometric curve and behavioral strategies for whisker-based texture discrimination in rats. *PLoS One* 6:e20437. [CrossRef Medline](#)
- O'Connor DH, Clack NG, Huber D, Komiyama T, Myers EW, Svoboda K (2010) Vibrissa-based object localization in head-fixed mice. *J Neurosci* 30:1947–1967. [CrossRef Medline](#)
- Paxinos G, Watson C (2009) *The rat brain in stereotaxic coordinates*, 6th ed. Amsterdam: Academic Press Elsevier.
- Ritt JT, Andermann ML, Moore CI (2008) Embodied information processing: vibrissa mechanics and texture features shape micromotions in actively sensing rats. *Neuron* 57:599–613. [CrossRef Medline](#)
- Sachidhanandam S, Sreenivasan V, Kyriakatos A, Kremer Y, Petersen CC (2013) Membrane potential correlates of sensory perception in mouse barrel cortex. *Nat Neurosci* 16:1671–1677. [CrossRef Medline](#)
- Saraf-Sinik I, Assa E, Ahissar E (2015) Motion makes sense: an adaptive motor-sensory strategy underlies the perception of object location in rats. *J Neurosci* 35:8777–8789. [CrossRef Medline](#)
- Schroeder JB, Ritt JT (2016) Selection of head and whisker coordination strategies during goal-oriented active touch. *J Neurophysiol* 115:1797–1809. [CrossRef Medline](#)
- Sturgeon RD, Fessler RG, Meltzer HY (1979) Behavioral rating scales for assessing phencyclidine-induced locomotor activity, stereotyped behavior and ataxia in rats. *Eur J Pharmacol* 59:169–179. [CrossRef Medline](#)
- Towal RB, Hartmann MJ (2006) Right-left asymmetries in the whisking behavior of rats anticipate head movements. *J Neurosci* 26:8838–8846. [CrossRef Medline](#)
- Voigts J, Herman DH, Celikel T (2015) Tactile object localization by anticipatory whisker motion. *J Neurophysiol* 113:620–632. [CrossRef Medline](#)
- von Heimendahl M, Itskov PM, Arabzadeh E, Diamond ME (2007) Neuronal activity in rat barrel cortex underlying texture discrimination. *PLoS Biol* 5:e305. [CrossRef Medline](#)
- Zuo Y, Perkon I, Diamond ME (2011) Whisking and whisker kinematics during a texture classification task. *Philos Trans R Soc Lond B Biol Sci* 366:3058–3069. [CrossRef Medline](#)

1.4.2. Additional unpublished results

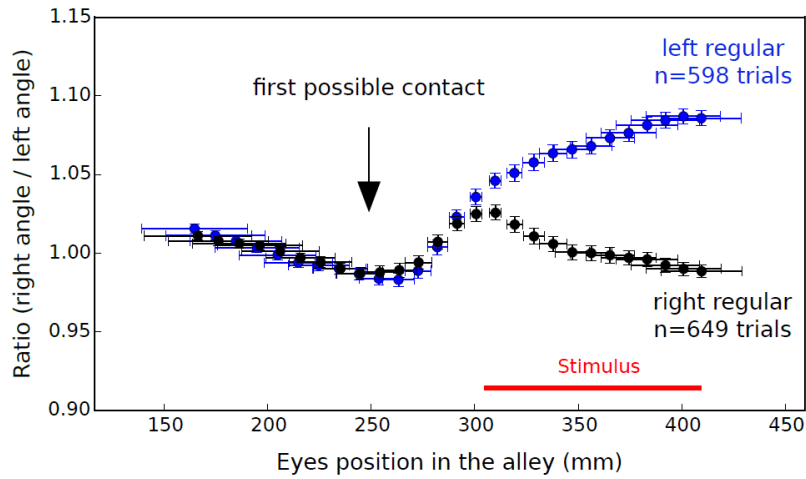
In this section, we report a few observations which were not included in the article for lack of space.

1.4.2.1. Increased retraction is not due to contact with the rougher stimulus

One possible explanation for the increased retraction on the side of regular series during successful trials, displayed on Figure 7 of the manuscript, could be that whiskers are passively pushed backward by the rougher stimulus. If this hypothesis were correct, then we should observe the same effect during failed trials. Figure 11 shows the average results for three rats during successful (top panel) and failed (lower panel) trials. We found a tendency for an opposite shift during failed trials, that is, excess retraction on the smooth side. In other words, the rats tended to orient their whiskers to the side which they were about to choose for the turn at the end of the alley. However, this effect was transient, so that by the end of the stimulus, the curves were joining, which was quite surprising. Note that because the number of failed trials was much lower than successful trials (n = 378 failed trials vs. 1247 successful trials), the statistical power was diminished. The only difference between the two conditions, is that the whiskers are turning towards a rewarded (regular) or a non rewarded stimulus (smooth). In both cases, the rat is turning towards the side the whiskers are orienting. Thus, we can hypothesize that the sustained separation in ratio values observed in successful trials, and not in failed trials, is due to the rewarded/non rewarded state of the stimulus, and that it is maybe driven by attention.

We conclude that the whisker asymmetry which we observed in the task is not due to the physical surfaces, but to a goal-directed behavior of the animal.

Successful trials



Failed trials

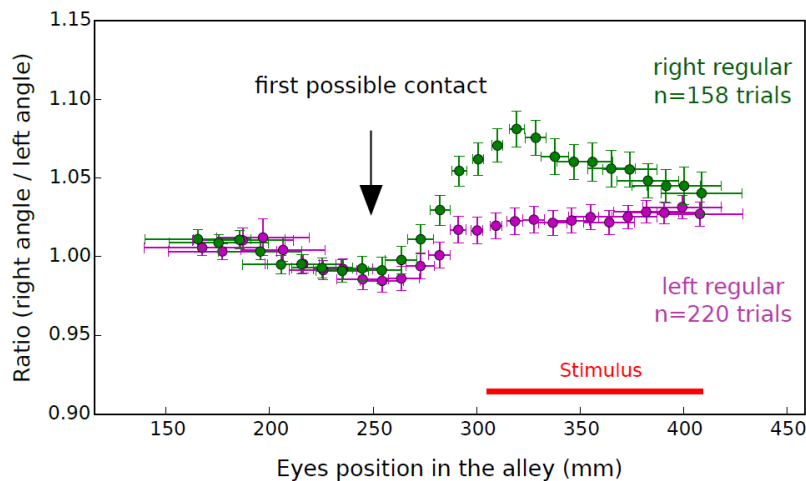


Figure 11: Increased retraction is not due to contact with the rougher stimulus

Mean (\pm SEM) whisker angle ratio (right / left) plotted as a function of the rat's eyes position in the central alley ($n = 3$ rats). Angle ratios have been divided by their baseline value before averaging across animals.

Top panel, the blue and black legends indicate the side of the regular (rewarded) series, and the rat systematically turned the same side from the regular series ("successful trials"). Lower panel: the green and pink legends indicate the side of the regular (rewarded) series, and the rat systematically turned the opposite side from the regular series ("failed trials").

1.4.2.2. Inactivation of the primary somatosensory cortex

To check the correct positioning of our implant and craniotomies above S1 (Figure 12A), we inserted a thin electrode covered with Dil in the cortex at the end of the experiments (Figure 12C). Histology confirmed that the implant designed for inactivation was indeed located above the barrel field region of S1 (S1BF, Figure 12B). In addition, Figure 12C shows the full time course of inactivation experiments on one rat. We repeated bilateral cortical inactivation twice and observed a significant decrease in performance of the task for the two muscimol sessions (Figure 12C).

1.4.2.3. Reminders are needed for learning the task

In the final protocol of the discrimination task, rats were trained in several phases, some of which included the presentation of reminders (copies of the rewarded surfaces) between the stimuli and the reward port. Before designing this protocol, we had tried to have rats learn the task without these reminders. During these preliminary experiments, rats were first trained on the detection of the regular series, meaning that there was no smooth surface facing the regular series. The idea was to introduce the smooth surface after the animals had already learnt the detection of the regular series. We helped the animals by 1) introducing some guided trials (with only one door open at the end of the alley) at the beginning of the session and 2) repeating at trial (n) the same stimulus than the one displayed at trial (n-1) if the rat failed consecutively for three trials before trial (n). On Figure 13, the performance of the animals is shown for 22 sessions for animals trained on this detection task with helped trials (grey line) or on the discrimination task with reminders (black line, data from the article). We can see that rats trained with reminders were almost always better than the other group throughout the 22 sessions. Moreover, the animals trained without the reminders kept a performance at chance level, whereas the animals trained with the reminders stabilized their performance at a significantly higher level (above 60%, $P < 0.05$, Wilcoxon test) after the 15th session.

These results suggest that the discrimination between the regular series and smooth surface is a difficult task to learn for the animals. This was surprising to us, given the remarkable abilities described in the literature (Carvell & Simons 1990). We hypothesized that an

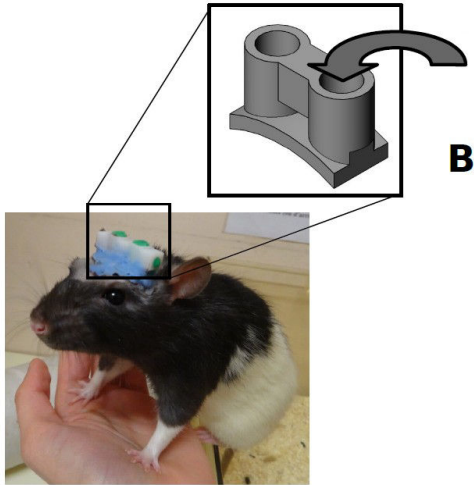
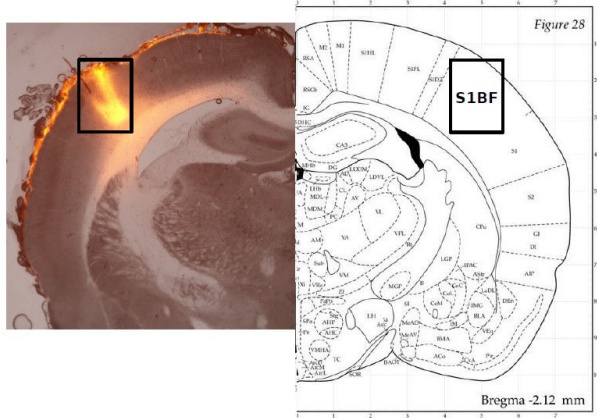
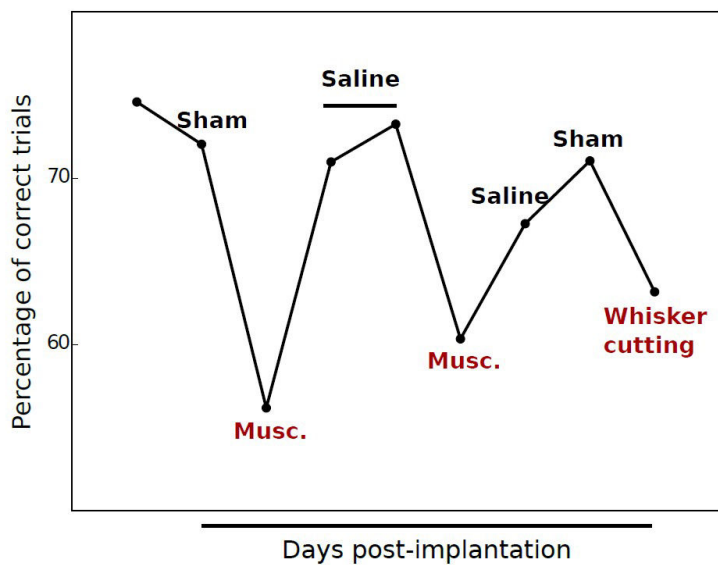
A**B****C**

Figure 12: Repeated inactivations of the primary somatosensory cortex

A: Picture of an implanted rat and structure of the implant designed in SolidWorks.

B: Plot of the behavioral performance (percentage of correct trials) as a function of the training sessions, during muscimol and control (saline or sham) sessions. During sham control sessions, the rats were not anesthetized and no solution was added in the implant reservoirs.

C: Coronal slice of the rat with Dil (yellow labelling) in the S1 Barrel Field (S1BF).

important source of variability could be the lack of spatial and temporal proximity between the stimuli and the reward. Thus, we set reminders of the rewarded stimulus in the learning protocol, as previously described in a visual task (Harvey et al. 2012).

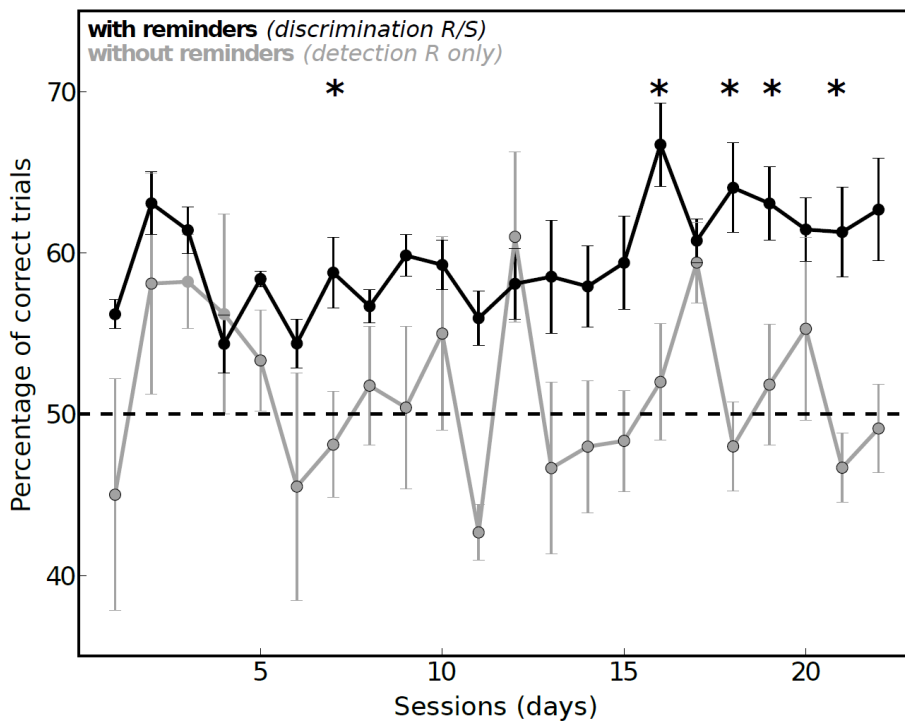


Figure 13: Reminders are needed for learning

Learning curves of the detection of the regular series (grey, $n=5$ rats, mean \pm SEM) and the discrimination of regular series/smooth surface (black, $n=5$ rats, mean \pm SEM) after training respectively without and with reminders of the regular series. The reminders were placed at the end of the alley and at the reward sites, as indicated in Figure 1 of the article. The dashed line indicates the chance level.

*: significant difference, $P < 0.05$, Wilcoxon test.

1.4.3. Discussion

1.4.3.1. No whisking: which consequences for the sensori-motor closed loop?

When rodents discriminate between stimuli placed in an arena, they typically whisk several times before making a choice. The speed and amplitude of the whisker movements can be adjusted from one whisking cycle to the next. This process is an example supporting the sensori-motor closed-loop hypothesis (see 1.3.). The speed of the whisker movement is not only a parameter that can be modulated to achieve good performance levels through learning (Harvey et al. 2001), but it is also a parameter that is kept unchanged under perturbing conditions, such as wind, after rats have learnt a localization task (Saraf-Sinik et al. 2015). The whisker speed parameter is stabilized at the cost of stability loss for other motor-related parameters, for instance head position or protraction and retraction amplitude. Along with the data presented in 1.3., this highlights the critical role of vibrissa angular speed during surface discrimination and spatial localization. In our study, there is no whisking and we can consider the whisker angular speed as negligible compared to the locomotion speed (0.03 mm/ms vs. 1 mm/ms). Consequently, we propose that locomotion can be a regulated motor output of the loop, to sweep the whiskers at a controlled velocity and achieve good performance levels in the discrimination task. This hypothesis is particularly relevant in our case, since locomotion speed shapes the temporal frequency of the whisker movement when brushed against a series of vertical bars (Jenks et al. 2010). We can also note that our behavioral configuration allows to test discrimination abilities of rodents at higher speed of scanning than with the whisking configuration. Indeed, whisking speed has been reported to be ~ 600 °/s (Carvell & Simons 1995), so the whisker is spanning an angle $\alpha = 0.6^\circ$ per ms. If we consider that the rat is at a distance where C2 can touch the stimulus, for instance $d_1 = 30$ mm (see Table 1), then the distance d_2 covered by the whisker when spanning 0.6° is: $d_2 = \tan(\alpha) \cdot d_1 = 0.3$ mm. Thus, the linear speed of the whisker during whisking is about 0.3 mm/ms, which is three times lower than the whisker speed (equal to the running speed) of about 1 mm/ms in our conditions.

Even though whisking as an oscillatory rhythm is not involved in the task, we would like to stress that the vibrissae are actively positioned during the discrimination process, since

retraction is stopped for 40-50ms at the beginning of contact (Figure 7 of Kerekes et al., 2017). Interestingly, this duration corresponds to the time range of sustained contact established by freely-moving rats when they whisk on an object (25-60ms, Hobbs et al. 2015). In our study, this period of stabilization of the whisker angle was directly followed by the orientation of the whisker arrays towards the rewarded stimulus, that is reflecting the rat's choice at every trial. Thus, we can hypothesize that this period of active positioning is also a motor strategy to improve the tactile signal acquisition and treatment.

1.4.3.2. Involvement of whiskers during discrimination

In the publication, we reported that after whisker cutting, the performance decreased at the beginning of the test session and then increased back to an intermediate level of performance. This indicates that the animals probably found an alternative strategy to partially solve the task. By tracking the head position and orientation, we concluded that discrimination could not involve the microvibrissae or the skin of the snout. However, the skin on the head posterior to the whisker pad as well as on the rest of the body could be involved. A change in the peripheral input entry is the only possible alternative for solving the task after whisker cutting, and we thus conclude that the performance after whisker cutting is probably rescued by trunk somatosensation.

1.4.3.3. Involvement of the primary somatosensory cortex during discrimination

Similarly to the whisker cutting experiment, inactivation of the primary somatosensory cortex led to a decrease followed by an increase in performance level throughout the test session. Tracking of the head position and orientation suggested that microvibrissae or snout skin can not account for the performance rescue. One can imagine that tactile signals are transmitted from the whiskers to a central pathway independent of the cortex. The superior colliculus is one of the sub-cortical structures involved in tactile sensori-motor processes in the rat (Hemelt & Keller 2008). This area contains neurons that not only respond to vibrissa movement, but that can also be tuned for a particular angle during deflection (Hemelt & Keller 2007). More interestingly, if the vibrissa is brushed against textures with different roughness levels, whisker-responding neurons in the superior colliculus fire significantly more for rougher surfaces (Bezudnaya & Castro-Alamancos 2011). In this work, the grain

diameter of the rougher and smoother stimuli is around 270 μm and 16 μm , respectively. These results show that neurons in the superior colliculus can report differences in grain size of about 250 μm , which is ten times lower than the thickness of the bars in our protocol. Therefore, we can hypothesize that, during cortical activity blockade, a parallel path involving the superior colliculus may participate in the rescue of behavioral performance. We can however note that most of the tactile tasks in rodents, such as spatial location (Krupa et al. 2001) (O'Connor et al. 2010), detection of tactile stimuli (Miyashita & Feldman 2013), and sandpaper discrimination (Guic-Robles et al. 1992), are cortex dependent. Some tactile tasks involving negative reinforcement during learning are cortex-independent (Hutson & Masterton 1986; Cohen & Castro-Alamancos 2007), and it has been proposed that the cortex would not be necessary in such negatively-reinforced tasks (Miyashita & Feldman 2013). The causal link between reinforcement value and cortex involvement in the task is nevertheless challenged by recent studies demonstrating the necessity of pyramidal cortical neurons activity for auditory fear learning (Letzkus et al. 2011), as well as important changes in the connectivity between cortical layers during tactile fear learning (Rosselet et al. 2011). These results could suggest that cortical activity is required during sensory learning of fear conditioning, but then becomes unnecessary once the task is learnt. To conclude, we can raise at least two hypotheses to explain the partial spontaneous performance rescue after cortical inactivation during our task: either the tactile input is transmitted from the head or trunk skin, and can then be treated by a part of the somatosensory cortex unrelated to the whiskers, or the input is transmitted from the whiskers to subcortical structures such as the superior colliculus. The fact that cortical inactivation tended to be more efficient than whisker cutting in decreasing task performance suggests that the first hypothesis could be the right one. To answer these questions, we could either inactivate the whisker- and trunk-related parts of the somatosensory cortex, or inactivate the superior colliculus. To gain in precision regarding the spatial extent of the inactivation, we could for instance use channelrhodopsin selectively expressed in inhibitory neurons and combined with a fluorescent protein (Sreenivasan et al. 2016).

1.4.3.4. Towards discrimination of tactile regularity?

In our study, we performed acute test sessions to assess whether rats are able to perceive the difference between regular (R) and irregular series (I) of bars. We designed five types of irregular series, all containing eighteen bars, that could be perceived as intermediate stimuli between the smooth surface and the regular series (Figure 3A of the publication). The irregular series included a maximal interval size between two consecutive bars of either 13, 30, 40, 48 or 50 mm, and are respectively named I13, I30, I40, I48, I50. We hypothesized that this wide smooth interval would be a feature similar to the smooth stimulus, and consequently that the wider this interval, the more easily the rats could discriminate the irregular series from the regular series. From the results we obtained, we inferred that the animals may associate only the presence of the bars to the reward, and not the fact that these bars are displayed regularly. If this hypothesis were correct, then the smooth stimulus might not be the best geometry to start with in order to achieve the regular/irregular discrimination. One possibility could be to start learning with the R vs. I40 combination with the additional two reminders. Once the rats are able to discriminate the two stimuli with no reminder, then the 40-mm wide interval could be progressively reduced. Indeed, we found that half of the rats performed above chance level during the acute R vs. I40 discrimination test, and that increasing the maximal interval size to 48 and 50mm increased the task performance. Therefore, the maximal interval constitutes a shared feature between the irregular series and the smooth surface, and may offer the opportunity to lead the rats to discriminate truly the regularity of series of bars, rather than only the presence or absence of bars on a surface.

II. Neuronal coding of tactile inputs by the whisker system

In this second part of the thesis, we will first focus on a general review of the literature on neuronal encoding of tactile inputs, in particular during sensory discrimination of object location and texture. Afterwards, we will present and discuss an ongoing project on the analysis of whisker deflections and neuronal responses evoked by the stimuli passing on the whiskers as during the task.

II.1. From the whiskers to the cortex

The purpose of this section is to give an overview of the different whisker-to-cortex pathways involved in sensori-motor processes. These pathways notably differ by their neurons receptive field size, by the thalamic nuclei involved, and by the connectivity established between the thalamo-cortical loop and other cortical areas such as the primary motor cortex. The strength of the connectivity between sensory and motor areas shapes behavior during tactile tasks, and the different pathways have been proposed to have complementary functional roles during such processes (Yu et al. 2006).

II.1.1. General introduction on whisker-to-cortex pathways

The mechanical deflection of a single whisker on the rat's snout first leads to emission of action potentials in a group of neurons of the trigeminal ganglion through the infraorbital nerve. This mechano-electrical transduction is operated by mechanoreceptors in the whisker follicle: the follicle inner elements are stretched or pressed upon, receptors are opened and a depolarizing ionic flux is established through the membrane. The information received by the TG neurons is then transmitted to the central nervous system by several sensory pathways (Figure 14 and also Figure 17, for review, see (Deschênes et al. 1998; Bosman et al. 2011)). The major pathway, called the lemniscal pathway, starts from the trigeminal ganglion and involves successively the trigeminal nucleus principalis (Pr5) in the brainstem, the ventro-postero-medial (VPM) nucleus of the thalamus and finally the primary somatosensory cortex (S1), which is the first cortical stage of tactile information integration. Two other routes, the para-lemniscal and the extra-lemniscal pathways, involve different areas at the brainstem, thalamic and cortical levels and are thus thought to carry out different information, albeit

overlapping, than the lemniscal pathway. Throughout the subsequent description of the different paths from the whiskers to the cortex, we will refer as «wS1» to the part of the somatosensory cortex specifically associated with the whiskers. Note that, as spatial areas in the primary motor cortex are predominantly dedicated to the movement of particular parts of the body (see I.3.2.3), every somato-sensitive part of the body is linked to a defined area within S1.

II.1.2. The lemniscal pathway

II.1.2.1. Somatotopy and definition of the principal whisker

Throughout the lemniscal pathway, the tactile information is received and processed in remarkable anatomo-functional structures named barrelettes in the principal nucleus 5 (Pr5) of the brainstem, barreloids in the dorso-medial part of the VPM (VPMdm) and barrels in wS1 (Woolsey & Van der Loos 1970). Notably, there is a strict topographic correspondence between the maps of whiskers, barrelettes, barreloids and barrels, which is called somatotopy (Figure 14, Deschênes et al. 1998). There are barrels only in layer 4, but we can define barrel-related regions in other layers: they correspond to the regions of the cortical column above and below the barrel. We call "septa" the regions between the well-defined barrels. Due to this strict somatotopy, the canonical description of the system is that of a "labeled line", where one whisker connects preferentially neurons of one barrel in the cortex. Deflection of this whisker, which we may call the "anatomical principal whisker", triggers action potentials with a high probability and short latency down to 7 ms in cortical neurons (Simons 1985). However, despite this dedicated line from one whisker to one barrel, neurons from the PrV, VPM and barrel cortex can also significantly respond to whiskers adjacent to the principal one, though with a higher latency and less action potentials (Brecht & Sakmann 2002; Moore & Nelson 1998). Besides the anatomical principal whisker, defined by the barrel the recorded neuron belongs to, we can define a functional principal whisker that corresponds to the whisker evoking the most action potentials with the lowest latency. Although they usually match, in some cases, anatomical and functional principal whisker may not be the same. For instance, Le Cam and colleagues (2011) found that according to the direction of the stimulation (caudal or rostral), the identity of the functional principal whisker

can change. For example, a single neuron in layer 4 of barrel C2 may show the strongest response for whisker C3 in the rostral direction and for whisker C2 in the opposite direction. Despite this complexity, there is usually good agreement between the anatomy and function so that most of studies refer to « the principal whisker » of a neuron defined functionally.

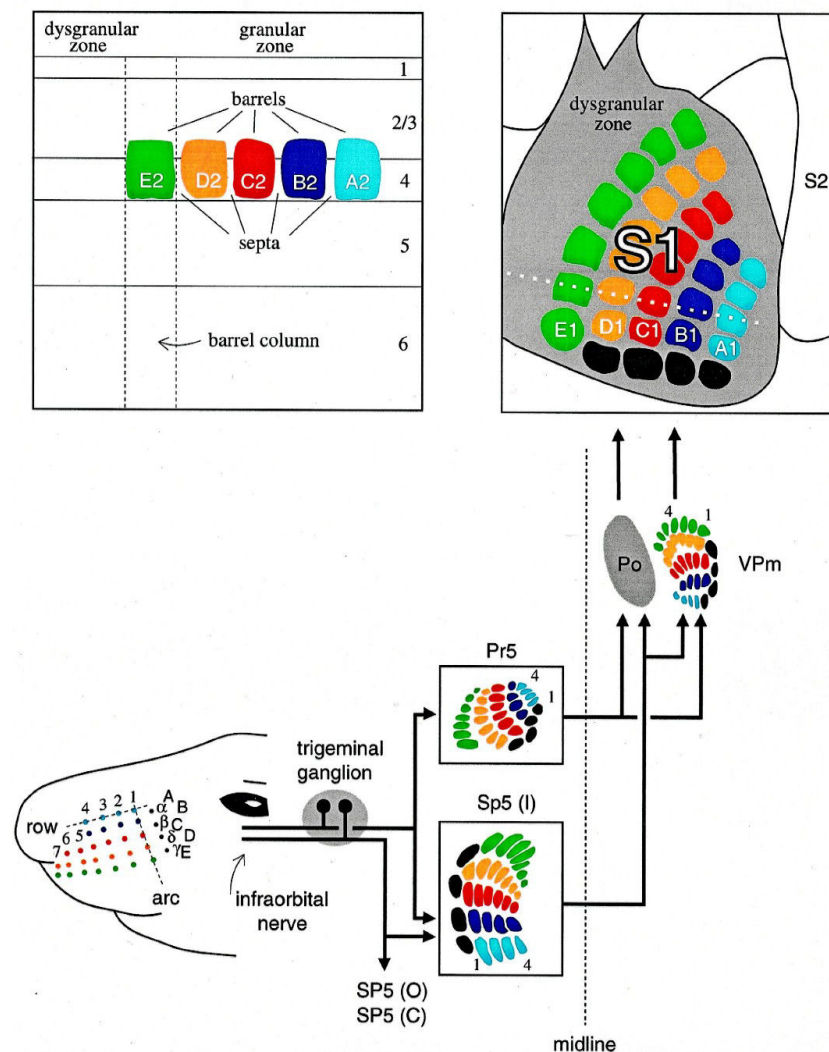


Figure 14: From the whiskers to the cortex

Schematic summary of the vibrissal sensory system of the rat. The whisker array on the snout is represented centrally by arrays of cellular aggregates in the brainstem PR5 and SP5i, thalamus VPm and PoM. and somatosensory cortex S1. The upper left hand frame shows the layout of cortical barrels in a frontal section passing through the second arc of barrels. Abbreviations: SP5O spinal trigeminal nucleus pars oralis, SP5C spinal trigeminal nucleus pars caudalis and S2 second somatosensory area. From Deschênes et al., 1998.

II.1.2.2. Beyond the dedicated labeled line: multi-whisker integration

In the barrel cortex, the response to the principal whisker can be facilitated or suppressed by the simultaneous deflection of one of the adjacent whiskers (Brumberg et al. 1996) (Ego-Stengel et al. 2005). This phenomenon depends notably on the type of recorded neuron (regular or fast spiking cell), the frequency of stimulation and the position (along the rostro-caudal and the dorso-ventral axis) of the adjacent whisker relative to the principal one. In order to study the functional properties of receptive fields in the whisker system, a stimulation matrix composed of 24 independent piezo-actuators has been built in the laboratory (Jacob et al. 2010). Using this device, it has been reported that around two thirds of neurons have a multi-whisker receptive field in the rat (Le Cam et al. 2011). Moreover, single cortical neurons can encode global properties of multi-whisker stimuli (Jacob et al. 2008)(Estebanez et al. 2012) levels of the lemniscal pathway. For example, neurons in the center of barrels are tuned to different multi-whiskers stimulations compared to those located at the barrel/septum border (Estebanez et al. 2016). In this study, applying uncorrelated stimuli between the principal whisker and the other whiskers of the pad elicited the strongest responses in the barrel center. On the contrary, applying correlated stimuli resulted in strongest responses at the barrel/septum border. Another study in the laboratory (Vilarchao et al., under revision), showed that rostral barrels in the mouse are more tuned to detect global motion of multi-whisker stimuli in the caudo-ventral direction.

This multi-whisker integration of tactile inputs probably arises from feedforward connections between the different pathways and from horizontal connections at the different levels (Lavallée & Deschênes 2004).

II.1.2.3. Two pathways through dorso-medial VPM

Within the VPMdm, anatomical and functional differences were also described along the dorso-ventral axis. Indeed, the dorsal-most area of the VPMdm (VPMdm « head ») contains neurons with multi-whisker receptive fields, and is thought to be contacted by multi-whisker receptive field neurons from the Pr5 (Urbain & Deschênes 2007a) (Veinante & Deschênes 1999). On the contrary, neurons from the more ventral part of the VPMdm respond predominantly to single whiskers, and are connected by Pr5 neurons displaying the same

activation properties. In addition, the head of VPMdm is anatomically connected by M1 (Urbain & Deschênes 2007a), and this connection could be involved in the coding of whisking movement by VPM cells (Yu et al. 2006; Urbain et al. 2015). The differences between the two regions also extend to the type of thalamo-cortical connections, since the head and the ventral section of VPMdm respectively connect the septa (Furuta et al. 2009) and barrel structures of the cortex. This additional disparity in targeted cortical regions reinforces the idea that there are two different lemniscal pathways, one passing through the dorsal-most part of the VPMdm, encoding multi-whisker touch signals as well as whisker movement, and another one connecting individual barrels and encoding single whisker touch signals.

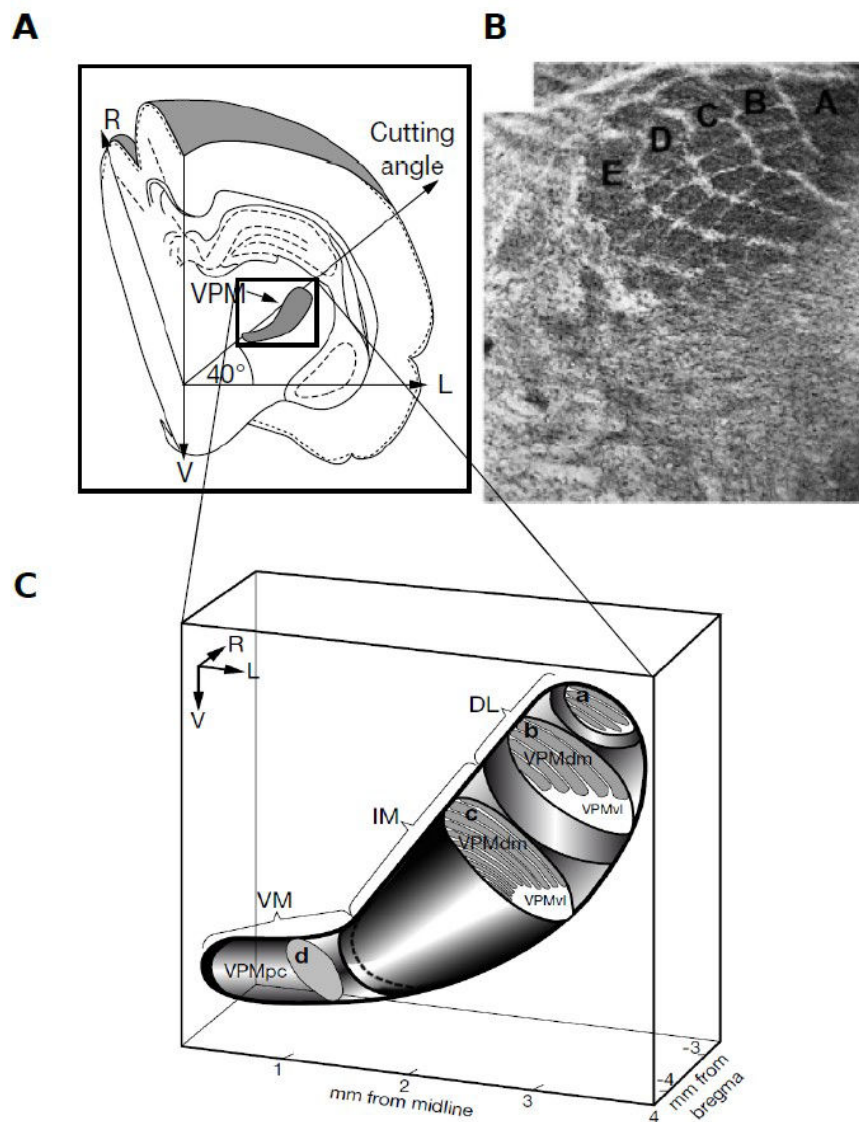


Figure 15: Map and individual structure of barreloids in the thalamus

A: Schematic drawing showing the VPM nucleus location in the rat brain and the optimized for barreloid visualization cutting plane.

B: Example slice cut along the plane shown in A, where the barreloid map is visible. Letters A-E indicate the rows locations.

C: Three-dimensional model of the intrinsic organization of the rat VPM. DL, the dorsolateral portion, which contains large barreloids that represent four straddlers (section a) and five rows of mystacial vibrissae (section b). IM, the intermediate portion, which contains multiple thin barreloids (section c). VM, ventromedial portion. The border of the VPM is depicted by a thick solid line. The thick dotted line separates the IM portion from the VM. a, b, c, and d are schematic oblique cutting planes through the VPM. L, lateral; R, rostral; V, ventral.

Adapted from Haidarliu et al., 2008.

II.1.3. The extra-lemniscal pathway

In the tactile thalamus, the VPM nucleus can be subdivided in two components along the length of the barreloids: a dorso-medial (VPMdm) and a ventro-lateral (VPMvl) part (Figure 15, Haidarliu et al. 2008; Pierret et al. 2000). Each barreloid is defined by a core section belonging to the VPMdm and a tail belonging to the VPMvl.

Barreloid structures within the VPM are, similarly to cortical barrels, anatomo-functional clusters of neurons that form a thalamic topographical copy of the whisker map. As described previously in II.1.2.2, each VPM barreloid is composed of a core part in the VPMdm and a tail part in the VPMvl. The barreloid tails have less well-defined contours than the core part, notably due to the fact that the density of cells is lower (Pierret et al. 2000) and cytochrome oxydase labelling is thus less homogenous. Nonetheless, they appear as thin strips in brain coronal slices (Haidarliu et al. 2008). Besides anatomical studies, functional analysis has shown that the core and tail of each barreloid are connected by different brainstem nuclei and target different cortical areas. The tail of the barreloids is connected by the interpolaris spinal nucleus (Sp5i) located in the brainstem (Bokor et al. 2008) and targets barrel cortex septa as well as secondary somatosensory cortex (S2) neurons (Pierret et al. 2000). Neurons from Pr5 projecting to VPMPvl were also observed by retro-tracing techniques along the thalamo-trigeminal pathway, however specific lesions of Pr5 do not inhibit VPMvl responses to tactile stimulation (Bokor et al. 2008). Similarly to the receptive fields described in the dorsal-most part of the VPMdm, individual neurons in VPMvl significantly respond to the deflection of several whiskers (Bokor et al. 2008); (Urbain & Deschênes 2007a). Electrophysiological recordings during artificial whisking (elicited by stimulation of the facial nerve) showed that VPMvl, and thus the extralemniscal pathway, is coding for touch responses rather than for free whisking movements in air (Yu et al. 2006).

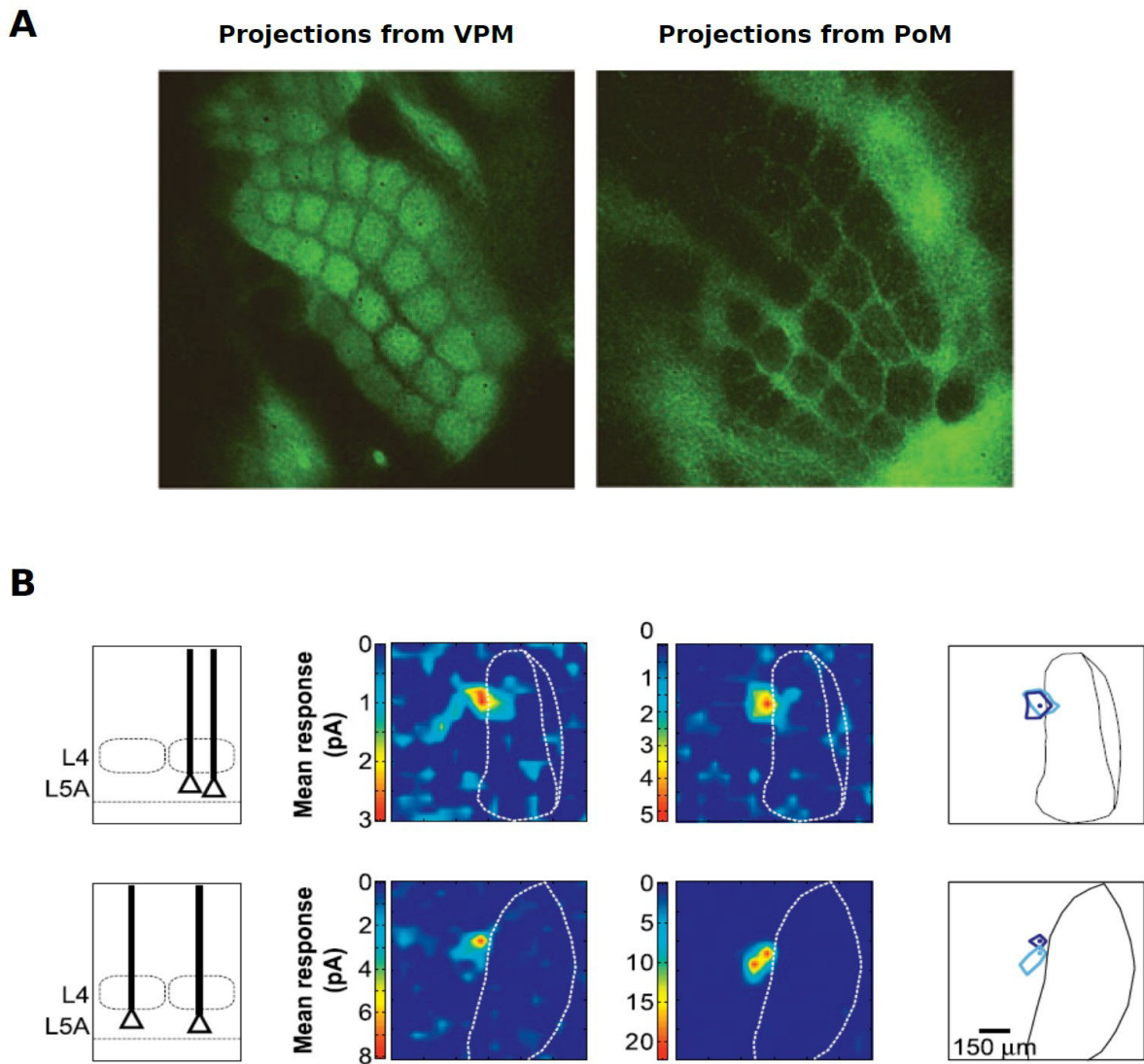


Figure 16: Thalamo-cortical projections in the paralemniscal and lemniscal pathways

A: Tangential slices showing anterograde labelling from the VPM thalamus (left) and from the PoM thalamus (right) to the cortical barrels and septa, respectively. Adapted from Wimmer et al., 2010.

B: Schematic of the locations of recorded neurons in the cortex (left), input domain maps in the thalamus (middle), and overlaid input domains in the thalamus (right). Circles in the input domains indicate the largest responses from a pair of L5A cells in the same column (first row) and a pair of L5A cells in neighboring columns (second row). From Bureau et al., 2006.

II.1.4. The paralemniscal pathway

Through the paralemniscal pathway, tactile inputs are conveyed from a rostral section of SP5i to a thalamic postero-medial nucleus (PoM) relative to VPM (Veinante et al. 2000). Similarly to VPMvl in the extralemniscal pathway, neurons in PoM connect wS1 septal regions (Wimmer et al. 2010) and the S2 area (Koralek et al. 1988). On Figure 16A, anterograde labellings from VPM (left panel) and PoM (right panel) are shown in the barrel cortex. These histological results show that VPM and PoM cells respectively target barrel and septal region of the cortex. In addition, PoM and M1 are reciprocally connected (Urbain & Deschênes 2007a)(Hooks et al. 2013).

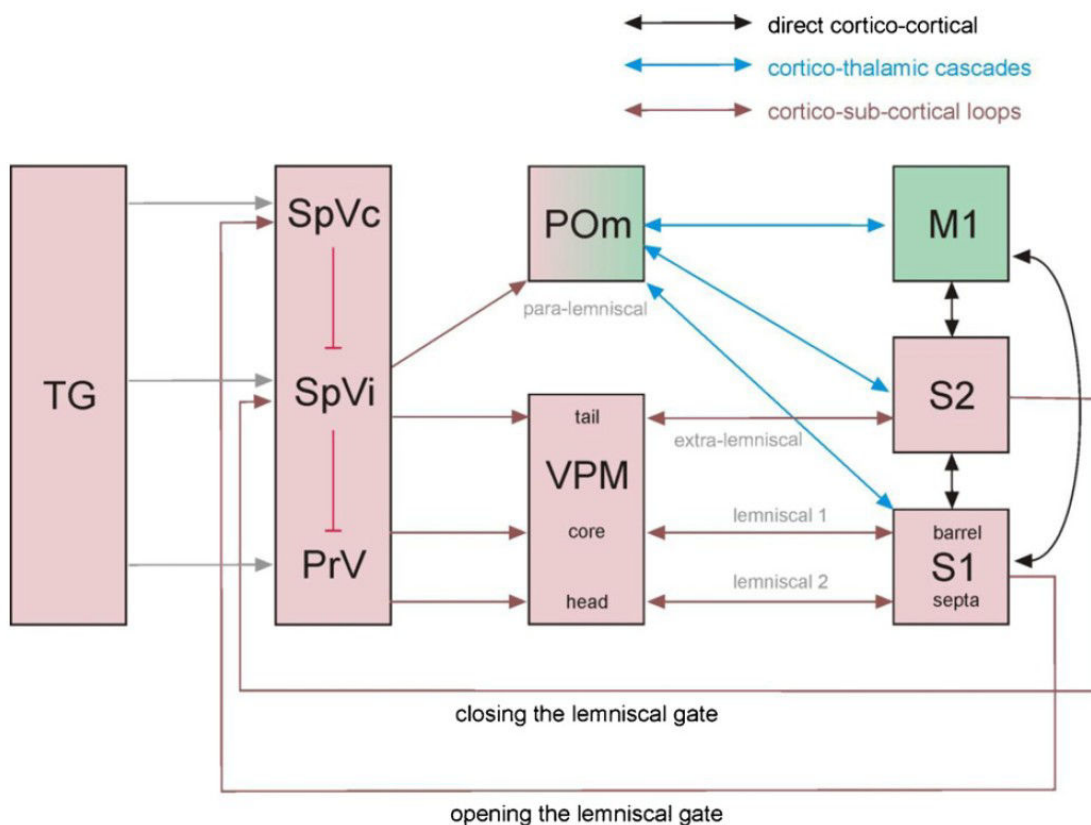


Figure 17: Summary of the cerebral structures involved in processing whisker information

From Feldmeyer et al. (2013)

This functional loop could play a role in whisker movement coding during whisking in air (Yu et al. 2006), even though encoding of whisker movement is performed less reliably than through the lemniscal pathway (Moore et al. 2015). Contrary to VPM, there are no barreloid structures described in the PoM. However, neurons from neighboring barrel-related columns in wS1 receive inputs from neighboring zones in the PoM, whereas neurons from the same barrel-related column receive inputs from superposed regions in PoM (Figure 16B, Bureau et al. (2006)). Moreover, the spacing between thalamic regions projecting to neighboring cortical barrels is similar between VPM and PoM (Bureau et al. 2006). This suggests that there is probably a representation of the whisker map at the level of the PoM, though it is not as precise as the barreloids map in the VPM. Studies of the lemniscal pathway brought the idea that the existence of a neuronal map of the whiskers does not necessarily imply that neurons' receptive fields are restrained to a single whisker. Similarly, extra- and intra-cellular recordings in the PoM revealed that neurons respond to several whiskers, and that receptive field sizes are also larger than those observed in the VPM (Chiaia et al. 1991). This broad receptive field property is shared by sensory cortical targets of PoM neurons (Jouhanneau et al. 2014)(Kwegyir-Afful & Keller 2004). In particular, PoM neurons and their target S2 cells respond with an equal maximal strength to several whiskers (Kwegyir-Afful & Keller 2004).

II.1.5. Further insights into the thalamo-cortical loops.

II.1.5.1. Connections within the loops.

In sections II.1.2 to II.1.4, we showed that the four different pathways described in the literature from whiskers to cortex involved both different input regions from the brainstem, different thalamic nuclei and different cortical targets (septal or barrel areas in wS1 ; S2 or M1, Figure 17). Besides these observations, wS1 layers targeted through lemniscal and paralemniscal pathways critically differ. Indeed, *in vivo* and *in vitro* analysis revealed that VPM neurons contact layer 4 (L4), L5B and L6A, whereas PoM first contacts L5A neurons (Constantinople & Bruno 2013; Bureau et al. 2006). In the lemniscal pathway, L4 then connects upper layers of the same barrel-related column, whereas through the paralemniscal pathway L5A connects directly upper layers neurons in several barrel-related columns (Bureau et al. 2006). From upper layers L2/3, evoked inputs are driven to infragranular layers.

Thus, according to the pathway, considered thalamorecipient layers differ and the connections from these thalamorecipient layers to upper layers spreads more across columns for the paralemniscal pathway. This observation goes along with the multi-whisker receptive fields described in the paralemniscal pathway. The dynamics of connections between layers impacts responses properties (magnitude, duration, latency) of cortical neurons. For instance, in behaving mice, whisker touch elicits responses with a lower amplitude and longer latency in L2 than in L3 (Crochet et al. 2011), and this could be likely due to the direct connection from thalamorecipient layers L4 and L5A onto L3. Note that the particular sequence of layer activation we describe here, with thalamorecipient cells activated first, followed by upper and then lower layers activation, is observed after a stimulus onset. This sequence is modified during spontaneous activity (Sakata & Harris 2009). Indeed, while evoked activity first emerges mainly in L4 and then spreads to supragranular and infragranular layers, spontaneous events arise in infragranular layers and then propagate up in the cortex.

In return, the thalamo-cortical loop is characterized by a strong feedback from cortical to thalamic neurons. In the lemniscal pathway, L6 establishes a large glutamatergic projections back to the VPM, involving metabotropic and ionotropic glutamatergic receptors (Alitto & Usrey 2003). In the paralemniscal pathway, L5 innervates the PoM nucleus back (Groh et al. 2013).

To conclude, the pattern of reciprocal connections between the thalamus and the cortex varies according to the pathway involved (lemniscal or paralemniscal). In particular, the cortical input and output layers differ in the two cases. Further, we can ask to what extent the activity of the cortex impacts the sensory evoked responses of the thalamus, and conversely. This question underlies the concept of first and higher order nuclei of the thalamus, described in the following section.

II.1.5.2. First and Higher-Order nuclei in the thalamus.

Sensory thalamic nuclei receive inputs from deeper layers of the sensory cortex and peripheral inputs through the trigeminal nuclei. The literature defines higher-order thalamic cells, which are primarily driven by cortical inputs, and first-order thalamic cells, whose activity is driven by peripheral inputs. In the literature, VPM has been proposed to be a first-

order nucleus, since VPM responses to whisker movements are not suppressed by cortical inactivation (Diamond et al. 1992). Excitatory connections from L6 cortico-thalamic neurons are thus not necessary to evoke VPM cells activity, and are described as «modulatory» and not «driver» inputs (Sherman 2016). For instance, enhancement of a barrel-related column facilitates and suppresses evoked activity in homologous and neighboring barreloids respectively (Temereanca & Simons 2004), and sharpens the direction tuning of VPM neurons sharing the same selectivity (Li & Ebner 2007). This demonstrates that cortical feedback modulates VPM receptive fields. On the contrary, PoM responses to whisker touch are dependent on cortical activity, and are thus characterized as higher order cells (Diamond et al. 1992). In this latter study, the authors furthermore showed that the mean latency to evoke a response by peripheral stimulation is about 7 ms in the VPM compared to 19 ms in the PoM. Since the mean latency of cortical responses is around 10-15 ms, the authors conclude that the cortex has been activated before the PoM, and possibly drove PoM activity. Besides this result, functional studies have shown that a proportion of PoM single cells only respond to L5 activation (Mease et al. 2016a), and not to peripheral inputs. Note that this is only a fraction of the PoM cells, and that other single cells are connected by both cortical and peripheral inputs (Groh et al. 2013), through the paralemniscal pathway. Besides cortico-thalamic feedback, thalamo-cortical feedforward connections impact both evoked (Mease et al. 2016b) and spontaneous activity (Poulet et al. 2012) of the cortex. Overall, the tight and reciprocal communication between cortical and thalamic cells highlights the importance of thalamic activity in the cortical treatment of tactile information.

II.1.5.3. Regulation of the loop activity.

The thalamus has been defined as a structure organized in « building blocks » with four types of interactions: « reciprocal excitation », « reciprocal inhibition », « recurrent inhibition » and « parallel excitation and inhibition » (Steriade et al. 1993). Reciprocal excitation is achieved when thalamic cells activate cortical cells, and then receive excitatory cortical feedback. The three other types of interactions involve an inhibitory structure, the reticular thalamic nucleus (RTN), that contains GABA-expressing neurons, receives connections from both cortical and VPM neurons, and sends projections back to VPM. Reciprocal inhibition consists in inhibition between RTN cells, and recurrent inhibition in inhibition of VPM cells by RTN

cells. The last type of interaction, parallel excitation and inhibition, refers to cortical cells that on one hand directly excite VPM cells, and on the other hand indirectly inhibit VPM cells through prior activation of RTN cells. In addition, a sub-thalamic nucleus, the zona incerta (ZI), contains mainly GABA-expressing neurons which inhibit PoM cells. Inactivation of ZI neurons significantly reduces the mean response latency observed in PoM cells (Trageser & Keller 2004). Interestingly, activation of wM1 inhibits ZI activity (Urbain & Deschênes 2007b). This implies that while wM1 is activated, for instance while rats are scanning their environment by whisking, sensory information from trigeminal relays is transmitted to PoM cells.

We conclude from this review of the whisker tactile system that 1) it is organized along multiple pathways, which are each likely to be specialized in transmitting one type of information (for instance touch or whisker position) and 2) that these pathways are highly interconnected internally and with motor structures, forming multiple loops. These sensori-motor loops can be hypothesized to play a role in adapting the behavioral strategy of the animal in order to collect relevant information. In the next section, we will investigate the encoding of different types of tactile information.

II.2. Encoding object properties with the whisker system.

II.2.1. Where is the object: spatial localization.

II.2.1.1. Spatial localization along the rostro-caudal axis.

Rodents are able to discriminate positions of an object along the rostro-caudal axis, and this ability specifically requires wS1 neuronal activity (O'Connor et al. 2010). To discriminate such spatial position, one can hypothesize that cortical neurons encode the whisker angle as a function of time while they are whisking similarly to proprioceptive information from the limbs. Indeed, with this strategy, the whisker angle at the time of touch can be stored, and the different positions of the object can be distinguished. In general, different mechanisms can be involved for reporting proprioception signals in the sensory cortex.

Firstly, proprioceptive fibers located in muscles can send information on muscle tone to central structures. In this case, proprioceptive and tactile inputs would run in parallel pathways to reach the cortex. However, in whisker extrinsic and intrinsic muscles, the

amount of proprioceptive fibers is negligible compared to those found in other facial muscles (Moore et al. 2015; Semba & Egger 1986), and it is thus unlikely that this mechanism significantly accounts for proprioception coding in the sensory cortex.

Secondly, mechanoreceptors in whisker follicles could be sensitive to whisker movement, in addition to touch. In this case, proprioceptive and sensory information should run through the same pathway to reach cortical neurons. As mentioned in II.1., lemniscal and paralemniscal pathways are involved in whisker movement coding during whisking (Yu et al. 2006), and we will thus focus on these routes. Recently, studies on TG and brainstem neurons preference for whisking phase were performed in anesthetized rats, in which whisking was artificially induced by stimulation of the facial nerve (Wallach et al. 2016) (Szwed et al. 2003). Simultaneous whisker tracking allowed proper feedback to the facial nerve stimulator, so that the amplitude and frequency of whisking could be precisely controlled from cycle to cycle and reproduce natural patterns (Figure 18A). Results show that TG neurons fire selectively more for a particular whisking phase (Figure 18B). Wallach et al. (2016) also showed that phase selectivity of individual TG neurons does not change when the amplitude or frequency are modulated.

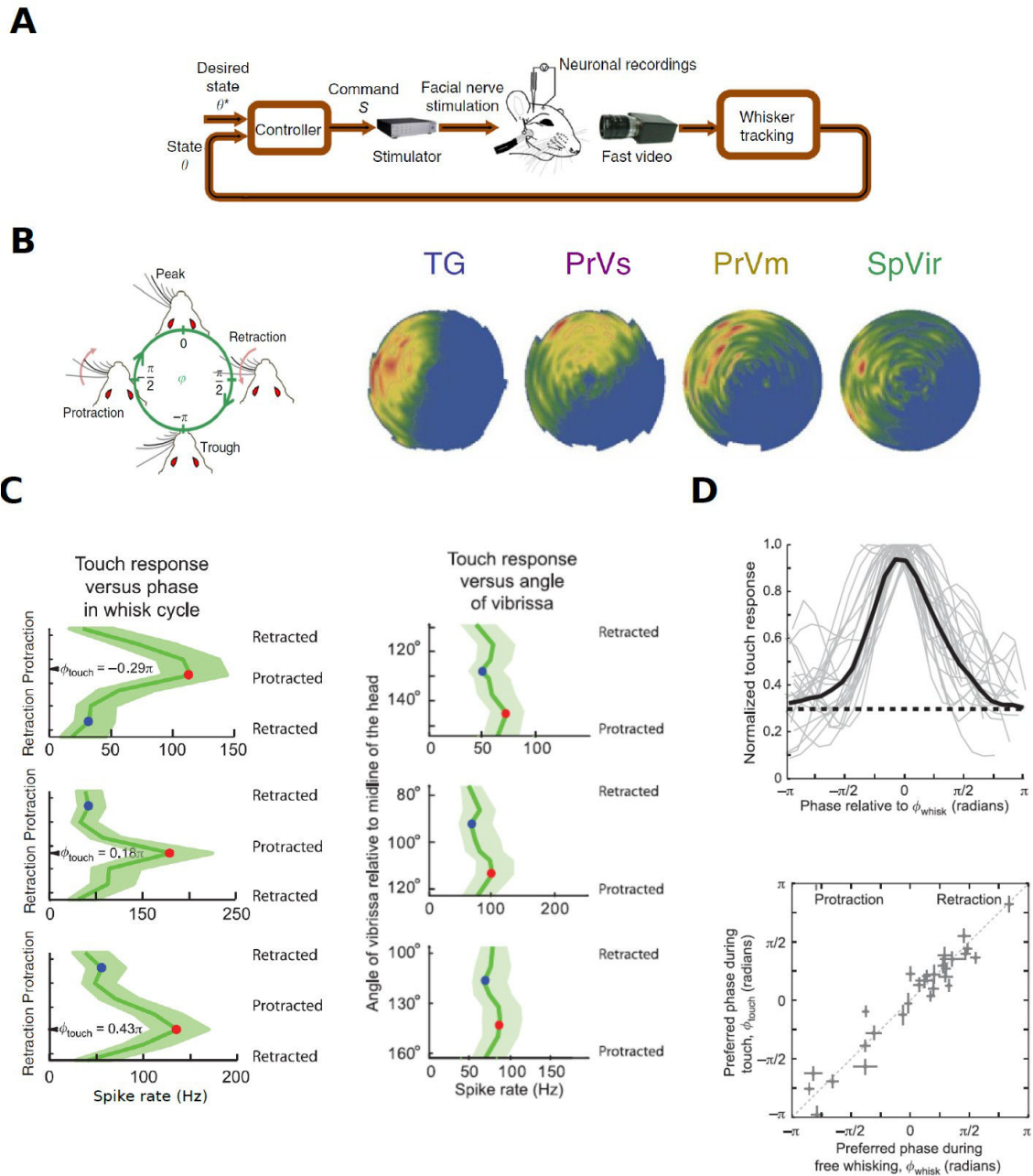


Figure 18: Neuronal selectivity for the whisking phase

A: Schematic representation of the artificial whisking protocol. From Wallach et al., 2016.

B: Left, value of the phase ϕ at the different stages of the whisking cycle. Right, the response of four example units to synthetic whisking phases, from different relay stations. From Wallach et al., 2016.

C: First column, responses of example wS1 neurons (X-axis) according to the whisking phase (Y-axis). Second column, responses of example wS1 neurons (X-axis) according to the angular position of the whisker during whisking (Y-axis). From Curtis and Kleinfeld, 2009.

D: Upper panel, normalized responses of all wS1 recorded cells as a function of the whisking phase. Thicker black trace represents the mean. Lower panel, correlation between the preferred phase of neurons during touch events (Y-axis) versus during free whisking (X-axis). From Curtis and Kleinfeld, 2009.

Thus, proprioceptive inputs could be relayed to the cortex through the same pathway than tactile inputs, provided that phase selectivity can be found in other relays of the lemniscal and / or paralemniscal pathway(s). In both Pr5 and SP5i in the brainstem, neurons are also tuned for a specific whisking phase (Figure 18B, (Wallach et al. 2016; Moore et al. 2015)). At the thalamus level, both VPM and PoM contain neurons that are selective for a particular whisking phase, even though these neurons are far more numerous in VPM (Moore et al. 2015). In L2/3 of wS1, membrane potential fluctuations are phase-locked to whisking oscillations (Crochet & Petersen 2006), and this correlation is not maintained if the infra-orbital nerve is cut (Poulet & Petersen 2008) This suggests that motion-related inputs are conveyed through the same pathway than tactile inputs. Moreover, touch supra-limbar responses in single neurons are of higher magnitude for specific phases of the whisking cycle in the barrel cortex (Curtis & Kleinfeld 2009; de Kock & Sakmann 2009). Figure 18C depicts the evoked response magnitude (X-axis), according to the phase of whisking (Y-axis, left panel) or to the angle of the whisker throughout each cycle (Y-axis, right panel). Results show that cortical wS1 neurons respond more when contact happens at a particular phase of the cycle (Figures 18C, left panel and 18D, upper panel), but does not display such selectivity towards precise angle values (Figure 18D, lower panel). In addition, the preferred phase during free-whisking in air corresponds to the preferred phase during touch events (Figure 18D, lower panel). Spike rate also particularly increases in L5A of the barrel cortex during whisking (de Kock & Sakmann 2009), adding evidence for a role of the paralemniscal pathway in coding whisking movements. Thus, both sub- and supra- limbar activity in wS1 can encode global whisking movements, and information on whisking phase is transmitted throughout the tactile lemniscal and paralemniscal pathways.

Lastly, single neurons in wM1 code for the amplitude and midpoint of the vibrissae during whisking, and encoding is not disturbed by cutting of the infra-orbital nerve (Hill et al. 2011). Indeed, some neurons monotonically increased or decreased their firing rate for increasing values of whisker amplitude. Thus, this may give a rate coding for angular positions of the whisker in time.

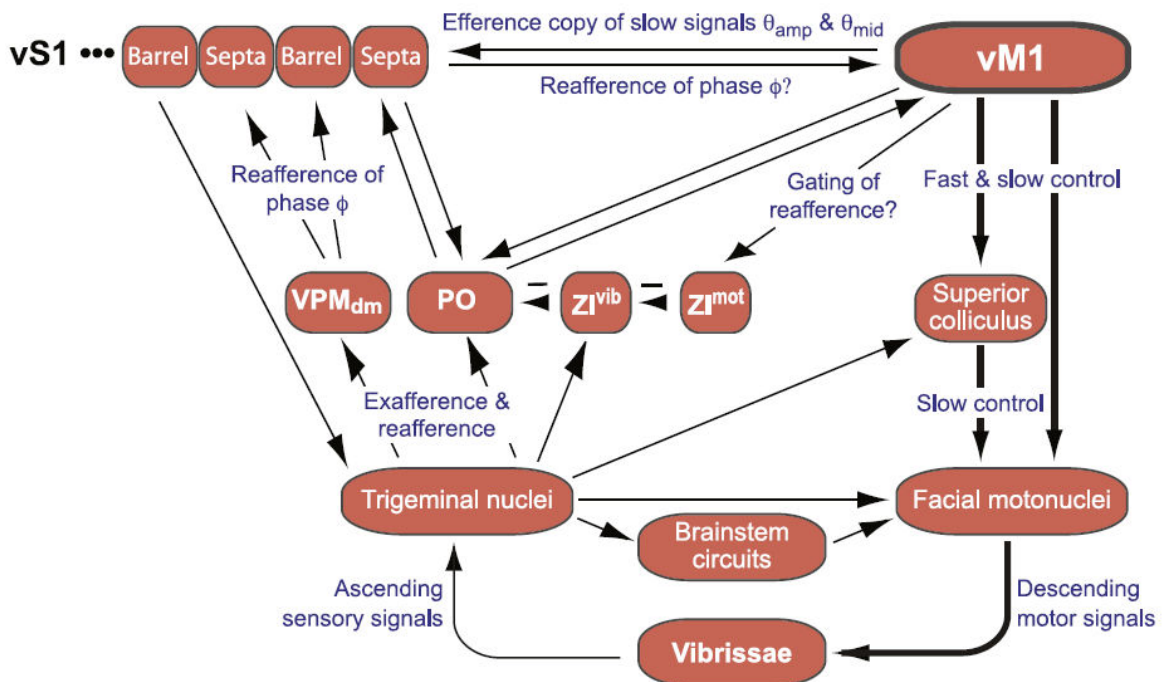


Figure 19: Connections involved in phase and amplitude selectivity

From Hill et al., 2009.

The authors propose that wM1 representation of the whisker amplitude and midpoint information could be transmitted to wS1, that lacks coding for precise whisker angle. The information on the whisker position, coupled to the encoding of touch, could underlie object spatial localization in rodents. A schematical view of the connections involved for coding phase and amplitude is shown in Figure 19.

The necessity for coupling precise whisker angle with touch responses in order to discriminate object positions has however been recently controversial (O'Connor et al. 2013). In this study, the authors showed that firing rate, rather than coupling of touch responses with a position of the whisker, underlies pole localization. This is consistent with findings showing that different positions of an object along the rostro-caudal axis evoke different magnitude of sub-limnar responses (Crochet et al. 2011).

Notably, the more rostral an object, the lower the curvature imposed on the whisker

(Bagdasarian et al. 2013) and curvature is encoded through firing rate in cortical neurons (Quist & Hartmann 2012). Indeed, a change in curvature could evoke a change in pressure in the follicle, and increase the firing rate of pressure-sensitive neurons in TG (Szwed et al. 2006), for review see Knutsen & Ahissar 2009). Another possibility is that whisking amplitude or speed may change between the exploration of the two locations, resulting in different inter-contacts intervals, and thus shaping different response magnitudes (Crochet et al. 2011).

In conditions where the forces applied on the whiskers and the interval between successive contacts would not differ significantly between two locations, we can hypothesize that monitoring precise whisker position in time would be necessary to solve the task.

II.2.1.2. Discrimination of stimulus distance to the snout.

Rats have also shown remarkable abilities in discriminating radial distance between a stimulus and their snout (Krupa et al. 2001). Radial distance could be inferred from the identification of which whisker is touching and which whisker is not. Indeed, since the whiskers have different lengths, if a whisker with a length L_1 is touching and a whisker with a length L_2 is not, with $L_1 > L_2$, then the contact position must be at a distance between L_2 and L_1 . However, it has been shown that rats can discriminate two aperture sizes of 60 and 68 mm, even though the whiskers were all contacting the two poles during the task (Krupa et al. 2001). Thus, in this case at least, the encoding mechanism can not be based on the determination of the touched or non touched state of each whisker. Theoretical models have shown that changing the radial position of contacts along the whisker elicits changes in the force moment applied at the whisker follicle (Solomon & Hartmann 2006). These mechanical variations in the follicle, along with significant changes in the whisker angle and curvature (Figure 20, Bagdasarian et al. 2013), carry information about the radial position of contact. In the TG, neurons encode radial positions by firing rate: the closer to the snout the contact point is, the more neurons fire spikes, and a subset of neurons also respond with a smaller latency to closer contact points (Szwed et al. 2006). In addition to changes in angle and curvature, the speed of the whisker is also different according to radial position of contact, at the time of touch (Figure 20D, middle panel, Bagdasarian et al. 2013), and this parameter is

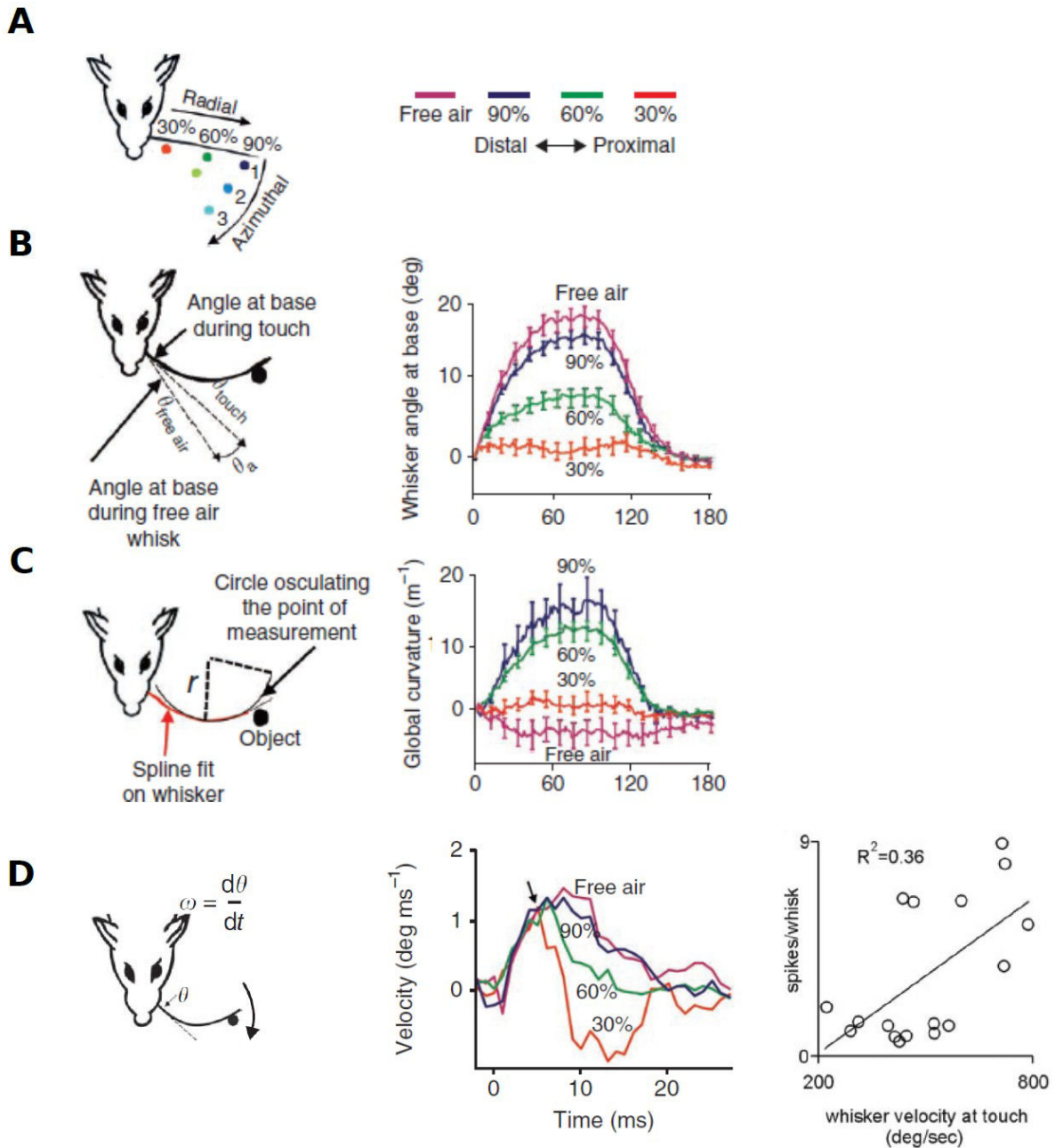


Figure 20: Encoding radial position

A: Left, Grid of pole positions. The curved arrow indicates the direction of whisker protraction. Right, color code applied in B-D for each of the three radial positions. From Bagdasarian et al., 2013.

B-D: Left, schematics of the measured variable (respectively whisker angle, curvature and speed at the time of contact). Middle, effect of the radial position of contact on the three variables. From Bagdasarian et al., 2013.

D: Right, correlation between neuronal activity in the TG and whisker speed at the time of contact during whisking cycles. From Szwed et al., 2006.

also encoded by TG neurons firing rate (Figure 20D, right panel, Szwed et al. 2006). At the cortical level however, in a majority of cases pre-contact whisker speed seems to not impact the magnitude of evoked sub-liminar responses (Crochet et al. 2011). Recently, a wall-tracking task in virtual environments has been carried out (Sofroniew et al. 2014), allowing a precise control of the stimulus radial distance freely-running mice. In this context, neurons in wS1 display diverse coding strategies. A proportion of the recorded cells increase their firing rate for closer objects, whereas other ones monotonically increase or decrease their firing rate while the walls were approached towards the mouse's snout (Sofroniew et al. 2015). More complex responses were also observed, with monotonically increasing firing rate of the cells till the wall has reached a certain distance to the snout, and decrease of the firing rate as the wall was brought closer. These results show that while first-order TG neurons activity seems exclusively negatively correlated with radial distance, somatosensory cortical neurons display more complexity and diversity in their firing responses.

II.2.2. What is the object: encoding surface properties

II.2.2.1. Encoding whisker movement over the whole stimulus

Encoding stimulus frequency

Spatial frequency is a parameter that can change with roughness, for instance on grooved surfaces (Carvell & Simons 1995) (Zuo et al. 2011). To better characterize the neuronal encoding of spatial frequency, several studies have been performed with temporal stimuli applied on the whiskers. These protocols allow to tightly control the frequency of stimulation, and to keep it constant throughout the protocol. In this section, we will focus on studies involving temporal stimulations to investigate stimulus frequency encoding.

(Zuo et al. 2011) Both rats and mice are able to discriminate 90 Hz pulses frequency applied on the whiskers from lower frequency stimuli ranging from 10 to 80 Hz (Mayrhofer et al. 2013). Calcium imaging studies showed that cortical neurons response transients increase for increasing frequencies in the same range (Mayrhofer et al. (2015), tested values: 10, 40, 90, and 110 Hz). Thus, stimulation frequency can be discriminated by cortical firing rate. Another possibility for encoding frequency could be to fire spikes time-locked to each pulse (Khatri et al. 2004), but it seems that this criterion is not necessary to achieve discrimination

performance of frequencies up to 40 Hz (Musall et al. 2014). Indeed, in this latter article, degrading temporal phase locking of cortical neurons to individual pulses did not decrease discrimination performance to chance level.

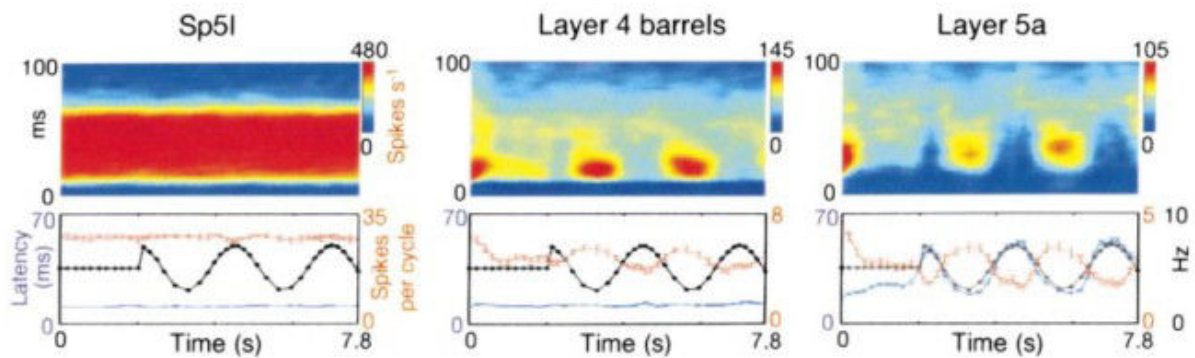


Figure 21: Encoding of stimulus frequency

Pooled data from all well localized local populations of Sp5i (left), cortical layer 4barrels (middle) and layer 5a (right) recorded during FM stimulations.

In each station, pooled data is represented by the population response composed of all spikes generated by the different units recorded from the same station in different subjects and at different times. Spike times were coordinated according to onset times of the stimulus trains. Top, PSTHs as a function of train time (vertical axis, PSTH time; horizontal, train time). Bottom, instantaneous stimulus frequencies (black), response latencies (blue) and spike counts (red) as a function of train time.

From Ahissar et al., 2000.

Encoding of frequencies lower than 10 Hz involves different neuronal treatments along the lemniscal and paralemniscal pathways (Ahissar et al. 2000). Figure 21 shows latency responses and firing rates in the brainstem nucleus SP5i and in cortical input layers of lemniscal and paralemniscal pathways (respectively L4 and L5A) and to a set of different stimulation frequencies. On lower panels of the Figure 21 are displayed the latencies in blue, the firing rate in orange and the frequency of the stimulation in dark. These plots show that firing rate is anti-correlated with the frequency values in both pathways, but in addition, latency values are positively correlated with frequency values in the paralemniscal pathway (lower right panel). This trend is not observed in the lemniscal pathway (lower middle panel), where latency values are not modulated by the frequency of stimulation. Upper panels of

Figure 21 show firing rate amplitude (color coded) and temporal decay per cycle of stimulation, according to the frequency of stimulation (represented by the dark curve in lower panels). The authors show that these tuning curves for particular frequencies are directly inherited from thalamic relays and do not exist at the brainstem level (upper and lower panels on the left). This supports the fact that thalamic neurons are not « simple » relays transmitting information from brainstem to cortex without transformation. On the contrary, there is an emergence of frequency selectivity at the level of the thalamus, and thus probably thalamic neurons have a role in discrimination processes. Note that, contrary to higher frequencies (Mayrhofer et al. 2015), low frequencies studied by (Ahissar et al. 2000) are encoded by firing rate values negatively correlated with frequency values. A critical parameter modulating neuronal responses to series of tactile stimulation is adaptation. This process consists in a decrease in neuronal response magnitude with an increasing number of pulses in a stimulation train (Khatri et al. 2004). In other words, responses are greater for the first pulse of a series and become progressively smaller for subsequent pulses. Adaptation is frequency-dependent and is in part due to depression at the thalamo-cortical synapse (Chung et al. 2002). As a consequence, responses are more decreased after adaptation in the cortex than in the thalamus (Khatri et al. 2004). Critically, adaptation is thought to decrease frequency discrimination abilities in rodents (Musall et al. 2014). This result has been obtained with optogenetic stimulation of wS1 calibrated such that evoked responses are close to those observed after neuronal adaptation. The authors in particular show that this adaptative-like stimulations significantly impair performance levels, whereas non-adaptative stimulations do not. However, adaptation leads to an increase in performance in other perceptual tasks, for instance deflection velocity by thalamic cells (Wang et al. 2010) and accuracy in identifying which whisker has been touched by cortical neurons (Ollerenshaw et al. 2014).

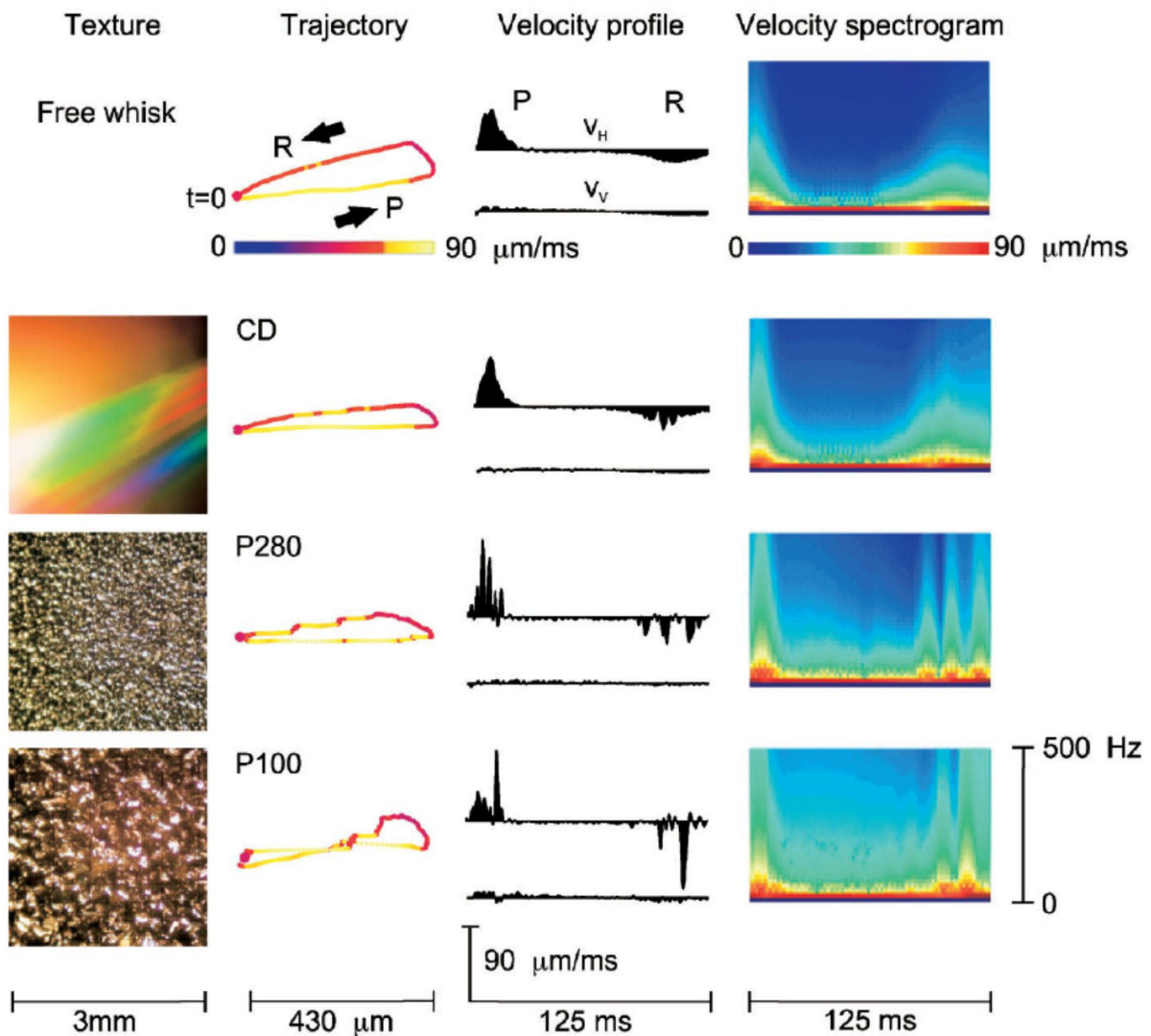


Figure 22: Whisker micromotions on sandpapers

“Texture” column: Photographs of the 5 surfaces used.

“Trajectory” column: Sample whisker trajectories. Each point, separated by 1 ms, gives the horizontal and vertical position; the trajectory begins with protraction (P) at $t = 0$ and terminates 125 ms later at the end of retraction (R). Speed is given by the color of each point. Note the irregularities—jumps, stops, and starts—induced by whisking on sandpaper.

“Velocity profile” column: Whisker trajectories displayed according to the horizontal and vertical velocities (V_H and V_V , respectively). P refers to protraction phase (positive V_H), and R to retraction phase (negative V_H).

“Velocity spectrogram” column: Velocity spectrograms for each texture.

From Arabzadeh et al., 2005.

Encoding whisker mean speed

A classical material used for this type of task is sandpaper surfaces, with varying grain size. Different types of sandpaper roughness evoke changes in local speed, amplitude of micromotions and frequency throughout the stimulus (Figure 22, Arabzadeh et al. (2005)). The value of the product (amplitude x frequency) is proportional to the mean speed of whisker oscillations (Arabzadeh et al. 2003), and behavioral studies have shown that rats are not able to discriminate two oscillations with similar mean speed values, even though these stimuli were differing in amplitude and frequency (Gerdjikov et al. 2010). This behavioral result was however recently challenged (Waiblinger et al. 2015a), suggesting that, in some other learning protocols, mean speed value is not a critical stimulus feature for discrimination. The mean speed is positively correlated with the roughness of a given surface (for review, see Diamond et al. 2008), and thus one can hypothesize that the rougher a surface is, the more cortical neurons should fire spikes. This hypothesis has been confirmed, in freely-moving rats performing a sandpaper discrimination task (von Heimendahl et al. 2007). To control the frequency and amplitude of incoming signals, TG and cortical neurons were recorded while surface-induced micro-motions were replayed on the whiskers (Arabzadeh et al. 2005). The authors found that neurons in both structures respond more to stimuli with increasing mean speed values. Similarly, a study involving sinusoidal stimulation of the whiskers, the more the value of the product (amplitude x frequency) was increased, the more evoked cortical response was of high magnitude (Arabzadeh et al. 2003). Taken together, these results show that TG and cortical neurons can encode stimulus parameters, such as speed, integrated over the whole stimulus, and that this tactile input is encoded by firing rate.

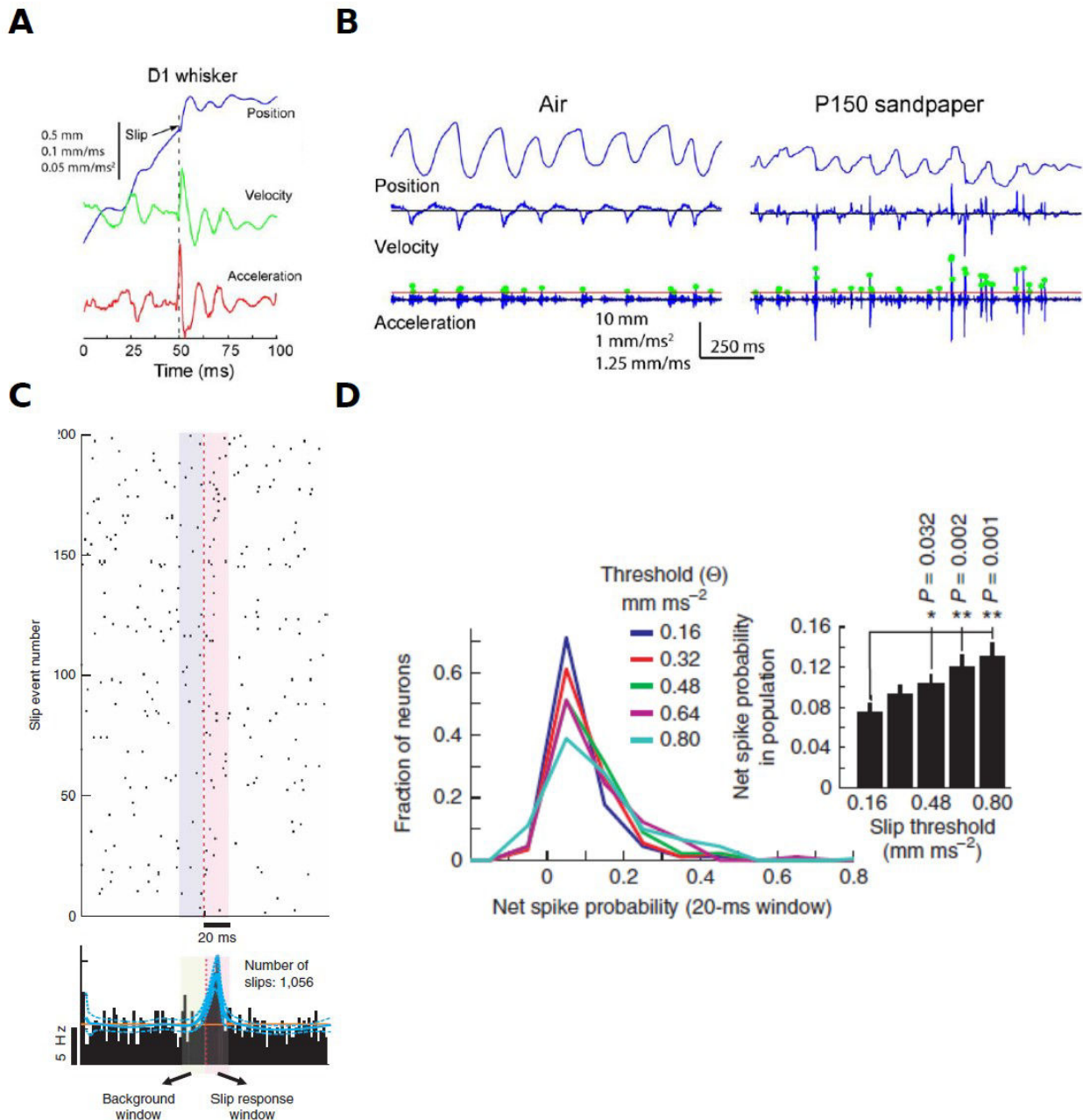


Figure 23: High-acceleration events during contact with a sandpaper surface

A: High-acceleration whisker movement for a D1 whisker. Movement event onset is marked by an acceleration peak (aligned at 50 ms), followed by transient, decaying ringing in acceleration, velocity, and position. From Wolfe et al., 2008.

B: Motion of the D2 whisker in air and on rough (P150) sandpaper. Dots indicate acceleration transients greater than 4 s.d. above mean acceleration in air (red line). From Wolfe et al., 2008.

C: First slip aligned raster for a representative neuron, illustrating sparse responses to slip events. From Jadhav et al., 2009.

D: Left, net spike probability (spikes per 20-ms window) above background probability for the population of 90 neurons, as a function of slip acceleration threshold. Right, mean net spike probability in the population for each threshold (mean \pm s.e.m.). From Jadhav et al., 2009.

II.2.2.2. Encoding acute variations in speed and acceleration

Replicating surface-induced micro-motions on the whiskers, Arabzadeh and colleagues (2005) also observed that TG and cortical neurons fire precise spike patterns, locked to local changes in speed or acceleration. In particular, high-acceleration events ("slip-stick events", for review see Jadhav & Feldman (2010) Schwarz (2016)) occur when the whiskers are swept onto sandpapers (Wolfe et al. 2008). A slip-stick event corresponds to an attachment (stick) of the whisker on a surface asperity, followed by its detachment. The detachment (slip) appears as an abrupt change in whisker position (Figure 23A, top panel), and is characterized by a high acceleration (Figure 23A,B), that crosses a pre-defined threshold (Figure 23B, lower panel, events that cross the threshold value are encircled in green). The number of slip-stick events increases with roughness of the surface (Ritt et al. 2008; Zuo et al. 2011), and is dependent on whisking amplitude (Chen et al. 2015). Also, a recent psychophysical study showed that rats can detect slip-like deflections embedded in a white noise background to mimic natural conditions of surface scanning (Waiblinger et al. 2015). At the cortical level, neurons encode slip acceleration with precise spike timing (Jadhav et al. 2009), since the peak of the evoked response is restrained to 20 ms post-slip (Figure 23C). In addition, spike emission probability at the population level is positively correlated with slip acceleration values (Figure 23D). These results strongly support the fact that cortical neurons encode acute kinematic cues, such as slip-stick events, in addition to encoding parameters integrated on the whole stimulus, such as frequency or mean speed. Interestingly, we know that VPM neurons respond to texture-evoked whisker movements by firing spikes precisely in time, and reliably across trials (Bale et al. 2015).

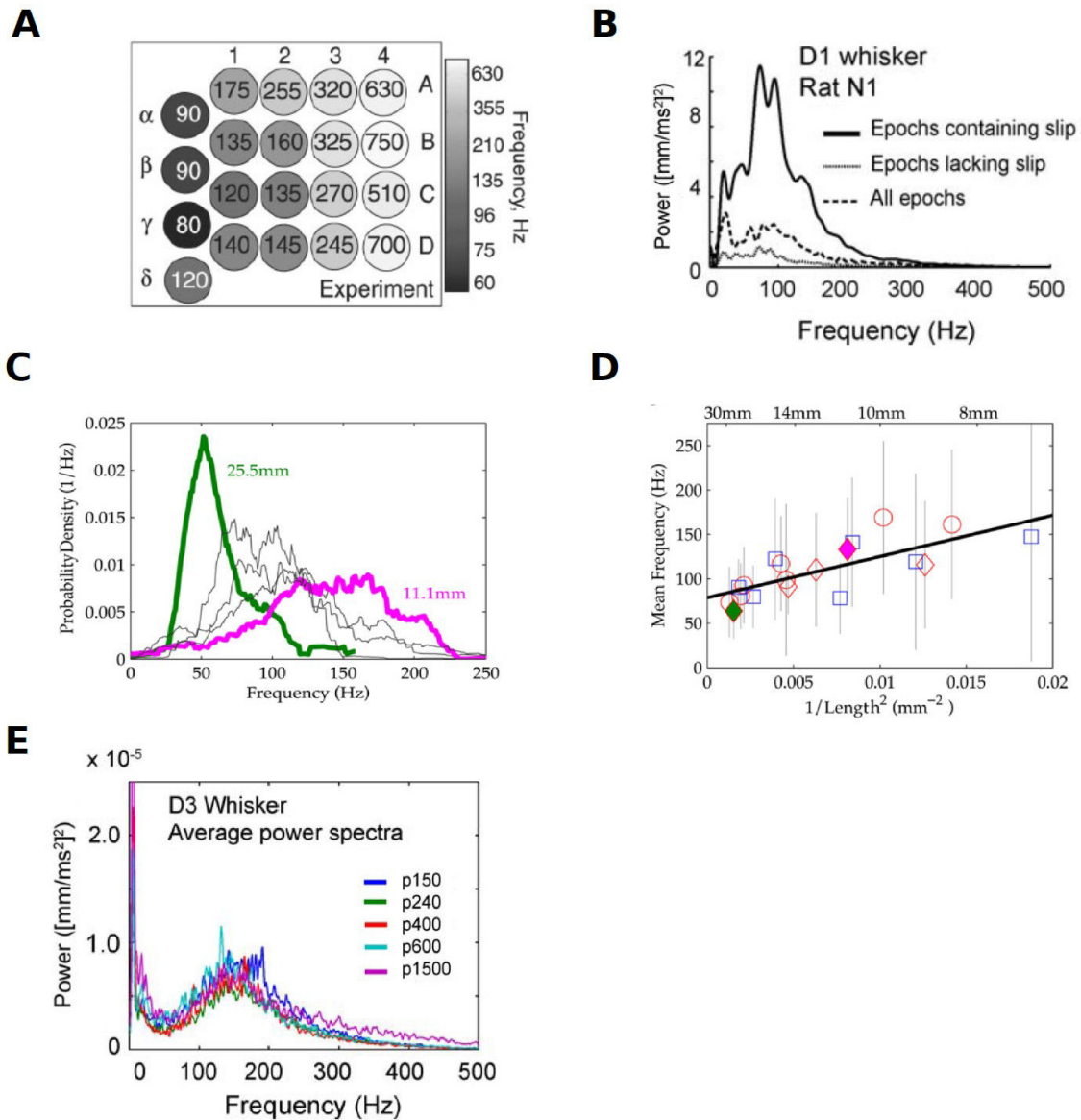


Figure 24: Whisker resonance during surface contact

A: Frequency of resonance of individual whiskers on rows A-D. From Neimark et al., 2003.

B: Average power spectra in 400-ms epochs containing a high-acceleration event (black), lacking such an event (dotted), or for all whisking epochs (dashed). Power spectra were derived from motion of the D3 whiskers in one rat, averaged across all textures. From Wolfe et al., 2008.

C: Distribution of micromotion frequencies for five vibrissae that contacted a rough surface during the same trial. Annotation provide the lengths of these vibrissa. From Ritt et al., 2008.

D: Mean frequency (symbols) and SD (gray bars) for all scanned vibrissae ($n = 19$) during surface contact is plotted against $1/\text{Length}^2$. Red and blue color indicate data from two rats, common symbols indicate samples from distinct vibrissae on the same trial. From Ritt et al., 2008.

E: Average power spectra of the D3 whisker on five different sandpapers (color-coded). From Wolfe et al., 2008.

II.2.2.3. The differential resonance theory

Whisker length and diameter increase from rostral to caudal position in the array, resulting in shorter whiskers vibrating at higher frequencies than longer ones when rats whisk in air (Figure 24A, (Neimark et al. 2003; Wolfe et al. 2008)). When rats sample textures, their whiskers stick on an asperity, slip from it and then resonate at the moment they stick on the next asperity (Ritt et al. 2008; Wolfe and collaborators 2008) confirmed this observation by finding a significant increase for particular frequencies in the power spectrum of whisker movements in trial epochs with slip events (Figure 24B). Resonance frequency is varying across whiskers during texture sampling (Figures 24C-D), following the same rule as during whisking in air: the longer the whisker, the lower the frequency (Ritt et al. 2008; Wolfe et al. 2008). The differential resonance theory states that the presence of resonance for each whisker is dependent on the spatial frequency of the stimulus, and thus on its roughness (for review, see Jadhav & Feldman 2010). More precisely, lower spatial frequencies would increase resonance in longer whiskers, and thus would increase neuronal activity in some barrels more than in others in the cortical map. This theory is also supported by the fact that cortical neurons can be tuned for the presence of resonance in whisker movement (Andermann et al. 2004). However, no significant differences were found between power spectra of whisker oscillations on different sandpaper textures (Figure 24E, Wolfe et al. 2008). The differential resonance theory thus seems irrelevant in classifying sandpaper roughness under these experimental conditions, but we can still ask if the results would be the same under a wider range of whisker speed. Indeed, whisker speed on texture can have an effect on the presence of resonance (Neimark et al. 2003). In addition, rodents adjust their whisker speed when trained on texture discrimination task (see I.3.3.3), and may search for an optimal speed to extract differences in resonance across whiskers. Thus, to assess more further the contribution of differential resonance in texture discrimination, one possible experiment could be to repeat the one of Wolfe and colleagues (2008) with a set of different speeds. To do so, whisker speed could be accurately controlled using an artificial whisking protocol (see Figure 20A) such as the one used in Wallach and colleagues (2016). In this section, we have focused on studies describing neuronal encoding of the sensory features known to be behaviorally significant. In particular, we have seen that the fine

features of a given surface are likely to produce kinetic events on whiskers, the stick/slip events, which are encoded at the sub-cortical and cortical level. In the following section, we will present an ongoing study in which we want to explore how different surfaces give rise to different spike patterns in the thalamo-cortical loop, thus allowing successful behavioral discrimination.

II.3. Study of thalamo-cortical responses evoked by a smooth surface, a regular or an irregular series of bars

In the behavioral experiment described in I.4, we have demonstrated that rats can be trained to discriminate tactile stimuli placed in an alley by sweeping their whiskers on them while running. In particular, the animals could perceive a difference between a surface exhibiting a regular series of bars versus a surface exhibiting an irregular series of bars. In order to understand the neuronal mechanisms underlying this difference in perception, we have developed an anesthetized preparation combining electrophysiological recordings in the thalamo-cortical system with the presentation of surface stimuli swept along the whisker pad.

II.3.1. Neuronal encoding of spatial patterns

We first present possible encoding mechanisms of surfaces, emerging from knowledge of the current literature.

II.3.1.1. Temporal responses locked to spatial series of bars

Probably the most straightforward way to encode regular and irregular spatial series would be to translate each bar position by precisely timed spikes. This would lead to temporally regular and irregular significant peaks of spike firing. However, if the series are scanned at fast rate, neurons might not be able to encode every bar. Indeed, cortical neurons can be locked to a particular phase of sinusoidal-shaped stimuli displayed at high frequencies, but do not fire at every cycle (Ewert et al. 2008). A representation of the phase locking found by Ewert and collaborators (2008) is shown on Figure 25A, and highlights the fact that although neurons can fire precisely one or a few spikes during a particular phase of the stimulus and for several successive stimuli, they do not systematically fire at each stimulus. This idea is strengthened by the fact that evoked cortical responses are sparse (Crochet et al. 2011), and are thus probably not the best candidates to strictly follow each contact at high frequency (Ewert et al. 2008)

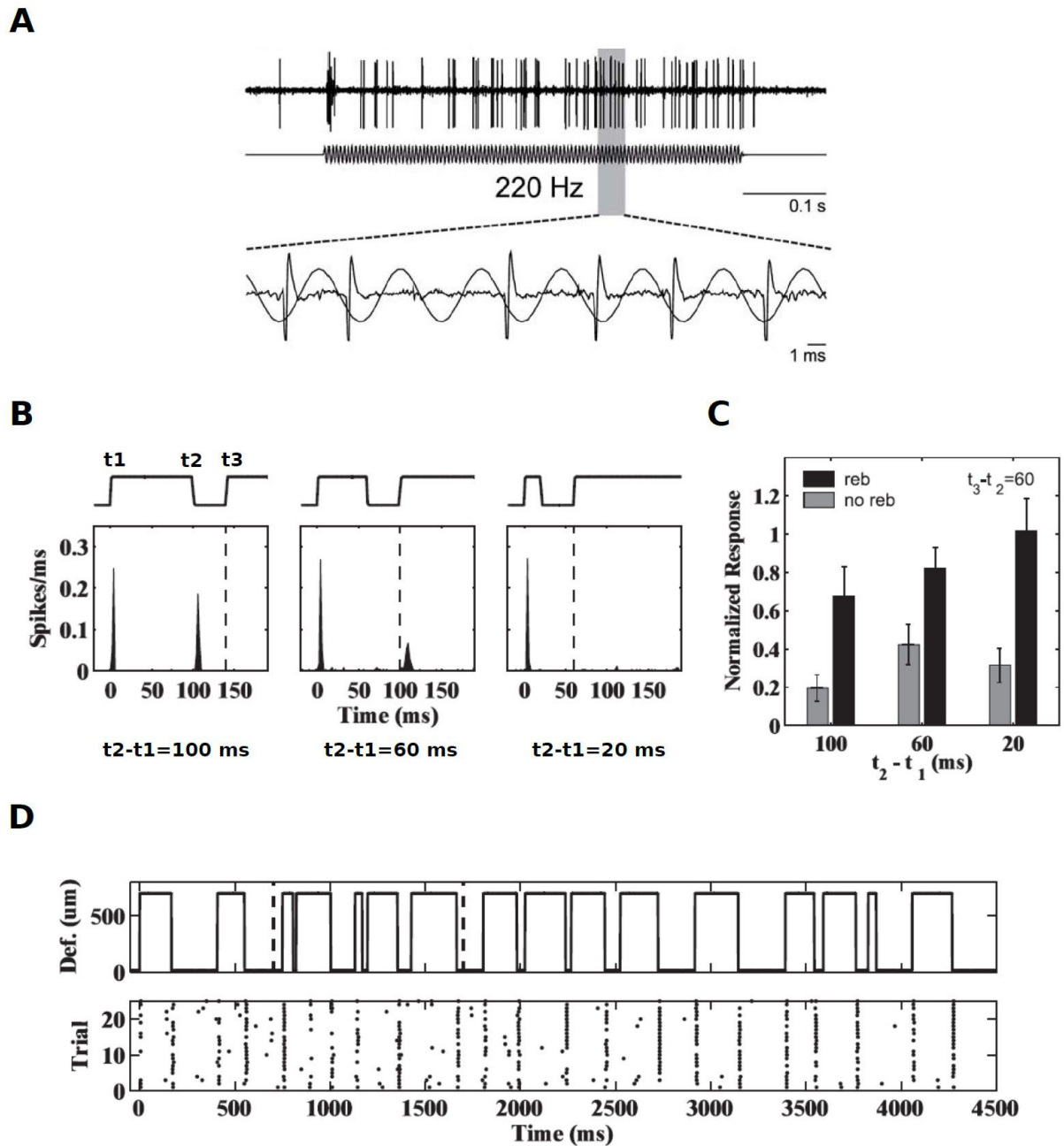


Figure 25: Neuronal responses to temporal series of whisker deflections

A: Single-unit responses to 220 Hz vibration of the principal whisker.

B: Neuronal responses to two consecutive deflections, characterized by onset and offset times of the first deflection (t_1 and t_2), and onset time of the second deflection (t_3).

C: Normalized neuronal responses according to the first deflection width (t_2-t_1) and to the type of response (with or without excitatory rebound).

D: Upper row, spatio-temporal pattern of deflections applied on the whisker. Lower row, raster plot of the responses during 25 repetitions (trials) of the deflection pattern.

An important constraint on possible temporal patterns of neuronal responses is the suppressive period following an evoked excitatory response (Carvell & Simons 1988; Webber & Stanley 2004). This suppressive period can be revealed by applying two whisker deflections successively: one triggers the first response, and a second one is a probe to determine the period during which responses are suppressed (Webber & Stanley 2004). On Figure 25B, the cortical responses to a series of three deflections at times t_1 , t_2 and t_3 . If (t_2-t_1) is equal to 100 ms are shown (left panel), then both the first and second deflections do evoke a response. However, if (t_2-t_1) is equal to 60 ms (middle panel), then the second deflection does not evoke a response. This shows that the suppression period lasts between 60 and 100 ms after the first deflection in this particular case. In addition, a proportion of cortical cells (~35%) also exhibit an excitatory response after the suppressive period, called « rebound activity » (Webber & Stanley 2004). The presence or absence of rebound activity shapes the response to the third deflection (dark vs. grey bars for each of the three values of (t_2-t_1) on Figure 25C). To conclude, there is a non-linear encoding of deflection patterns into temporal spike patterns, constrained by 1) the « history » of temporal deflections (Figure 25C, dark bars or grey bars across the three conditions), and 2) the presence or absence of rebound activity (Figure 25C, dark vs. grey bars for each of the three conditions). An example single neuron responding to a series of irregular deflections is depicted in Figure 25D, showing that responses are not linearly encoding the pattern; for instance these responses are not always evoked by the onset of each deflection. However, we can note that the pattern of responses is reliable from trial to trial. In awake behaving animals, the inter-contact interval also modulates the amplitude of the response (Crochet et al. 2011), supporting the dependence of responses on the history of previous deflections.

Taken together, these results suggest that the hypothesis that temporal responses should be precisely locked to the sequence of bars in order to encode regularity/irregularity is probably too naive.

II.3.1.2. Encoding stick/slip events

Since the regularity of the bars is not likely to be encoded by a temporal pattern of spikes locked to each physical bar, we hypothesize that regular and irregular series may evoke more complex differences in whisker velocity and acceleration profiles. Indeed, when a whisker is

brushed onto sandpaper and grooved surfaces, it attaches and detaches from grains, resulting in high-speed and high-acceleration events (“stick-slip events”, see II.2.2.2). First, we suppose that these events could vary in number and timing between the two series. Second, as for sandpapers grains, the size of bars and intervals may modulate acceleration magnitude during slip event, as well as the forces in the follicle during the stick phase. Thus, we expect the variability of slip acceleration values to be greater in irregular than in regular series. Furthermore, Jadhav et al. (2009) showed that the number of neurons activated by slip events is positively correlated with the acceleration magnitude. At the level of the population, we thus predict a high variability of spiking probability for the irregular series of bars.

To summarize, we hypothesize that several features of thalamo-cortical spike patterns will be affected by the regularity of the surface physical profile. We predict that an irregular series will evoke a different overall firing rate and more irregular spike patterns, both for individual neurons and at the level of the population. Further, we would like to relate thalamic and cortical neurons responses to the sequence of slip events during the passage of our particular stimuli. To tackle these questions, we designed a set-up for recording thalamo-cortical activity while moving the stimuli linearly along the whisker pad.

II.3.2. Materials and methods

II.3.2.1. Animals

All experimental and surgical procedures were approved by the French Ethical Committee (project n°526.01). So far, four male adult Long Evans rats were used. Before the electrophysiological recordings, two animals were trained on the tactile discrimination task (Kerekes et al., 2017). Two other animals were trained to perform an alternation task on the same maze but without stimuli placed in the central alley, in order to match the general physical activity and food intake of the trained rats.

II.3.2.2. Overview of the protocol

We present the different steps that were followed for each rat. The details of each technique are given in following sections of the materials and methods.

Steps of the protocol:

- 1- Building of the implant and surgical implantation of a rat.
- 2- Lowering of the tetrodes in the brain.
- 3- Determination of the receptive field of the neurons recorded on each tetrode using the matrix stimulator (Jacob et al. (2010)).
- 4- Selection of a whisker row that include the receptive fields found in step 3, and electrophysiological recording of a session during bar stimuli presentation.
- 5- Repetition of step 4, either with a different whisker row or with the same row. We change the recording site (by lowering the tetrode) from one session to the next.
- 6- When the series of recording sessions is done, rats are perfused with a 4 % paraformaldehyde solution. Post-mortem histology is performed afterwards to obtain tetrode location in the brain.

II.3.2.3. Implant making

These methods as well as surgical implantation have been adapted from those of the laboratory of Matt Wilson (MIT, Cambridge, USA). These methods are available online (Kloosterman et al., 2009; Nguyen et al., 2009).

Implant design and microdrives

First, we designed the « base » of the implant in SolidWorks (Figure 26, left panel). This base contains a support for the interface where tetrodes (Electrode Interface Board, EIB) are connected (top part of the implant) and pairs of holes to add a series of devices called « microdrives ». Microdrives are the parts of the implant that allow vertical movements of tetrodes in the brain, with a precision of about 20 μ m. Each tetrode is associated with one microdrive, consequently tetrodes can be individually displaced vertically. The top piece of a microdrive (Figure 26 right panel) is made of molded dental cement and contains the head of a custom-designed stainless steel screw (Faulcon, Saclay) and a piece of 23 gauge (Inner Diameter = 0.3mm; Outer Diameter = 0.6mm; abbreviated 23G) stainless steel cannula. The 23G cannula is embedded firmly in the top piece whereas the screw head can freely rotate inside. The screw and 23G cannula of each microdrive are inserted in the pairs of holes on the printed implant (Figure 26 middle panel). When turning the screw clockwise, the whole

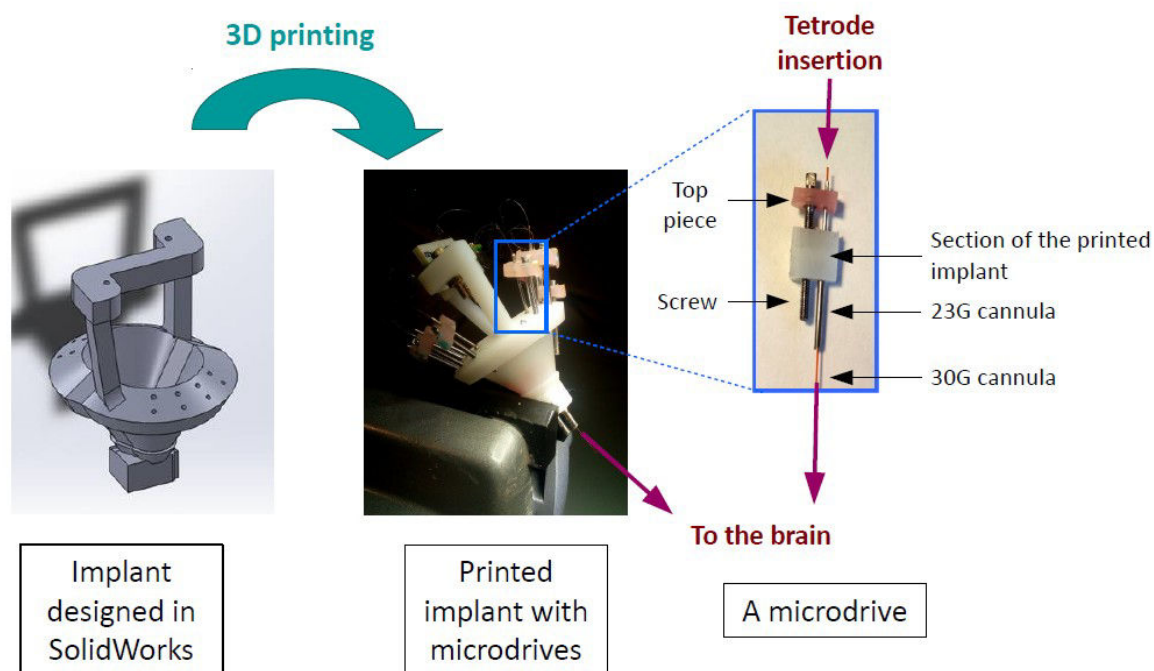


Figure 26: Tetrode implant

Left panel, schematic of the implant designed in 3D (SolidWorks). Middle panel, printed implant, with microdrives and tetrodes. Right panel, details of a microdrive.

top piece and the 23G cannula go down relative to the base, and go up when turning counterclockwise. This simple mechanism allows the experimenters to bring the tetrodes down in the brain during recording. Each full turn translates the screw by 250 μm . The custom-made screwdrivers adapted to the screw heads allow to lower by 1/8th to 1/16th of a turn, thus between 30 to 15 microns.

Tetrode making

To make the tetrodes, we first take a 50cm long electrode wire (20 μm NiCr insulated with Teflon, Kanthal Palm Coast, USA) and make a loop. The two ends of the wire are placed side by side between two fingers. Then, the loop is cut with thin scissors, yielding two 25cm wires. This double wire is looped around a rod and the four ends are clipped on a rotating device. The four wires are coiled for eighty turns clockwise and forty turns counter-clockwise. Finally, this helix is homogeneously heated at 250°C during 30 seconds. This step is very

important to fix the four wires in a coiled shape and glue them together so that they don't separate while entering the brain. Finally, the top loop is cut and the four ends are separated to form the “head” of the tetrode. Once tetrodes are made, they are inserted in the top piece as shown in Figure 26, right panel. Once fully inserted, tetrodes are glued to the 30G cannula, which is itself glued to the 23G cannula, so that if the screw is turned clockwise, the tetrode is going down with the screw. Once loaded, the tetrodes are connected to the EIB (see below).

Tetrode cutting and labelling with Dil

The microdrives are brought down to their lowest position, and the tetrodes that stick out of the bottom of the implant are cut to specific lengths according to the depth they have to reach in the brain. The barrel cortex is localized at a vertical depth of 0.5-4mm below the skull (taking into account its curvature). We take a margin of error of two millimetres and cut the tetrodes at 6mm targeting the S1 cortex. For the VPM nucleus, we take the same margin of error and cut at 9mm. Then, the tetrodes are covered by Dil, a fluorescent dye which marks cellular membranes. This allows confirming the tetrodes localization by immunochemistry after electrophysiological experiments. Indeed, after the recording period (which can last for a few weeks), the rat is sacrificed, and is then transcardially perfused with 4% PFA to fix the brain. The brain is cut in 80µm-thick slices. These slices are labelled with cytochrome oxydase, which highlights neuronal density in layer 4 of S1, thus indicates if the Dil prints of tetrodes are located in infragranular layers (below layer 4), granular or supragranular ones.

Tetrode gold plating

This step deposits gold on the tip of the tetrodes. This increases the contact surface with the extracellular medium, thus reducing the impedance value of the tetrode, without increasing the tip width. This improves the signal/noise ratio of the recordings.

To perform the plating, we place the tetrodes in a gold plating solution. We then deliver a negative current of 3µA through an electrode wire for approximately one second. We check the impedance value and pass more current if necessary. After plating each wire, all

impedance values should be comprised in [200-300 KOhms] for regular tetrodes and around 150 KOhms for reference tetrodes (four wires shortcut together).

Finally, the tetrodes are brought upward in order to be positioned just above the bottom of the base cannulae.

II.3.2.4. Surgical implantation

Rats were anaesthetized with an induction dose of isoflurane 3%. All the surgery was done under sterile conditions. Once anaesthetized, the animal was positioned on the surgical set-up. We used ear and mouth bars to position the top of the skull horizontally and immobile. In order to avoid eyes drying, we put ophthalmic gel on them. The nose was put in a tube that delivers the isoflurane at a concentration of 0.5 to 3% in air, and the respiratory activity was monitored by a piezoelectric sensor placed under the abdomen. Then, the skin of the skull was shaved and cleaned with alcohol first followed by betadine. The skin was cut with a scalpel along the median axis of the skull, and carefully stretched with counter-weights. The skull surface was scraped and cleaned with hydrogen peroxide. Craniotomies were made with a small drill at the following stereotaxic coordinates: S1 5.5mm laterally from the median axis, -2.5mm post-Bregma along the antero-posterior axis; VPM, 2.6mm laterally, -3mm post-Bregma. Then, the implant loaded with tetrodes was brought just above the craniotomies. In order to properly fix the implant on the skull with dental cement, we drilled holes around the craniotomies for stainless steel bone screws. One of them was chosen to be the ground screw and was soldered to the ground wire. Once all the bone screws were inserted in dedicated holes, the ground wire was connected on a ground pin hole of the EIB. Superglue was applied on the skull. Finally, the implant base cannulae, the top of the skull and the screw heads were embedded together in dental cement. A plastic protective cone was wrapped around the implant and its bottom embedded in the dental cement as well. The isoflurane incoming flux was then stopped and the rat was placed in a temporary cage to recover.

II.3.2.5. Determination of neurons receptive field with the matrix

In order to know which whisker row we should focus on during recording sessions, we had to

determine the receptive field of neurons recorded on each tetrode. To do so, we used a software developed in the laboratory by Gérard Sadoc (Elphy), combined with a stimulator composed of 25 independent piezoelectric actuators adapted to the five rows and the five caudal arcs of the whisker pad (Jacob et al., 2010). The actuators were driven with RC-filtered (time constant = 2 ms) voltage pulses of 30 ms duration (10 ms-rise, 10 ms-hold, 10 ms-fall time) to produce displacements of 0.93° along the rostro-caudal axis. For our experiments, we used sparse noise stimulation applied on the 24 whiskers. Every sequence of stimulation included the deflection of each of the 24 whiskers in both rostral and caudal directions in a random order at 20 Hz. This stimulator was adapted for trimmed whiskers, and stimulator tubes were blocked at 15-20mm. However, we needed to keep the whiskers full length for our subsequent recording sessions using surface stimuli. Thus we added a small plastic piece (designed in SolidWorks and printed by the Cresilas factory) on each stimulator tube to make the matrix compatible with full length whiskers. This piece was made of two holes, one for the stimulator tube, the other one for the whisker.

II.3.2.6. Typical recording session and hardware system to display the stimuli

Each session was composed of 30 blocks of 8 trials, i.e. 240 trials in total. Within each block, stimuli were pseudo-randomly presented, with each of the four stimuli type (regular series, irregular series, smooth surface or «no stimulus») being presented twice per block. The interval between two trials was 18 seconds, so a typical recording session lasted for 1h15. To display the stimuli, we used a linear motor that was moved at 20 cm/s along the rostro-caudal axis of the rat (Figure 27). During stimulation trials, the motor was moved towards the caudal direction, and between trials it was moved rostrally back to its initial position. On the linear motor was attached a stepper (rotative) motor that held the tactile stimuli. The stimuli were gathered on a square structure, one stimulus per face so that each time the stepper was rotating by a quarter, another stimulus was presented (Figure 27). The «no stimulus» condition was a control: the linear motor was moved along its axis in the caudal direction, but no object touches the whiskers. We designed this control to check that the mechanical

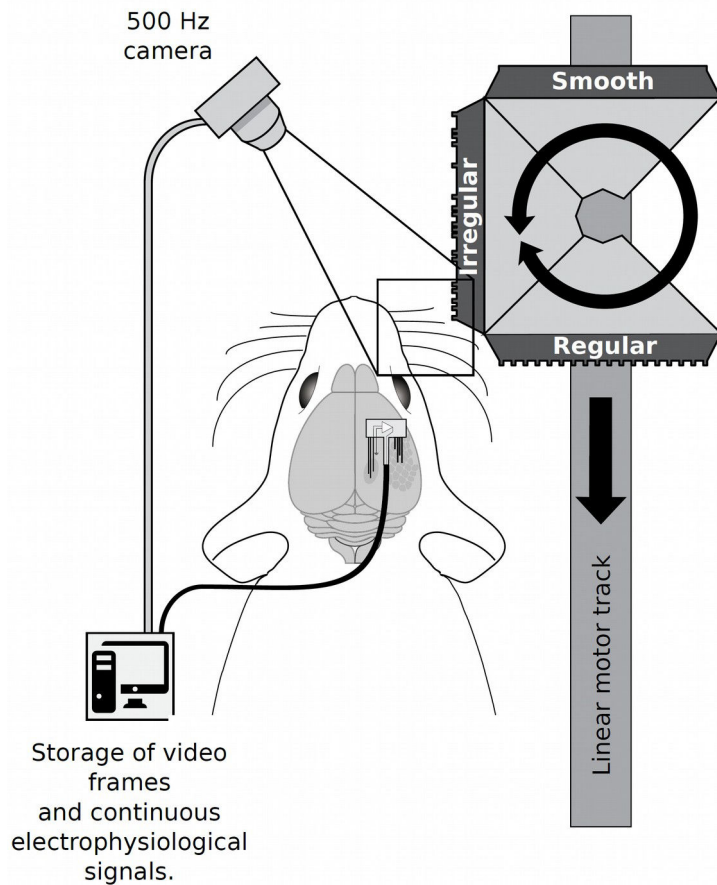


Figure 27: Set-up for recording in anesthetized rats

Schematic representation of the set-up to stimulate the whiskers with the smooth surface, the irregular series or the regular series of bars. Note that one side of the square stimuli holder is kept empty, for «no stimulus» (control) trials. During each trial, one of the stimuli or the empty side is swept on the whiskers, following a linear track and at a speed of 20cm/s. Once the stimulus has been displayed (the stimulus holder now behind the rat's head), the stimulus holder is systematically rotated back to the «no stimulus» position and translated back to its initial position (in front of the rat). This allows to not touch the whiskers during the inter-trial period. Each trial is video-recorded at 500Hz by a high-speed camera placed above the whiskers. The video is synchronized with the electrophysiological acquisition by TTL pulses emitted by the microcontroller at the beginning of each trial.

Drawing by Timothé Jost-Mousseau.

vibrations or the wind possibly induced by the running linear motor do not account for the neuronal activity recorded when the «real» stimuli are brushed on the whiskers. Between two trials, when the linear motor was coming from caudal to rostral ends, the stepper was set on the « no stimulus » position to avoid touching the whiskers. An Arduino mega2560 controller was used to move the stepper motor, and send TTL to trigger frame acquisition at the beginning of each trial. The same TTLs was sent to the electrophysiological acquisition system, so that we could synchronize frame and spike timing offline.

II.3.2.7. Electrophysiological recordings and analysis

Recording hardware

We recorded neuronal activity with a Blackrock Microsystems acquisition system. The electrophysiological signals were transmitted through the following components: EIB => Cereplex => Digital Hub => Neural Signal Processor (NSP). We briefly describe below the functions of these different stages.

The EIB is a small printed circuit board physically attached on top of the implant. It is a passive interface where tetrode wires are connected. The tetrode wires are inserted into conductive holes of the EIB, before tiny gold pins are pressed into them. Insertion of the pins removes the insulating coat of the tetrode wire, and thus connects the wire to the EIB hole.

The Cereplex is a digitalizing headstage directly connected to the EIB, via a miniature Omnetics connector (also called bank), matching the connector on the EIB. It allows recording and direct digitalization of the analog signals provided by the tetrodes.

The Digital Hub transforms the electrical digital signals to optic digital ones, travelling through an optic fiber to the NSP. This conversion to optic signals reduces the noise caused by signal transmission in long cables.

In the NSP, signals can be low- and/or high-pass filtered to specifically record Local Field Potentials (LFP) or spikes.

Multi- and single- units recordings

We acquired electrophysiological signals using the Central software from the Blackrock Microsystems company. Through this software, two types of files were acquired: files that contain spikes and TTL times (.nev) and files that contain continuous signals (.ns). Multi-unit

activity is directly available in the .nev files. In this type of file, every voltage signal that crosses a threshold defined in Central is considered as a spike. However, possible artefacts also appear as spikes with this method, so results must be interpreted with care. In the near future, we will perform spike sorting offline in order to eliminate artefacts and most importantly to identify clusters of spikes originating from single neurons. For this, we will use the .ns file, and run the spike sorting software Phy developed by the Harris team (previously KlustaKwik).

II.3.2.8. Whisker movement filming and tracking

Acquisition of the frames

To facilitate tracking of single whiskers, we chose to stimulate only one whisker row per session. To do so, we used a parafilm surface with a rectangle-shaped opening to let one row of whiskers stick out while maintaining the others flattened against the rat's face (Figure 28). We were very careful that the edges of the rectangle opening did not touch the whiskers of the selected row, to not modify the resting position and evoked movements of those whiskers. By following this procedure, we avoid cutting the whiskers around the selected row. This presents two advantages.

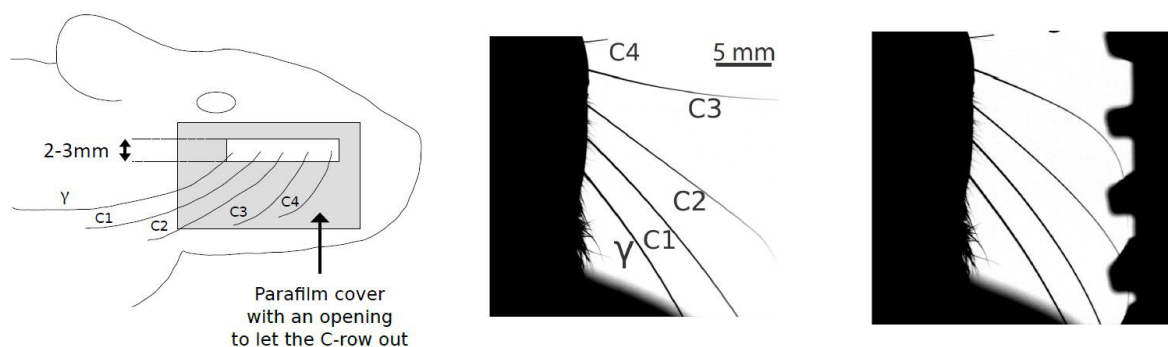


Figure 28: Tracking one whisker row

Left panel, schematic representation of the procedure to stimulate and track only one whisker row without cutting others: a parafilm surface with a rectangle opening is applied on the pad, and all the whiskers but the row of interest are flattened against the rat's face. On middle and right panels, top views of the rat's head during rest and stimulation are shown.

First, we avoid map plasticity between successive sessions that could result from whisker cutting (Feldman & Brecht 2005). Second, cutting all the whiskers but one row would result in not being able to test functional properties of neurons that respond to other rows. On the contrary, the use of parafilm allows to stimulate different rows on different sessions. Frames were acquired with a 500 Hz camera and software from the R&D Vision factory. Each frame (600 x 608 pixels) acquisition is triggered by a TTL sent by the Arduino controller, and is directly saved to the computer hard disk. Tracking of the whisker angle in time is then performed with a custom-built Python program from the lab (developed by Yves Boubenec and Valérie Ego-Stengel). Briefly, first the image is inverted (so the whiskers appear white on a dark background). Every pixel value (range 0-255) below a given threshold is set to black to get rid of background inhomogeneity. A weighted average of the whisker's transversal profile of intensity is computed, from a location close to the snout to the last visible point near the tip. This method allows to track the profile of the whisker shaft with sub-pixel resolution.

Low-pass filtering of the signal

To remove the high-frequency noise of the whisker movement trace, the signal was low-pass filtered twice: first the angular values were low-pass before we calculated the angular speed (threshold=140Hz), and second the angular acceleration values were also low-pass (threshold=100Hz).

Extraction of stick and slip events

Slip and stick events were characterized by their high acceleration, and were thus detected by applying a threshold on the acceleration values collected during the stimulation. This threshold was calculated on the acceleration values collected during the smooth surface stimulation, such that $\text{threshold} = (\text{mean} + (3 \times \text{SD}))$.

To avoid having several detected points for the same event, we systematically only kept the first detected point per event.

II.3.3. Results

In this part, we present first detailed analysis of whisker angular movements, for one session taken as a case study. We also include preliminary results obtained from one cortical recording site during that session, performed on a rat that had previously learnt the regular vs smooth discrimination task. The analysis we describe here will be applied to all sessions and all thalamic and cortical sites we recorded from (39 sites, in 4 rats), after isolation of single unit activity by spike sorting.

II.3.3.1. Whisker movement evoked by bar series: stick and slip events

We performed recording sessions during which we stimulated the whiskers with a regular series, an irregular series, or a smooth surface. We also collected control trials where the motor was moved but no stimulus contacted the whiskers (cf Methods). The mean whisker movement evoked by each of the four trial types during one session is shown in Figure 29A for whisker C2. Decreasing angle values indicate that the whisker is pushed backward, and conversely increasing values reflect forward movements. Stimulation periods typically began with a large backward movement when the whisker first hits the surface, and then the whisker was moved forward and backward successively following bar contacts. More precisely, the whisker angle increased when it fell in between two bars, and decreased when it stuck to a bar and was pushed back by it. On the top left panel of Figure 29A (irregular series stimulation) some of the biggest bar intervals when the whisker was falling between two bars are indicated in red, corresponding to an angle value increase. For the regular series, the whisker movements displayed angular peaks at each bar interval: the 17 bar intervals on the stimulus, lead to 17 one-to-one movement profile peaks. Finally, the smooth surface elicited the initial backward movement but little change after that. As expected, the no stimulation trials did not elicit any whisker movements, confirming that we could use it as a control for evaluating neuronal activity evoked solely by the experimental conditions (see Methods). Note that, to further confirm that none of the whiskers were touched, we plan to perform the tracking of gamma, the longest whisker of the stimulated row.

We examined the whisker movements to search for high acceleration events such as those described in previous studies (Jadhav et al., 2009). A threshold was applied to identify these

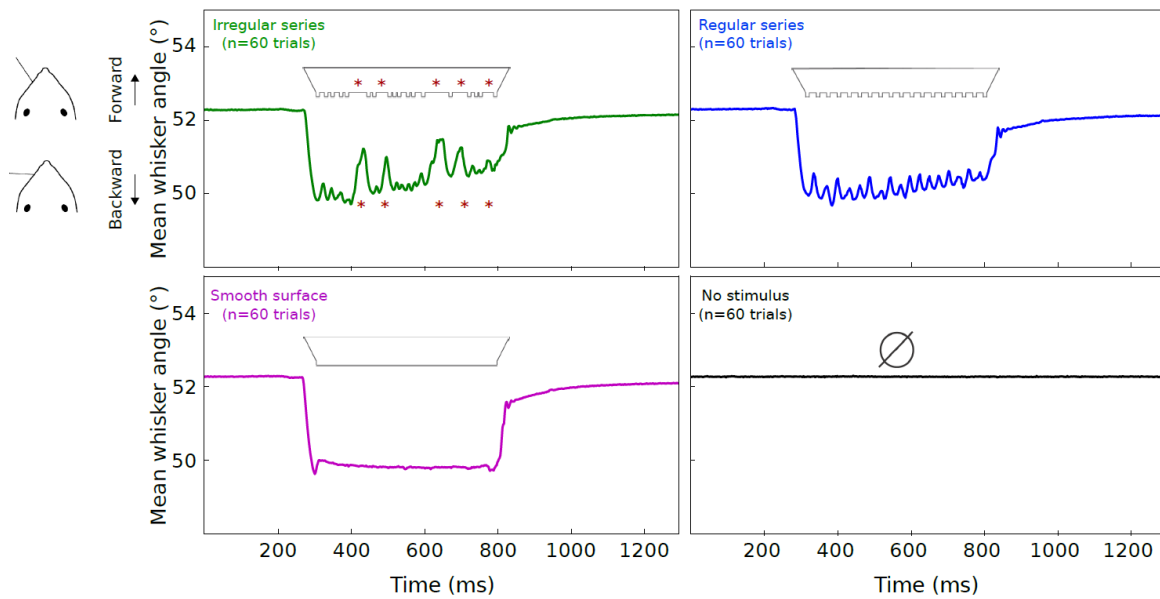
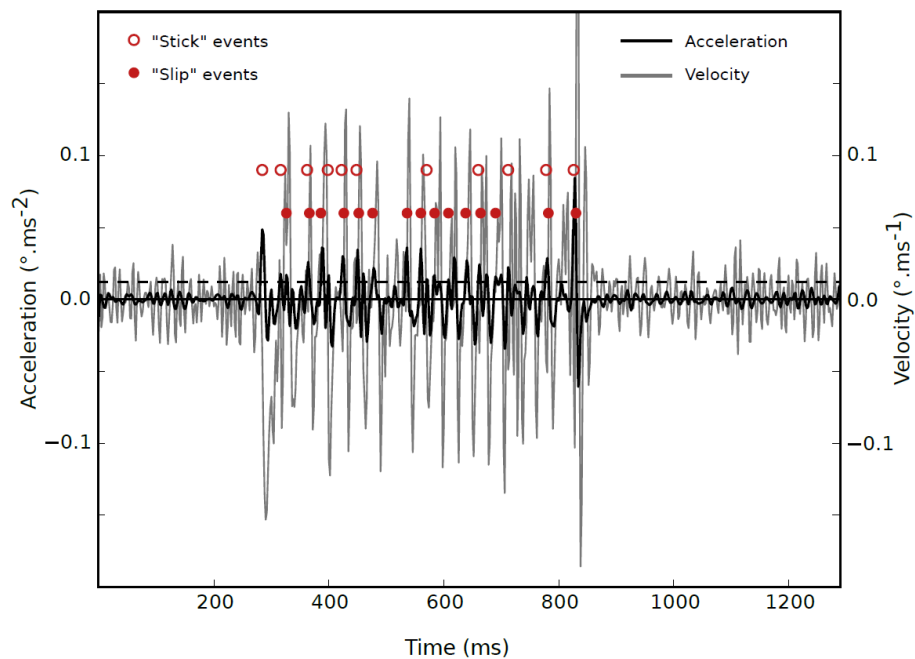
A**B**

Figure 29: Whisker movement and "stick/slip" events during stimulation

A: Mean (1 session, $n=60$) angular position of the C2 whisker as a function of time for the three stimuli (irregular series, regular series and smooth surface) and the «no stimulus» condition. Red lines on the top left panel indicate correspondence between some bar intervals and high-amplitude whisker forward movement.

B: Example traces of the velocity (grey line) and the acceleration (dark line) of whisker C2, during one sweep of the regular series. Stick and slip events (open and filled red circles, respectively) are characterized by an acceleration value (calculated from the absolute value of the angular speed) above the threshold (dashed line), concomitant with either a positive velocity for slips or a negative velocity for sticks.

events: each movement with an acceleration (calculated on the absolute value of the angular speed) superior to this threshold was kept as a high-acceleration event. In the analysis presented here, the threshold was equal to $(\text{mean} + (3 \times \text{SD}))$ of acceleration values obtained when the whisker was brushed on the smooth surface. Indeed, we expected the high-acceleration events to be triggered by the bars of the stimulus, and thus used the smooth surface (without bars) as a baseline. Among the positive high-acceleration events we separated two cases, one with positive whisker velocity and another with negative whisker velocity. Positive-velocity events correspond to a slip of the whisker from a bar, since the angular position was increasing with time. Conversely, negative-velocity events correspond to periods where the whisker is stuck on a bar and pulled backwards by it.

Through this results section, we will refer to positive-velocity events as «slip» events, and negative-velocity events as «stick» events. In both cases, only positive-acceleration events higher than the threshold were kept for analysis. However, we can already emphasize that the stick and slip events we describe may not correspond exactly to the ones characterized by the Feldman group (for review, Jadhav and Feldman 2010), since their studies were performed using micro-patterns (sandpaper grains). On Figure 29B, we report stick and slip events occurring during a typical trial with a regular series stimulation. This particular example displays 11 sticks and 15 slips, showing that slips were not systematically preceded by a stick event. The fact that our analysis did not extract one stick/slip event for every bar on the surface, despite the one-to-one peak shown in Figure 29A, could come from the parameters used (threshold and filters), and we will investigate this in more details in the future.

An overview of the slip and stick events for the whole session is depicted by raster plots in Figure 30A. Stick and slip events were almost absent during the smooth stimulation, except at onset and offset of the stimulation period. Moreover, the observation that sticks are less numerous than slips (Figure 29B) seems to be generalized at the level of the session. The sharpness of the peaks in the sum profiles (on top of each raster plot) observed in regular and irregular trials indicate that stick and slip events encode precisely in time some features of the surfaces, and the height of these peaks reflects the reliability of the events across trials. In particular, from the peak heights we can infer that slip events seem to signal the

regular series features more reliably across trials than stick events. For the same reasons, we can also infer that stick events reliably signal features that are sparser (since large height-peaks are sparser) than those signalled by slip events in the irregular series.

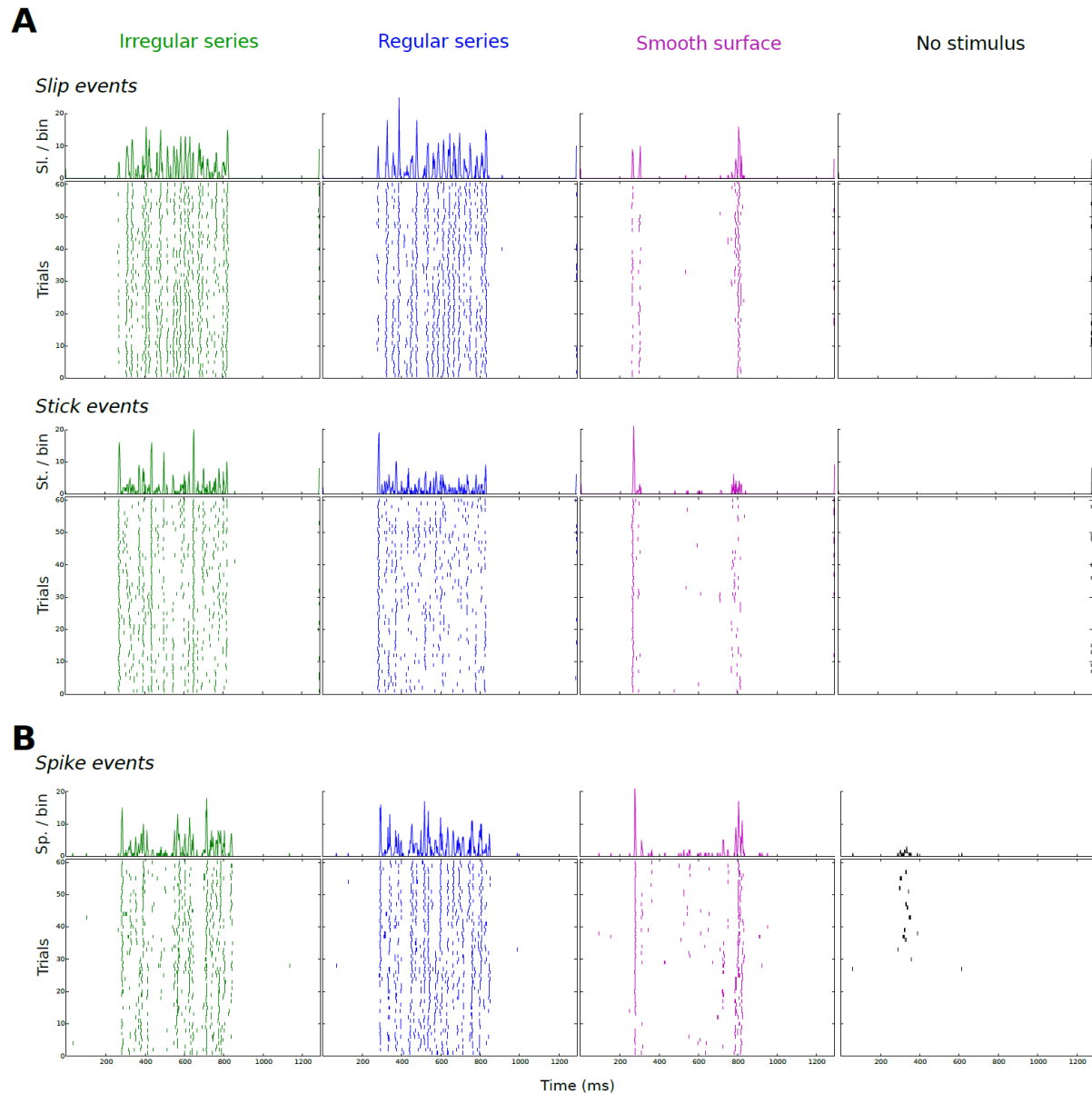


Figure 30: Raster plots of slips, sticks, and spikes

Raster plots on 60 trials for stick, slip (A) and spike (B) events are shown along rows 1-3 respectively, and for the four different stimuli types along columns 1-4. On top of each raster plot, we indicated the sum of events per bin as peri-stimulus time histograms (each bin is 2ms-wide).

To further characterize stick and slip series according to the stimulus type, we determined the mean number of events, the mean time interval between two consecutive events, and the mean coefficient of variation of these time intervals (equal to $SD/mean$) per trial (respectively Figure 31A, B and C). For this analysis, we focused on the regular and irregular series, since the smooth surface elicited almost no stick or slip events except during stimulation onset and offset. Results show that the number of stick events is significantly lower during regular compared to irregular stimulation (Wilcoxon test, $P < 0.05$, Figure 31A), which expectedly led to a significant increase in time interval during regular stimulation (Wilcoxon test, $P < 0.05$, Figure 31B). On the contrary, the number of slip events and the time interval between two consecutive events did not change according to the stimulus type (Figure 31A,B). To determine whether the events were more regularly or irregularly timed according to the bar series, we calculated the mean coefficient of variation ($CV = SD/mean$) per stimulus and per trial. In a case where events would be at the maximal level of regularity, all time intervals would be equal and the SD would be equal to 0. We found a significant difference between CV of the slip interval during regular surface stimulation compared to irregular stimulation (Wilcoxon test, $P < 0.05$). The CV during regular stimulation was lower than those during irregular stimulation, indicating that slip event patterns were significantly more regularly spaced in time, as the bars in space.

To conclude, we found stick and slip events during both regular and irregular stimulations. The number of stick events significantly varied between regular and irregular stimulations, which was not the case for slip events. Additionally, the temporal pattern of slip events was significantly more regular during regular stimulation, compared to irregular stimulations. Thus, stick and slip events encode differently regular and irregular series, and are potential candidate features of whisker movement for underlying discrimination of these two stimuli.

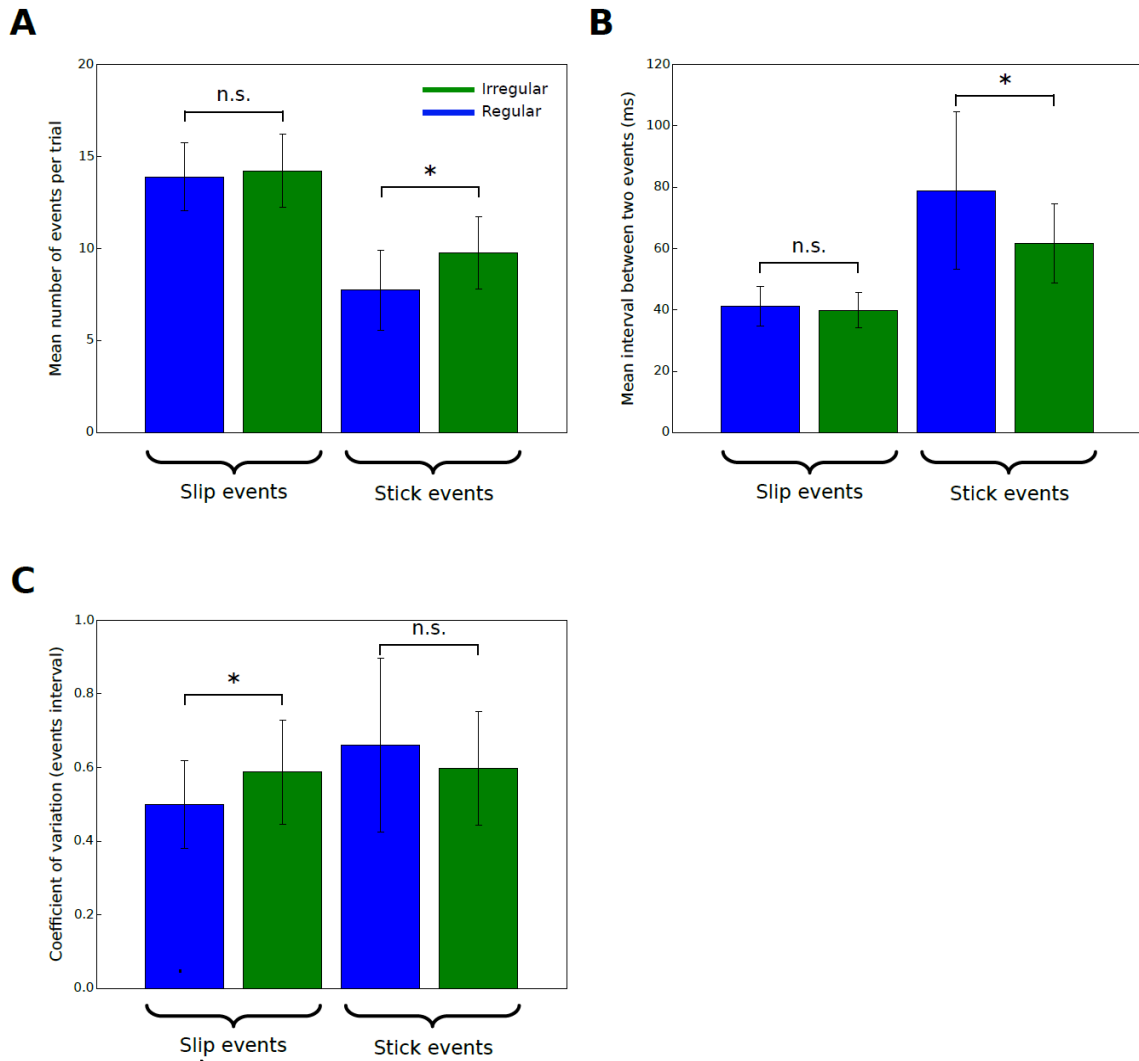


Figure 31: Characterization of stick/slip event temporal patterns

Number of events (A), interval between two consecutive events in ms (B), and coefficient of variation ($CV = SD/mean$) of the intervals between two consecutive events (C) for irregular (green) and regular (blue) stimuli.

For A-C: * : significantly different ($P < 0.05$, Wilcoxon test), n.s.: non significantly different ($P > 0.05$, Wilcoxon test). Error bars are SD across trials.

II.3.3.2. Multi-unit responses to stick and slip events

One goal of this study is to determine whether stick and slip events evoked by passive surface stimulation are encoded at the cortical level, thus whether cortical neurons do respond to such movement features. To answer this question, we have started to develop an analysis method that will be applied to the spike time series of individual neurons, obtained after offline spike sorting. Here, we present the results obtained from one multi-unit site.

We plotted the peri-stimulus time histogram of the responses centered on the event to determine whether spiking activity would significantly increase after the event (Figure 32).

We separated four cases, according to the surface type (regular or irregular series) and to the event type (stick or slip). In order to detect a potential peak in activity, we applied a threshold (mean + (2 SD)) calculated on the 80ms preceding the event (baseline). With this method, we found a peak in spiking activity within 20ms following the event in the four different cases (Figure 32A-D). Indeed, the latency from event ($t=0$ ms) to first peak after the event (surrounded in red) was of 14ms after slip events during both regular and irregular stimuli, 10ms after stick events during regular series and 18ms after stick events during the irregular stimulus. The thresholding method we use here does not necessarily detect accurately the beginning of the evoked response, which may explain the relatively long latency observed for stick events in irregular stimulation (Figure 32C), above the typical evoked cortical responses latencies (10-15ms). In fact, we do see another peak preceding the detected peak, which may be part of the response. We can also note that other activity peaks could be detected before and after the event in this case (Figure 32C). They may be due to other events (slip or stick) evoked close to the event of interest. To conclude, we found on this multi-unit example that both stick and slip events evoked a significant cortical response, and that the peak of this response occurred within 20ms after the event. To further investigate whether discrimination between irregular and regular series could be based on stick or slip events, we determined the probability of spiking within 20ms after each type of event and during the two bar series stimulation. We calculated this probability on every trial, and the mean \pm SD across trials is presented in Figure 33. We found that the spiking probability after slip events is significantly greater during regular compared to irregular stimuli (Wilcoxon test, $P < 0.05$). A similar increase in probability occurs after stick

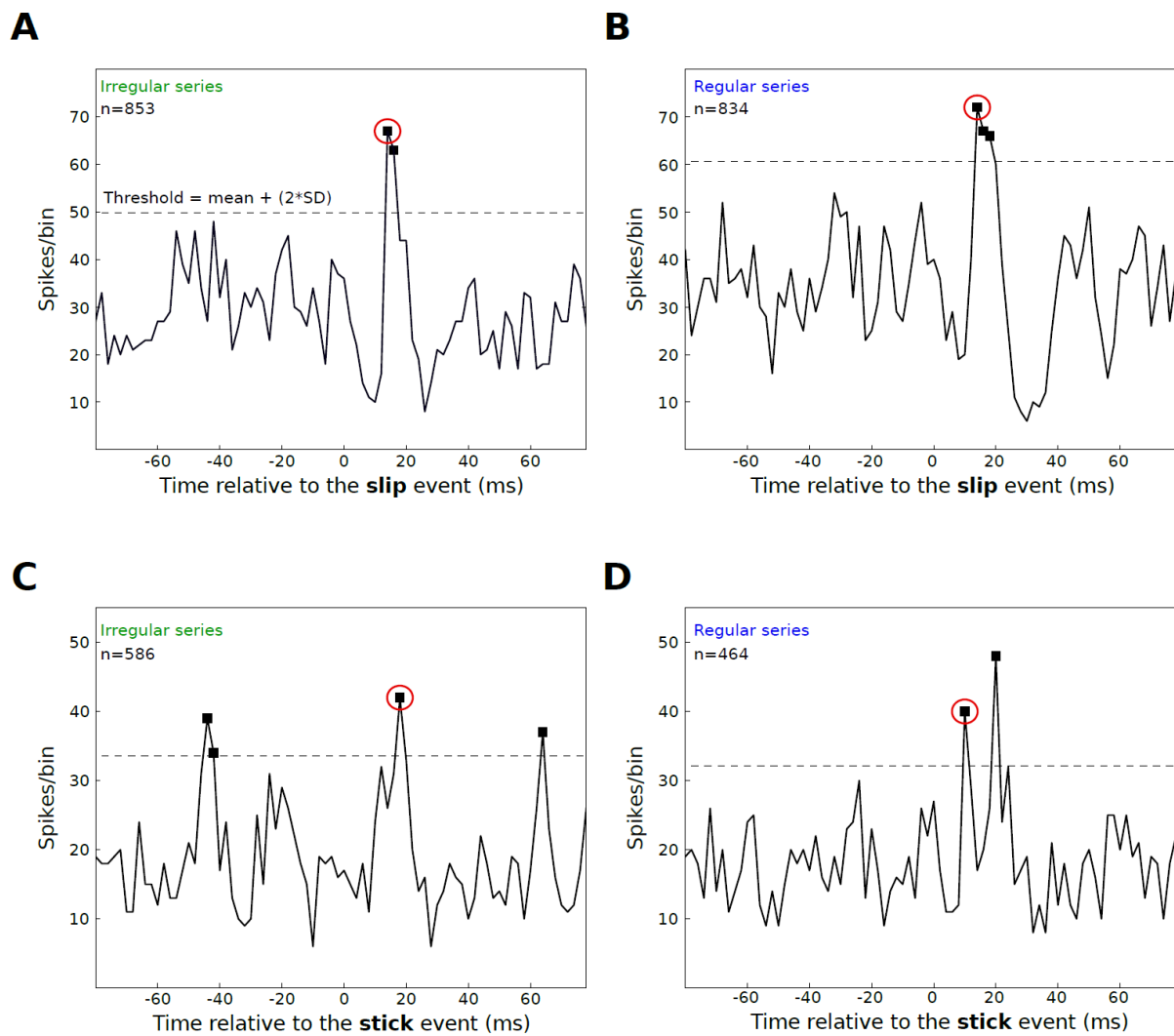


Figure 32: Neuronal responses to stick and slip events

A-D: Spiking activity evoked 80ms before to 80ms after a slip (upper row) or a stick (lower row) event. Responses to the irregular and to the regular stimuli are shown on the left and right columns respectively. The spikes are summed for all events occurring in one session (60 trials for each stimulus type). Note that here the level of activity is not normalized by the number of events (n) on which the sum is performed, which accounts for the different overall levels observed between stick and slip peristimulus plots. To detect peaks of activity, we applied a threshold equal to the mean + (2 SD) calculated on the 80ms preceding the event. Each peak of activity is labeled by a black square, and the first peak detected after the event is surrounded in red.

n is equal to the number of events.

events during regular stimuli, although the difference with irregular stimuli was not found to be significant (Wilcoxon test, $P > 0.05$). This result is consistent with the higher overall firing rate observed during regular surface presentation compared to the irregular surface (Figure 30B).

In conclusion for this particular recording site, since slip events evoked different firing probability according to the type of bar series, they could be potential candidates for underlying these stimuli discrimination. In the following section, we will thus focus on cortical responses to slip events only.

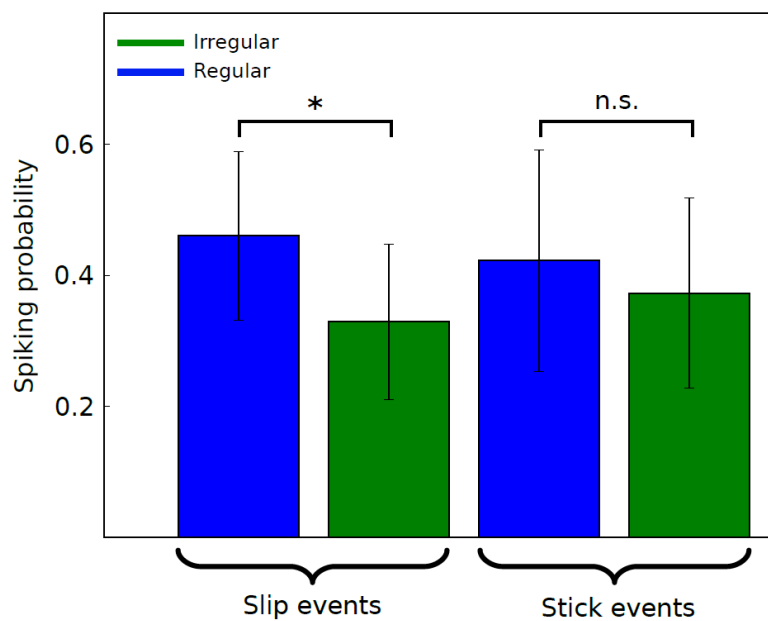


Figure 33: Spiking probability according to regular and irregular series

Mean \pm SD across trials of the spiking probability in a 20ms time window after the event according to the type of stimulation (irregular in green, regular in blue).

* : significantly different ($P < 0.05$, Wilcoxon test), n.s.: non significantly different ($P > 0.05$, Wilcoxon test).

II.3.3.3. Effect of slip amplitude and timing on multi-unit responses

To investigate what causes the difference in spiking probability after slip events during regular or irregular stimuli, we first examined whether the neuronal response was modulated by the slip acceleration value. Indeed, it was previously shown with sandpaper stimulations that slip acceleration is positively correlated with spiking probability (Jadhav et al. 2009). We cut the whole range of slip acceleration values into three ranges, and the probability of response across these ranges is shown in Figure 34A. We note a positive correlation between the slip acceleration and the response probability during the irregular stimulation. Indeed, the probability almost doubled, from 0.29 to 0.53, with increasing acceleration values. This observation is in contrast with the response probability observed during regular stimulation, which remains quite stable across the three acceleration ranges (values ranging from 0.44 to 0.49). In conclusion, for the same range of acceleration values, response probability can change according to the bar series, and thus very likely according to the history of contacts preceding the event of interest. To start investigating this hypothesis, we calculated the spiking probability after a slip event (n) according to time interval between this event (n) and the previous event ($n-1$). The preliminary results are shown in Figure 34B. Note that we did not span here the complete range of possible time intervals, since the maximal slip interval was of 148ms for irregular series and 166ms for regular series. We only compare here events with similar acceleration values. For the regular stimulation, the time interval between slip($n-1$) and slip(n) seems to impact the spiking probability after slip(n). For instance, intervals included either in $[0 ; 20\text{ms}[$ or $[80 ; 100\text{ms}[$ result in different levels of probability (Figure 34B, respectively 0.63 and 0.18). If only the time interval between the slip(n) and slip($n-1$) accounted for spike probability, then we should find similar probability level for similar ranges of time intervals, no matter the bar series involved. However, even in this case it seems on the contrary that the series regularity impacts the probability at slip(n). Indeed, for same time intervals in $[40 ; 60\text{ms}[$, spiking probability was about 0.58 and 0.31 during respectively regular and irregular stimulations. Thus, the time interval with the immediately previous event is not the only parameter accounting for spiking probability, and it seems here that the history (previous to event ($n-1$)) of contact-induced events must participate in the response generation.

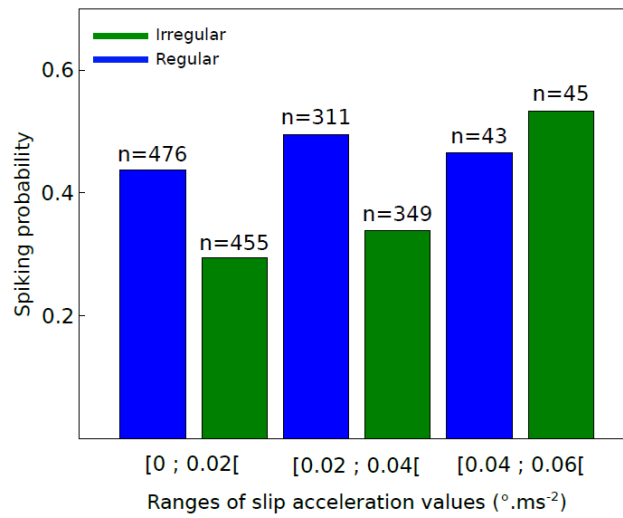
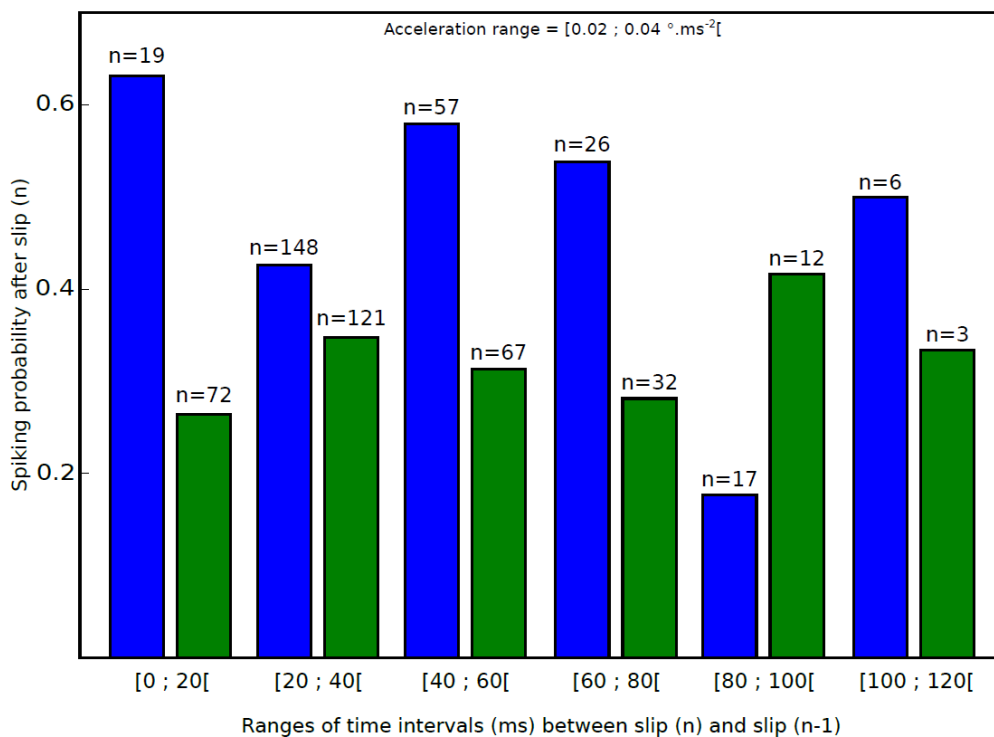
A**B**

Figure 34: Effect of slip amplitude and inter-slip interval on spiking probability

A: Spiking probability after slip events according to the type of stimulation (irregular in green, or regular in blue) and to the amplitude of the slip acceleration.

B: Spiking probability after slip events according to the type of stimulation (irregular in green, or regular in blue) and to the time interval (ms) with the immediately preceding slip event. n is equal to the number of events.

II.3.4. Conclusion and discussion

II.3.4.1. Stick and slip events during bar series stimulation

Detection of stick/slip events

With a thresholding method similar to that used by Jadhav and colleagues (2009), we detected stick and slip events occurring during bar series stimulation. These events are characterized by a high acceleration, and differ in the direction of the whisker movement: during stick events the whisker is pulled backwards (negative velocity) by a bar on the surface presented, whereas during slip events the whisker is moving forwards (positive velocity) while falling in between two bars. We found that the smooth surface elicited stick and slip events almost exclusively during onset and offset of the stimulus, and only rarely during the stimulus course. On the contrary, stick and slip events patterns occurred during the whole time course of presentation of bar surfaces, and their precise sequence in time varied according to the bar series type (regular or irregular). We found that the number of stick events significantly differed, which is not the case for slip events. Also, the temporal pattern of slip events was significantly more regular during regular stimulations, compared to irregular stimulations. These variations according to the bar series type suggest that stick and slip events could be important features of the whisker movement and participate in the discrimination between regular and irregular stimuli.

Factors impacting stick and slip temporal patterns

The results described above were obtained by tracking the C2 whisker in one session. As described in I.2.1., whisker length and diameter vary according to the position in the whisker array. We can expect that both the length and the diameter of the shaft impact the timing of stick and slip movements of the whisker on the bars, as well as the amplitude of the acceleration during slip events. Indeed, for instance if the whisker is shorter, the duration of contact with a given bar may be shorter, and thus a slip event may arrive sooner. This process would probably in turn impact stick patterns, since the timing of slip events condition the timing of subsequent stick events. Also, the diameter of the whisker may modify the contact geometry of the whisker on the bar, and thus impact the pattern of stick events. We could

determine the impact of whisker length and diameter on stick/slip events by tracking arc 3 of straddler whiskers (arc 4 did not touch the stimulus), and perform the same analysis as in Figure 33.

Another important factor that must impact stick and slip event patterns is the speed of stimulation. In this study, because of the limitations of the motor, the speed of the stimulus swept on the whiskers is 0.2m/s. We have to acknowledge the fact that, at greater speeds of stimulation, such as described during tactile discrimination of bar series by freely-behaving animals (Kerekes et al., 2017), the temporal pattern of stick/slip events is very likely to be changed. First, the time interval between successive bar contacts would obviously be shorter, but also the acceleration of individual slip or stick event would probably be affected, and this may change the number and temporal arrangement of detected events.

II.3.4.2. Neuronal responses to stick and slip events

Summary of the results on the multi-unit responses to stick and slip events

For the particular recording site presented in the results, we observed that the spiking activity significantly increases after both stick and slip events, and during both regular and irregular stimulations. We also found that the spiking probability was higher after slip events during the regular stimulation compared to the irregular stimulation. When we separated events by acceleration peak values, we found that the spiking probability was around 50% for all ranges of slip acceleration values during the regular stimulation, whereas the spiking probability during irregular stimulation gradually increased from 30% to 50% with increasing values of acceleration. This means that for the lower ranges of acceleration values, the spiking probability was greater during regular stimulation than during irregular stimulation (comparing the blue and the green bars on the left and in the middle, Figure 34A). We also looked at whether the history of slip event patterns of the regular and the irregular series differently impacts the probability of spiking after a given slip event.

In summary, the slip-evoked spiking probability seems to be in general greater during regular stimulation than during irregular stimulation, independently from the slip acceleration amplitude or the time interval with the previous slip.

Future analysis

The analysis steps shown in the results will be applied to the thirty-nine thalamic and cortical sites we recorded from, in order to characterize neuronal responses to stick and slip events during regular and irregular stimulations. We will analyze these responses at the single-neuron level, by first performing spike sorting offline (Klustakwik software).

In our preliminary analysis, we looked at the probability of emitting at least one spike within 20ms after a slip or a stick event. However, other features of the response can be analyzed: for instance, the spike count on a longer time-window, or the latency to emit the first spike. On Figure 32D, we can see that the response to stick events during the regular stimulation is composed of two peaks, whereas the response to slip events is composed of one peak followed by a decrease in activity compared to pre-stimulus baseline (Figure 32B). Furthermore, after stick events, two peaks are detected in the response during the regular stimulation (Figure 32C), whereas only one peak is detected during the irregular stimulation (Figure 32D). This suggests that the spike count response to stick events could be of higher magnitude during the regular stimulation. Thus, we could also look at the spike count within 40ms after the event, to determine if we could find differences in the response to stick events between regular and irregular stimulations.

Tuning for regularity after learning?

Previous studies in the tactile and visual systems showed that neuronal evoked responses are modulated by task learning (Wiest et al. 2010; Poort et al. 2015). Poort and colleagues (2015) notably showed that neuronal selectivity for one given stimulus is changing throughout learning. Their task consists in visual discrimination between angled (non-rewarded) and vertical (rewarded) gratings in a virtual-reality environment, and a neuron is classified as selective for one of the two gratings if it does respond significantly more for this grating compared to the other one. In this context, the authors found that after learning, more neurons are selective for one of the two stimuli, and that this selectivity gets more reliable from one recording session to another. Thus, properties of sensory evoked responses are modulated by learning.

In our study, we recorded neuronal responses from four anesthetized rats, that were trained on different tasks. Two of these rats were trained on the regular/smooth discrimination task

(see I.4.), while the two other rats were trained on a simple alternation task on the same maze. During the alternation task, the regular and smooth stimuli were not displayed in the central alley, and rats had to choose alternatively the right or left side at the end of the alley to get a reward. This alternation task is similar to the pre-learning stage of the discrimination task, where rats are trained to run in the maze without stopping in the central alley. By using this 2-tasks configuration, we could observe differences in evoked responses due to the fact that the rats learnt the task or not. In the results presented in II.3.3., we show the multi-unit evoked responses in one cortical recording site of a rat trained on the discrimination task. For this particular site, we found that the response probability after slip events is significantly higher during one stimulus (regular series, rewarded) compared to the other one (irregular series, non-rewarded). By further analyzing recording sites from discrimination trained or untrained rats, we will be able to report whether this neuronal selectivity for slip events during one stimulus is also observed in alternation-trained animals or not, and thus whether it could be an effect of learning. However, we have to acknowledge the fact that our conditions are not optimal to examine the effect of learning on sensory-evoked responses. Indeed, recording of the same neurons before and after learning, as experimented by Poort and colleagues (2015), would offer a more appropriate way to analyze such process. The next section will present our ongoing project aimed at obtaining such data.

II.3.5. Perspectives for recording in awake behaving animals

Our preparation in anesthetized animals will allow us to explore how surface stimuli are translated into whisker movements, and how they are encoded at the neuronal level. However, a direct link between behavior and neuronal activity can be established exclusively in awake freely-behaving preparations. In parallel to the two projects that were presented in this thesis, we have developed a set-up for recording neuronal activity in freely-moving rats while they are performing a behavioral task on the maze. The technical steps that we achieved for this ambitious project are presented in the following sections.

II.3.5.1. The maze and electrophysiological acquisition

In order to record from freely-moving animals, the neuronal acquisition system must follow the rat movements, even at high-speed running or when the animal is turning. To avoid damage of the acquisition cables due to repetitive turns of the animal in the maze, we bought and installed a multi-channel commutator from BlackRock Microsystems. The commutator is installed at about 50cm above the rat's head, and attached to the implant by an acquisition cable. Next, to follow the rat motion, we installed a system of pulleys above the maze. Thanks to this pulley system, the acquisition cable and the commutator attached to it can follow the rat's head position in the center alley as well as in the lateral arms of the maze. Electrophysiological recordings in walking or running animals can be achieved with tetrode implants (Ego-Stengel & Wilson 2010). We tested neuronal recording in awake behaving animals on the maze with two implanted rats. Rats were able to run in the central alley and turn in the lateral arms with the commutator and pulleys system. We could record neuronal activity in a freely-moving rat on the maze (Figure 35).

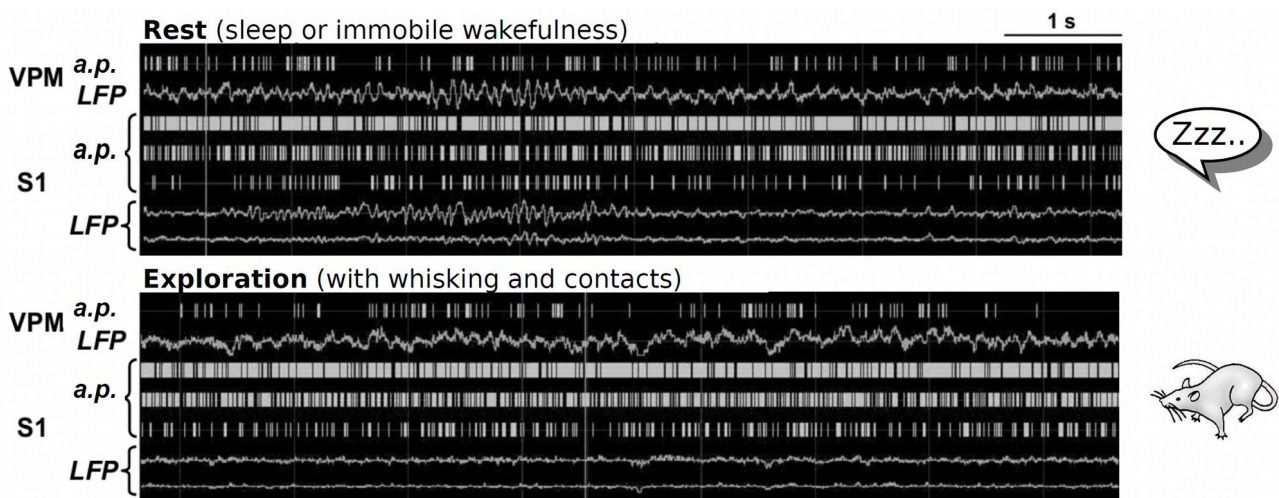


Figure 35: Example recordings in a freely-behaving rat

Multi-unit activity and LFPs recorded simultaneously in VPM and S1 during a rest period and an exploration period.

II.3.5.2. Recording whisker movements

In order to interpret spike patterns in relation to the movements of the whiskers while contacting the stimuli, we need to measure the whiskers position in time during the trials, at least in the stimuli zone.

The recording of whisker movement in freely-moving rats can be performed with the same hardware system than the one used in the anesthetized preparation: high-speed camera and image acquisition with triggering TTL pulses. As a first step, we installed and tested a photodetector placed just before the stimuli in the maze to send a TTL from the Arduino to the electrophysiological acquisition system at the beginning of each stimulation trial. This system works reliably and could thus trigger video acquisition during whisker-surfaces contact. However, two points must be considered before the transition from anesthetized to awake animals.

First, the vertical cable plugged on the implant and carrying the electrophysiological signals must not be blocked by the camera when the rat is running through the alley. The camera is a cube with an edge of 5cm, and we will center it on one side of the stimuli (contra-lateral to the implanted hemisphere). Thus, the camera should cover ~ 2.5 cm of the maze central alley. Since the stimuli are separated by 5.4cm, the camera is not blocking the center of the alley. But we have to take into account the thickness of the implant cable, and the fact that rats will probably not run perfectly in the center at each trial. Thus, to be sure that the cable will not get blocked by an angle of the camera, we will have to add a curved surface around the camera, to smooth the cable trajectory.

Second, we should also add an infra-red light under the stimuli to see the whiskers (as done in the set-up for behaving rats of Jenks and collaborators (2010) and as we do in the anesthetized preparation).

Once we solve these technical issues, we will be able to record simultaneously neuronal activity and whisker movements on the discriminanda, while the animals are performing the task. We will be able to study spike patterns encoding different surfaces in the awake animal, and to determine whether these spike patterns are modified during learning.

III. General conclusion and discussion

III.1. Summary of the Ph.D. results

Throughout the first part of this Ph.D. work, we showed that rats are able to discriminate between a regular series of bars and a smooth surface while running and without whisking on the stimuli (Kerekes et al., 2017). This bilateral and simultaneous discrimination is the first one to have been carried out under such freely-moving conditions. These conditions share common aspects with the natural behavior a rat could display in the wild: the animals are contacting surface features bilaterally, simultaneously, and while running, as they would probably do in underground tunnels that tightly fit their body size (Calhoun, 1963). We showed that the whiskers and the primary somatosensory cortex are involved in this behavioral process, and that whiskers are actively positioned in a stereotypical manner few tens of milliseconds after the first touch. We also showed evidence suggesting that rats are able to discriminate regular and irregular series of vertical bars, under the same conditions than the regular/smooth task.

A second project of the Ph.D. work is focused on the analysis of whisker movements and thalamo-cortical neuronal responses evoked by stimuli such as those used during the behavioral task. These experiments are carried out in chronically implanted anesthetized rats. We recorded from four rats, and currently have data from thirty-nine neuronal recording sites that we need to analyze. Preliminary results show the presence of high-acceleration events occurring during whisker movements on the stimuli, and the analysis of one recording site shows that these events evoke cortical responses. Evoked responses probability differs according to the stimulus type (regular or irregular series of bars). We will pursue this work to search for characteristics of the whisker movement that could be differentially encoded according to the stimulus type by the thalamo-cortical loop.

III.2. Perspectives: information processing in freely-behaving rodents

This thesis has been part of a larger ongoing project in the team, aimed at understanding neuronal coding of tactile information and its changes during learning. Thus, the behavioral task has been specifically designed so that it would be possible to record populations of neurons in the thalamo-cortical system while animals learned and performed the task. The anesthetized preparation study allows us to have a first look at neuronal patterns evoked by complex tactile stimuli brushed on by whiskers, and thus to optimize the acquisition and analysis of electrophysiological signals before stepping up to the awake freely-running condition. We have now almost all elements ready to start these recordings. Here, we discuss the experiments that we wish to perform, and how they relate to our previous work.

Stimulus encoding during the task

We will first record neuronal activity while rats contact the bar series stimuli in the central alley. This will require training a new group of rats to perform the task, so that they brush their whiskers past the stimuli while running. As in the anesthetized preparation, we hope to observe different neuronal spike patterns for the different bar series presented.

However, several differences in information coding will be extracted between the anesthetized and awake preparations.

First of all wakefulness and sleep/anesthetized state involve global brain states changes that can act as strong modulators of neuronal activity.

Second, the speed of scanning differs: in the anesthetized preparation, the motor speed is equal to 0.2m/s, which is a value close to whisking speed during discrimination tasks (see I.4.4.1). In the freely-running rats, the speed stands around 1m/s. As mentioned in II.3.4.1, the speed of whisker scanning must impact the occurrence and magnitude of stick and slip events, and thus the neuronal encoding of these events. With these two complementary studies, we would be able to extract the potential differences in stick/slip events timing and magnitude when the whisker is swept with a whisking-like speed or with a rat running speed. We could for instance see whether the change in slip interval coefficient of variation between regular and irregular series (Figure 31) would also be observed at the running speed scale.

Third, the muscular control of the whisker is changing between the anesthetized and awake preparations. Indeed, though rats are not whisking during the discrimination task, they stabilize their whiskers at a stable position for few tens of milliseconds during the stimulation (Kerekes et al. 2017), whereas we can suppose that the muscular tone is lower in anesthetized animals. This hypothesis is partly confirmed by tracking of the cut and labelled C2 whisker in behaving rats (Figure 7 of the article) and tracking of the C2 whisker in anesthetized rats (Figure 29A). Indeed, in the first case, the cut whiskers are set at an angle at least equal to 90° before and during the stimulation, whereas in the second case the resting position of the whisker is more retracted ($\sim 52^\circ$). Similarly to varying speed, this change in the whisker-associated muscular tone could significantly impact stick or slip event timing and magnitude.

Effect of stimulus relevance on sensory coding

Thalamic and cortical neuronal activity in behaving animals are modulated by several higher-order processes, and in particular by the level of attention (Otazu et al. 2009). Attention can be driven by the behavioral relevance of a stimulus during a sensory task, for instance by the rewarded regular series in the behavioral task we developed. To extract the effect of the stimulus relevance on the evoked neuronal response, we should have control trials in which the rats contact the stimuli but do not need to analyze them to perform the task. For this purpose, we could for instance first train rats on the discrimination task, and then train them on an alternation task. The alternation task could take place on the same maze, with only one door open at the end of the alley for each trial, whereas two doors are open in the discrimination task. The two tasks could be intermingled in a same session: successive blocks of trials could be dedicated to either the alternation task or the discrimination task, as it was described in a previous auditory/olfactory task (Otazu et al. 2009). During both tasks, the rats would run in the central alley and touch the stimuli, but contrary to the discrimination task, the stimuli would not be useful to obtain a reward. By comparing the two types of trials, we may be able to extract the effect of stimulus relevance on the thalamic and cortical treatment of tactile information.

Choice coding during the task

Decision making in rodents typically involves the posterior parietal cortex, as well as several cortical frontal areas (for review, see Carandini & Churchland (2013)). However, recent studies have suggested that sensory areas, including primary cortices, might already contribute to decision making. A recent study has highlighted the important role of the primary somatosensory cortex in the selection of a response during a detection task (Yang et al. 2016). The animals had to respond to a tactile sinusoidal stimulation by licking to a reward port. If the animal licked in a defined period after the stimulation, it obtained a reward and was thus successful («hit trial»), and if it did not respond to the stimulation, it did not get a reward and failed («miss trial»). If no stimulus was presented during the stimulation period, the animals had to not lick to be successful («correct rejection trials»). In this study, sub- and supra-limbar evoked activity were of higher magnitude in hit trials compared to miss trials. Activity in wS1 thus accurately predicted the choice of the animal. Our task differs from this detection task because it involves two different stimuli and requires the animal to make an action at each trial. We are recording from one hemisphere, and thus we record the response to only one of the two stimuli at each trial. Consequently, we will have two types of successful trials: those in which we record neuronal response to the non-rewarded stimulus (S-), and those in which we record responses to the rewarded stimulus (S+), in both cases during a successful trial. Using this data, we could for instance ask whether in the particular case of successful trials, the choice-associated response would change in duration or magnitude after the S+ compared to the S-. We could also contrast successful and unsuccessful trials as in Yang et al. (2016).

In addition to these possibilities to explore the neuronal encoding of bar series stimuli during the discrimination task, we are interested in how learning could impact such coding. Indeed, learning can induce significant changes in stimulus neuronal tuning, as well as response latency and magnitude in both visual and tactile systems (Poort et al. 2015; Wiest et al. 2010). The experimental strategy here will be to record changes in neural activity during, and not only after, the acquisition of the task.

IV. Bibliography

- Ahissar E, Assa E (2016) Perception as a closed-loop convergence process. *ELife* 5, e12830.
- Ahissar E, Sosnik R, Haidarliu S (2000) Transformation from temporal to rate coding in a somatosensory thalamocortical pathway *Nature* 406:302-6.
- Alitto HJ, Usrey WM (2003) Corticothalamic feedback and sensory processing. *Curr Opin Neurobiol* 13:440-445.
- Andermann ML, Ritt J, Neimark MA, Moore CI (2004) Neural correlates of vibrissa resonance; band-pass and somatotopic representation of high-frequency stimuli *Neuron* 42:451-63.
- Arabzadeh E, Zorzin E, Diamond ME (2005) Neuronal encoding of texture in the whisker sensory pathway *PLoS Biol* 3:e17.
- Arkley K, Grant RA, Mitchinson B, Prescott TJ (2014) Strategy change in vibrissal active sensing during rat locomotion. *Curr Biol* 24:1507-1512.
- Bagdasarian K, Szwed M, Knutsen PM, Deutsch D, Derdikman D, Pietr M, Simony E, Ahissar E (2013) Pre-neuronal morphological processing of object location by individual whiskers. *Nat Neurosci* 16:622-631.
- Bale MR, Ince RAA, Santagata G, Petersen RS (2015) Efficient population coding of naturalistic whisker motion in the ventro-posterior medial thalamus based on precise spike timing. *Front Neural Circuits* 9:50.
- Berdoy M (2002) The laboratory rat: a natural history. <http://www.ratlife.org/>
- Berg RW, Kleinfeld D (2003) Rhythmic whisking by rat: retraction as well as protraction of the vibrissae is under active muscular control. *J Neurophysiol* 89:104-117.
- Bezudnaya T, Castro-Alamancos MA (2011) Superior colliculus cells sensitive to active touch and texture during whisking. *J Neurophysiol* 106:332-346.
- Blanchard RJ, Takahashi LK, Fukunaga KK, Blanchard DC (1977) Functions of the vibrissae in the aggressive and defensive behavior of the rat. *Aggressive Behavior* 3:231-240
- Bokor H, Acsády L, Deschênes M (2008) Vibrissal responses of thalamic cells that project to the septal columns of the barrel cortex and to the second somatosensory area. *J Neurosci* 28:5169-5177.
- Bosman LWJ, Houweling AR, Owens CB, Tanke N, Shevchouk OT, Rahmati N, Teunissen WHT, Ju C, Gong W, Koekkoek SKE, Zeeuw CID (2011) Anatomical pathways involved in generating and sensing rhythmic whisker movements. *Front Integ Neurosci* 5:53.
- Brecht M, Krauss A, Muhammad S, Sinai-Esfahani L, Bellanca S, Margrie TW (2004) Organization of rat vibrissa motor cortex and adjacent areas according to cytoarchitectonics,

microstimulation, and intracellular stimulation of identified cells. *J Comp Neurol* 479:360-373.

Brecht M, Preilowski B, Merzenich MM (1997) Functional architecture of the mystacial vibrissae *Behav Brain Res* 84:81-97.

Brecht M, Sakmann B (2002) Dynamic representation of whisker deflection by synaptic potentials in spiny stellate and pyramidal cells in the barrels and septa of layer 4 rat somatosensory cortex *J Physiol* 543:49-70.

Brecht M, Schneider M, Sakmann B, Margrie TW (2004b) Whisker movements evoked by stimulation of single pyramidal cells in rat motor cortex. *Nature* 427:704-710.

Brumberg JC, Pinto DJ, Simons DJ (1996) Spatial gradients and inhibitory summation in the rat whisker barrel system *J Neurophysiol* 76:130-40.

Bureau I, von Saint Paul F, Svoboda K (2006) Interdigitated paralemniscal and lemniscal pathways in the mouse barrel cortex. *PLoS Biol* 4:e382.

Calhoun JB (1963) The ecology and sociology of the norway rat. Public Health service Publication n°1008.

Carandini M, Churchland AK (2013) Probing perceptual decisions in rodents. *Nat Neurosci* 16:824-831.

Carvell GE, Simons DJ (1988) Membrane potential changes in rat Sml cortical neurons evoked by controlled stimulation of mystacial vibrissae *Brain Res* 448:186-91.

Carvell GE, Simons DJ (1990) Biometric analyses of vibrissal tactile discrimination in the rat *J Neurosci* 10:2638-48.

Carvell GE, Simons DJ (1995) Task- and subject-related differences in sensorimotor behavior during active touch *Somatosens Mot Res* 12:1-9.

Chen JL, Margolis DJ, Stankov A, Sumanovski LT, Schneider BL, Helmchen F (2015) Pathway-specific reorganization of projection neurons in somatosensory cortex during learning. *Nat Neurosci* 18:1101-1108.

Chiaia NL, Rhoades RW, Fish SE, Killackey HP (1991) Thalamic processing of vibrissal information in the rat: II. Morphological and functional properties of medial ventral posterior nucleus and posterior nucleus neurons *J Comp Neurol* 314:217-36.

Chung S, Li X, Nelson SB (2002) Short-term depression at thalamocortical synapses contributes to rapid adaptation of cortical sensory responses in vivo *Neuron* 34:437-46.

Cohen JD, Castro-Alamancos MA (2007) Early sensory pathways for detection of fearful conditioned stimuli: tectal and thalamic relays. *J Neurosci* 27:7762-7776.

Constantinople CM, Bruno RM (2013) Deep cortical layers are activated directly by thalamus.

Science 340:1591-1594.

Cramer NP, Keller A (2006) Cortical control of a whisking central pattern generator. *J Neurophysiol* 96:209-217.

Cramer NP, Li Y, Keller A (2007) The whisking rhythm generator: a novel mammalian network for the generation of movement. *J Neurophysiol* 97:2148-2158.

Crochet S, Petersen CC (2006) Correlating whisker behavior with membrane potential in barrel cortex of awake mice *Nat Neurosci* 9:608-10.

Crochet S, Poulet JFA, Kremer Y, Petersen CCH (2011) Synaptic mechanisms underlying sparse coding of active touch. *Neuron* 69:1160-1175.

Curtis JC, Kleinfeld D (2009) Phase-to-rate transformations encode touch in cortical neurons of a scanning sensorimotor system *Nat Neurosci* 12:492-501.

Deschênes M, Veinante P, Zhang Z-w (1998) The organization of corticothalamic projections: reciprocity versus parity *Brain Res Brain Res Rev* 28:286-308.

Deutsch D, Pietr M, Knutsen PM, Ahissar E, Schneidman E (2012) Fast feedback in active sensing: touch-induced changes to whisker-object interaction. *PLoS one* 7:e44272.

Diamond ME, Armstrong-James M, Budway MJ, Ebner FF (1992) Somatic sensory responses in the rostral sector of the posterior group (POm) and in the ventral posterior medial nucleus (VPM) of the rat thalamus: dependence on the barrel field cortex *J Comp Neurol* 319:66-84.

Donoghue JP, Wise SP (1982) The motor cortex of the rat: cytoarchitecture and microstimulation mapping. *J Comp Neurol* 212:76-88.

Dörfl J (1982) The musculature of the mystacial vibrissae of the white mouse *J Anat* 135:147-54.

Dörfl J (1985) The innervation of the mystacial region of the white mouse. A topographical study *J Anat* 142:173-184.

Ebara S, Kumamoto K, Matsuura T, Mazurkiewicz JE, Rice FL (2002) Similarities and differences in the innervation of mystacial vibrissal follicle-sinus complexes in the rat and cat: a confocal microscopic study. *J Comp Neurol* 449:103-119.

Ebbesen CL, Doron G, Lenschow C, Brecht M (2017) Vibrissa motor cortex activity suppresses contralateral whisking behavior. *Nat Neurosci* 20:82-89.

Ego-Stengel V, Le Cam J, Shulz DE (2012) Coding of apparent motion in the thalamic nucleus of the rat vibrissal somatosensory system. *J Neurosci* 32:3339-3351.

Ego-Stengel V, Mello e Souza T, Jacob V, Shulz DE (2005) Spatiotemporal characteristics of neuronal sensory integration in the barrel cortex of the rat *J Neurophysiol* 93:1450-67.

Ego-Stengel V, Wilson MA (2010) Disruption of ripple-associated hippocampal activity during rest impairs spatial learning in the rat. *Hippocampus* 20:1-10.

Estebanez L, Bertherat J, Shulz DE, Bourdieu L, Léger J-F (2016) A radial map of multi-whisker correlation selectivity in the rat barrel cortex. *Nature Commun* 7:13528.

Estebanez L, Boustani SE, Destexhe A, Shulz DE (2012) Correlated input reveals coexisting coding schemes in a sensory cortex. *Nat Neurosci* 15:1691-1699.

Ewert TA, Vahle-Hinz C, Engel AK (2008) High-frequency whisker vibration is encoded by phase-locked responses of neurons in the rat's barrel cortex *J Neurosci* 28:5359-68.

Favaro PDN, Gouvêa TS, de Oliveira SR, Vautrelle N, Redgrave P, Comoli E (2011) The influence of vibrissal somatosensory processing in rat superior colliculus on prey capture. *Neuroscience* 176:318-327.

Feldman DE, Brecht M (2005) Map plasticity in somatosensory cortex *Science* 310:810-5.

Feldmeyer D, Brecht M, Helmchen F, Petersen CCH, Poulet JFA, Staiger JF, Luhmann HJ, Schwarz C (2013) Barrel cortex function. *Prog Neurobiol* 103:3-27.

Ferezou I, Bolea S, Petersen CC (2006) Visualizing the cortical representation of whisker touch: voltage-sensitive dye imaging in freely moving mice *Neuron* 50:617-29.

Friedman WA, Zeigler HP, Keller A (2012) Vibrissae motor cortex unit activity during whisking. *J Neurophysiol* 107:551-563.

Fundin BT, Rice FL, Pfaller K, Arvidsson J (1994) The innervation of the mystacial pad in the adult rat studied by anterograde transport of HRP conjugates *Exp Brain Res* 99:233-46.

Furuta T, Kaneko T, Deschênes M (2009) Septal neurons in barrel cortex derive their receptive field input from the lemniscal pathway. *J Neurosci* 29:4089-4095.

Gamzu E, Ahissar E (2001) Importance of temporal cues for tactile spatial- frequency discrimination *J Neurosci* 21:7416-27.

Gao P, Bermejo R, Zeigler HP (2001) Whisker deafferentation and rodent whisking patterns: behavioral evidence for a central pattern generator *J Neurosci* 21:5374-80.

Gao P, Hattox AM, Jones LM, Keller A, Zeigler HP (2003) Whisker motor cortex ablation and whisker movement patterns. *Somatosens Mot Res* 20:191-198.

Grant RA, Mitchinson B, Fox CW, Prescott TJ (2009) Active touch sensing in the rat: anticipatory and regulatory control of whisker movements during surface exploration. *J Neurophysiol* 101:862-874.

Graziano MSA, Aflalo TN (2007) Mapping behavioral repertoire onto the cortex. *Neuron* 56:239-251.

Grinevich V, Brecht M, Osten P (2005) Monosynaptic pathway from rat vibrissa motor cortex to facial motor neurons revealed by lentivirus-based axonal tracing. *J Neuro* 25:8250-8258.

Groh A, Bokor H, Mease RA, Plattner VM, Hangya B, Stroh A, Deschenes M, Acsady L (2013) Convergence of Cortical and Sensory Driver Inputs on Single Thalamocortical Cells. *Cereb Cortex* 26:3534-3543.

Guic-Robles E, Jenkins WM, Bravo H (1992) Vibrissal roughness discrimination is barrelcortex-dependent *Behav Brain Res* 48:145-52.

Haidarliu S, Simony E, Golomb D, Ahissar E (2010) Muscle architecture in the mystacial pad of the rat. *Anat Rec (Hoboken)* 293:1192-1206.

Haidarliu S, Yu C, Rubin N, Ahissar E (2008) Lemniscal and Extralemniscal Compartments in the VPM of the Rat. *Front Neuroanat* 2:4.

Hall R, Lindholm E (1974) Organization of motor and somatosensory neocortex in the albino rat *Brain Res* 66:23-38.

Harvey CD, Coen P, Tank DW (2012) Choice-specific sequences in parietal cortex during a virtual-navigation decision task. *Nature* 484:62-68.

Harvey MA, Bermejo R, Zeigler HP (2001) Discriminative whisking in the head-fixed rat: optoelectronic monitoring during tactile detection and discrimination tasks. *Somatosens Mot Res* 18:211-222.

von Heimendahl M, Itskov PM, Arabzadeh E, Diamond ME (2007) Neuronal activity in rat barrel cortex underlying texture discrimination *PLoS Biol* 5:e305.

Hemelt ME, Keller A (2007) Superior sensation: superior colliculus participation in rat vibrissa system. *BMC neuroscience* 8:12.

Hemelt ME, Keller A (2008) Superior colliculus control of vibrissa movements. *J Neurophysiol* 100:1245-1254.

Hill DN, Bermejo R, Zeigler HP, Kleinfeld D (2008) Biomechanics of the vibrissa motor plant in rat: rhythmic whisking consists of triphasic neuromuscular activity. *J Neurosci* 28:3438-3455.

Hill DN, Curtis JC, Moore JD, Kleinfeld D (2011) Primary motor cortex reports efferent control of vibrissa motion on multiple timescales. *Neuron* 72:344-356.

Hobbs JA, Towal RB, Hartmann MJZ (2015) Spatiotemporal Patterns of Contact Across the Rat Vibrissal Array During Exploratory Behavior. *Front Behav Neurosci* 9:356.

Hooks BM, Mao T, Gutnisky DA, Yamawaki N, Svoboda K, Shepherd GMG (2013) Organization of cortical and thalamic input to pyramidal neurons in mouse motor cortex. *J Neurosci* 33:748-760.

Huet LA, Schroeder CL, Hartmann MJZ (2015) Tactile signals transmitted by the vibrissa

during active whisking behavior. *J Neurophysiol* 113:3511-3518.

Hutson KA, Masterton RB (1986) The sensory contribution of a single vibrissa's cortical barrel *J Neurophysiol* 56:1196-223.

Ibrahim L, Wright EA (1975) The growth of rats and mice vibrissae under normal and some abnormal conditions. *J Embryol Exp Morphol* 33:831-844.

Jacob V, Estebanez L, Le Cam J, Tiercelin J-Y, Parra P, Parésys G, Shulz DE (2010) The Matrix: a new tool for probing the whisker-to-barrel system with natural stimuli. *J Neurosci Methods* 189:65-74.

Jacob V, Le Cam J, Ego-Stengel V, Shulz DE (2008) Emergent properties of tactile scenes selectively activate barrel cortex neurons *Neuron* 60:1112-25.

Jadhav SP, Feldman DE (2010) Texture coding in the whisker system. *Curr Opin Neurobiol* 20:313-318.

Jadhav SP, Wolfe J, Feldman DE (2009) Sparse temporal coding of elementary tactile features during active whisker sensation. *Nat Neurosci* 12:792-800.

Jenks RA, Vaziri A, Bolori A-R, Stanley GB (2010) Self-motion and the shaping of sensory signals. *J Neurophysiol* 103:2195-2207.

Jin T-E, Witzemann V, Brecht M (2004) Fiber types of the intrinsic whisker muscle and whisking behavior. *J Neurosci* 24:3386-3393.

Johnson KO, Hsiao SS (1992) Neural mechanisms of tactual form and texture perception. *Annual Rev Neurosci* 15:227-250.

Jouhanneau J-S, Ferrarese L, Estebanez L, Audette NJ, Brecht M, Barth AL, Poulet JFA (2014) Cortical fosGFP expression reveals broad receptive field excitatory neurons targeted by POM. *Neuron* 84:1065-1078.

Kerekes P, Daret A, Shulz DE, Ego-Stengel V (2017) Bilateral discrimination of tactile patterns without whisking in freely-running rats. *J Neurosci*

Khatri V, Hartings JA, Simons DJ (2004) Adaptation in thalamic barreloid and cortical barrel neurons to periodic whisker deflections varying in frequency and velocity *J Neurophysiol* 92:3244-54.

Kleinfeld D, Ahissar E, Diamond ME (2006) Active sensation: insights from the rodent vibrissa sensorimotor system *Curr Opin Neurobiol* 16:435-44.

Kleinfeld D, Deschênes M (2011) Neuronal basis for object location in the vibrissa scanning sensorimotor system. *Neuron* 72:455-468.

Kloosterman, F.; Davidson, T. J.; Gomperts, S. N.; Layton, S. P.; Hale, G.; Nguyen, D. P. & Wilson, M. A. (2009) Micro-drive array for chronic in vivo recording: drive fabrication. *J Vis*

Exp <http://www.jove.com/index/Details.stp?ID=1094>

Knutsen PM, Ahissar E (2009) Orthogonal coding of object location. *Trends Neurosci* 32:101-109.

Knutsen PM, Derdikman D, Ahissar E (2005) Tracking whisker and head movements in unrestrained behaving rodents. *J Neurophysiol* 93:2294-2301.

de Kock CPJ, Sakmann B (2009) Spiking in primary somatosensory cortex during natural whisking in awake head-restrained rats is cell-type specific. *Proc Natl Acad Sci U S A* 106:16446-16450.

Koralek KA, Jensen KF, Killackey HP (1988) Evidence for two complementary patterns of thalamic input to the rat somatosensory cortex. *Brain Res* 463:346-51.

Krupa DJ, Matell MS, Brisben AJ, Oliveira LM, Nicolelis MA (2001) Behavioral properties of the trigeminal somatosensory system in rats performing whisker-dependent tactile discriminations *J Neurosci* 21:5752-63.

Kwegyir-Afful EE, Keller A (2004) Response properties of whisker-related neurons in rat second somatosensory cortex. *J Neurophysiol* 92:2083-2092.

Lang EJ, Sugihara I, Llinás R (2006) Olivocerebellar modulation of motor cortex ability to generate vibrissal movements in rat. *J Physiol* 571:101-120.

Lavallée P, Deschênes M (2004) Dendroarchitecture and lateral inhibition in thalamic barreloids. *J Neurosci* 24:6098-6105.

Le Cam J, Estebanez L, Jacob V, Shulz DE (2011) Spatial structure of multiwhisker receptive fields in the barrel cortex is stimulus dependent. *J Neurophysiol* 106:986-998.

Letzkus JJ, Wolff SBE, Meyer EMM, Tovote P, Courtin J, Herry C, Lüthi A (2011) A disinhibitory microcircuit for associative fear learning in the auditory cortex. *Nature* 480:331-335.

Li L, Ebner FF (2007) Cortical modulation of spatial and angular tuning maps in the rat thalamus *J Neurosci* 27:167-79.

Martinez R, Morato S (2004) Thigmotaxis and exploration in adult and pup rats. *Revista de Etologia* 6:49-54.

Matyas F, Sreenivasan V, Marbach F, Wacongne C, Barys B, Mateo C, Aronoff R, Petersen CCH (2010) Motor control by sensory cortex. *Science* 330:1240-1243.

Mayrhofer JM, Haiss F, Helmchen F, Weber B (2015) Sparse, reliable, and long-term stable representation of periodic whisker deflections in the mouse barrel cortex. *Neuroimage* 115:52-63.

Mayrhofer JM, Skreb V, von der Behrens W, Musall S, Weber B, Haiss F (2013) Novel two-alternative forced choice paradigm for bilateral vibrotactile whisker frequency discrimination

in head-fixed mice and rats. *J Neurophysiol* 109:273-284.

Mease RA, Metz M, Groh A (2016b) Cortical Sensory Responses Are Enhanced by the Higher-Order Thalamus. *Cell Rep* 14:208-215.

Mease RA, Sumser A, Sakmann B, Groh A (2016a) Cortical dependence of whisker responses in posterior medial thalamus In Vivo. *Cereb Cortex* 26:3534-3543.

Melaragno HP, Montagna W (1953) The tactile hair follicles in the mouse. *Anat Rec* 115:129-149.

Mitchinson B, Martin CJ, Grant RA, Prescott TJ (2007) Feedback control in active sensing: rat exploratory whisking is modulated by environmental contact *Proc Biol Sci* 274:1035-1041.

Mitchinson B, Prescott TJ (2013) Whisker movements reveal spatial attention: a unified computational model of active sensing control in the rat. *PLoS Comput Biol* 9:e1003236.

Miyashita E, Mori S (1995) The superior colliculus relays signals descending from the vibrissal motor cortex to the facial nerve nucleus in the rat. *Neuroscience Letters* 195:69-71.

Miyashita T, Feldman DE (2013) Behavioral detection of passive whisker stimuli requires somatosensory cortex. *Cereb Cortex* 23:1655-1662.

Moore CI, Nelson SB (1998) Spatio-temporal subthreshold receptive fields in the vibrissa representation of rat primary somatosensory cortex. *J Neurophysiol* 80:2882-2892.

Moore JD, Deschênes M, Furuta T, Huber D, Smear MC, Demers M, Kleinfeld D (2013) Hierarchy of orofacial rhythms revealed through whisking and breathing. *Nature* 497:205-210.

Moore JD, Mercer Lindsay N, Deschênes M, Kleinfeld D (2015) Vibrissa Self-Motion and Touch Are Reliably Encoded along the Same Somatosensory Pathway from Brainstem through Thalamus. *PLoS Biol* 13:e1002253.

Morita T, Kang H, Wolfe J, Jadhav SP, Feldman DE (2011) Psychometric curve and behavioral strategies for whisker-based texture discrimination in rats. *PLoS One* 6:e20437.

Musall S, von der Behrens W, Mayrhofer JM, Weber B, Helmchen F, Haiss F (2014) Tactile frequency discrimination is enhanced by circumventing neocortical adaptation. *Nat Neurosci* 17:1567-1573.

Neimark MA, Andermann ML, Hopfield JJ, Moore CI (2003) Vibrissa resonance as a transduction mechanism for tactile encoding. *J Neurosci* 23:6499-6509.

Nieder L, Cagnin M, Parisi V (1982) Burrowing and feeding behavior in the rat. *Anim Behav* 30:837-844

Nguyen Q-T, Kleinfeld D (2005) Positive feedback in a brainstem tactile sensorimotor loop. *Neuron* 45:447-457.

Nguyen, D. P.; Layton, S. P.; Hale, G.; Gomperts, S. N.; Davidson, T. J.; Kloosterman, F. & Wilson, M. A. (2009) Micro-drive array for chronic in vivo recording: tetrode assembly. *J Vis Exp* <http://www.jove.com/index/Details.stp?ID=1098>

O'Connor DH, Clack NG, Huber D, Komiyama T, Myers EW, Svoboda K (2010) Vibrissa-based object localization in head-fixed mice. *J Neurosci* 30:1947-1967.

O'Connor DH, Hires SA, Guo ZV, Li N, Yu J, Sun Q-Q, Huber D, Svoboda K (2013) Neural coding during active somatosensation revealed using illusory touch. *Nat Neurosci* 16:958-965.

Otazu GH, Tai L-H, Yang Y, Zador AM (2009) Engaging in an auditory task suppresses responses in auditory cortex. *Nat Neurosci* 12:646-654.

Pierret T, Lavallée P, Deschênes M (2000) Parallel streams for the relay of vibrissal information through thalamic barreloids *J Neurosci* 20:7455-62.

Poort J, Khan AG, Pachitariu M, Nemri A, Orsolich I, Krupic J, Bauza M, Sahani M, Keller GB, Mrsic-Flogel TD, Hofer SB (2015) Learning Enhances Sensory and Multiple Non-sensory Representations in Primary Visual Cortex. *Neuron* 86:1478-1490.

Poulet JFA, Fernandez LMJ, Crochet S, Petersen CCH (2012) Thalamic control of cortical states. *Nat Neurosci* 15:370-372.

Poulet JF, Petersen CC (2008) Internal brain state regulates membrane potential synchrony in barrel cortex of behaving mice *Nature* 454:881-5.

Proville RD, Spolidoro M, Guyon N, Dugue GP, Selimi F, Isope P, Popa D, Lena C (2014) Cerebellum involvement in cortical sensorimotor circuits for the control of voluntary movements. *Nat Neurosci* 17:1233-1239.

Quist BW, Hartmann MJZ (2012) Mechanical signals at the base of a rat vibrissa: the effect of intrinsic vibrissa curvature and implications for tactile exploration. *J Neurophysiol* 107:2298-2312.

Reig R, Silberberg G (2016) Distinct Corticostriatal and Intracortical Pathways Mediate Bilateral Sensory Responses in the Striatum. *Cereb cortex* 26:4405-4415.

Rice FL, Kinnman E, Aldskogius H, Johansson O, Arvidsson J (1993) The innervation of the mystacial pad of the rat as revealed by PGP 9.5 immunofluorescence *J Comp Neurol* 337:366-85.

Rice FL, Mance A, Munger BL (1986) A comparative light microscopic analysis of the sensory innervation of the mystacial pad. I. Innervation of vibrissal follicle-sinus complexes *J Comp Neurol* 252:154-74.

Ritt JT, Andermann ML, Moore CI (2008) Embodied information processing: vibrissa mechanics and texture features shape micromotions in actively sensing rats *Neuron* 57:599-613.

Rosset C, Fieschi M, Hugues S, Bureau I (2011) Associative learning changes the organization of functional excitatory circuits targeting the supragranular layers of mouse barrel cortex. *Front Neural Circuits* 4:126.

Sachdev RN, Sellien H, Ebner F (2001) Temporal organization of multi-whisker contact in rats *Somatosens Mot Res* 18:91-100.

Sachdev RNS, Berg RW, Champney G, Kleinfeld D, Ebner FF (2003) Unilateral vibrissa contact: changes in amplitude but not timing of rhythmic whisking. *Somatosens Mot Res* 20:163-169.

Sakata S, Harris KD (2009) Laminar structure of spontaneous and sensory-evoked population activity in auditory cortex. *Neuron* 64:404-418.

Saraf-Sinik I, Assa E, Ahissar E (2015) Motion makes sense: an adaptive motor-sensory strategy underlies the perception of object location in rats. *J Neuro* 35:8777-8789.

Schroeder JB, Ritt JT (2016) Selection of head and whisker coordination strategies during goal-oriented active touch. *J Neurophysiol* 115:1797-1809.

Schwarz C (2016) The Slip Hypothesis: Tactile Perception and its Neuronal Bases. *Trends Neurosci* 39:449-462.

Semba K, Egger MD (1986) The facial "motor" nerve of the rat: control of vibrissal movement and examination of motor and sensory components *J Comp Neurol* 247:144-58.

Semba K, Komisaruk BR (1984) Neural substrates of two different rhythmical vibrissal movements in the rat *Neuroscience* 12:761-74.

Sherman SM (2016) Thalamus plays a central role in ongoing cortical functioning. *Nat Neurosci* 19:533-541.

Simons DJ (1985) Temporal and spatial integration in the rat SI vibrissa cortex *J Neurophysiol* 54:615-35.

Sofroniew NJ, Cohen JD, Lee AK, Svoboda K (2014) Natural whisker-guided behavior by head-fixed mice in tactile virtual reality. *J Neurosci* 34:9537-9550.

Sofroniew NJ, Svoboda K (2015) Whisking. *Curr Biol* 25:R137-R140.

Sofroniew NJ, Vlasov YA, Hires SA, Freeman J, Svoboda K (2015) Neural coding in barrel cortex during whisker-guided locomotion. *ELife* 4, e12559.

Solomon JH, Hartmann MJ (2006) Biomechanics: robotic whiskers used to sense features. *Nature* 443:525.

Sreenivasan V, Esmaili V, Kiritani T, Galan K, Crochet S, Petersen CCH (2016) Movement Initiation Signals in Mouse Whisker Motor Cortex. *Neuron* 92:1368-1382.

- Steriade M, McCormick DA, Sejnowski TJ (1993) Thalamocortical oscillations in the sleeping and aroused brain *Science* 262:679-85.
- Szwed M, Bagdasarian K, Ahissar E (2003) Encoding of vibrissal active touch *Neuron* 40:621-30.
- Szwed M, Bagdasarian K, Blumenfeld B, Barak O, Derdikman D, Ahissar E (2006) Responses of trigeminal ganglion neurons to the radial distance of contact during active vibrissal touch *J Neurophysiol* 95:791-802.
- Takahashi LK, Lore RK (1980) Foraging and food hoarding of wild *Rattus norvegicus* in an urban environment. *Behav Neural Biol* 29:527-531.
- Takato H, Nelson A, Zhou X, Bolton MM, Ehlers MD, Arenkiel BR, Mooney R, Wang F (2013) New modules are added to vibrissal premotor circuitry with the emergence of exploratory whisking. *Neuron* 77:346-360.
- Temereanca S, Simons DJ (2004) Functional topography of corticothalamic feedback enhances thalamic spatial response tuning in the somatosensory whisker/barrel system *Neuron* 41:639-51.
- Tomomura S, Ebara S, Bagdasarian K, Uta D, Ahissar E, Meir I, Lampl I, Kuroda D, Furuta T, Furue H, Kumamoto K (2015) Structure-function correlations of rat trigeminal primary neurons: Emphasis on club-like endings, a vibrissal mechanoreceptor. *Proceedings of the Japan Academy*. 91:560-576.
- Towal RB, Hartmann MJ (2006) Right-left asymmetries in the whisking behavior of rats anticipate head movements. *J Neurosci* 26:8838-8846.
- Trageser JC, Keller A (2004) Reducing the uncertainty: gating of peripheral inputs by zona incerta. *J Neurosci* 24:8911-8915.
- Urbain N, Deschênes M (2007) A new thalamic pathway of vibrissal information modulated by the motor cortex *J Neurosci* 27:12407-12.
- Urbain N, Deschênes M (2007) Motor cortex gates vibrissal responses in a thalamocortical projection pathway. *Neuron* 56:714-725.
- Urbain N, Salin PA, Libourel P-A, Comte J-C, Gentet LJ, Petersen CCH (2015) Whisking-Related Changes in Neuronal Firing and Membrane Potential Dynamics in the Somatosensory Thalamus of Awake Mice. *Cell Rep* 13:647-656.
- Veinante P, Deschênes M (1999) Single- and multi-whisker channels in the ascending projections from the principal trigeminal nucleus in the rat *J Neurosci* 19:5085-95.
- Veinante P, Jacquin MF, Deschênes M (2000) Thalamic projections from the whisker-sensitive regions of the spinal trigeminal complex in the rat *J Comp Neurol* 420:233-43.
- Vincent S (1912) The function of the vibrissae in the behavior of the white rat *Behavior*

Monographs 1:7-85.

Voigts J, Herman DH, Celikel T (2015) Tactile object localization by anticipatory whisker motion. *J Neurophysiol* 113:620-632.

Waiblinger C, Brugger D, Whitmire CJ, Stanley GB, Schwarz C (2015) Support for the slip hypothesis from whisker-related tactile perception of rats in a noisy environment. *Front Integr Neurosci* 9:53.

Wallach A, Bagdasarian K, Ahissar E (2016) On-going computation of whisking phase by mechanoreceptors. *Nat Neurosci* 19:487-493.

Webber RM, Stanley GB (2004) Nonlinear encoding of tactile patterns in the barrel cortex *J Neurophysiol* 91:2010-22.

Wiest MC, Thomson E, Pantoja J, Nicolelis MAL (2010) Changes in S1 neural responses during tactile discrimination learning. *J Neurophysiol* 104:300-312.

Wimmer VC, Bruno RM, de Kock CPJ, Kuner T, Sakmann B (2010) Dimensions of a projection column and architecture of VPM and POr axons in rat vibrissal cortex. *Cereb Cortex* 20:2265-2276.

Wolfe J, Hill DN, Pahlavan S, Drew PJ, Kleinfeld D, Feldman DE (2008) Texture coding in the rat whisker system: slip-stick versus differential resonance *PLoS Biol* 6:e215.

Wolfe J, Mende C, Brecht M (2011) Social facial touch in rats. *Behavioral neuroscience* 125:900-910.

Woolsey TA, Van der Loos H (1970) The structural organization of layer IV in the somatosensory region (SI) of mouse cerebral cortex. The description of a cortical field composed of discrete cytoarchitectonic units *Brain Res* 17:205-42.

Yang H, Kwon SE, Severson KS, O'Connor DH (2016) Origins of choice-related activity in mouse somatosensory cortex. *Nat Neurosci* 19:127-134.

Yu C, Derdikman D, Haidarliu S, Ahissar E (2006) Parallel thalamic pathways for whisking and touch signals in the rat *PLoS Biol* 4:e124.

Zuo Y, Perkon I, Diamond ME (2011) Whisking and whisker kinematics during a texture classification task. *Philos Trans R Soc Lond B Biol Sci* 366:3058-3069.

Index des illustrations

Figure 1: Detailed representation of a typical burrow.....	12
Figure 2: Macro- and micro-vibrissae on the rat's snout.....	14
Figure 3: Structure of the Follicle-Sinus Complex.....	16
Figure 4: From the whisker follicle to the brainstem.....	18
Figure 5: Whisking spatio-temporal properties.....	22
Figure 6: Muscles of the whisker pad.....	24
Figure 7: Generation of whisking patterns in the brainstem.....	27
Figure 8: The primary motor cortex can trigger whisking.....	29
Figure 9: Movement amplitude as a function of wM1 stimulation frequency.....	31
Figure 10: Whisking modulation according to behavioral contexts.....	32
Figure 11: Increased retraction is not due to contact with the rougher stimulus.....	52
Figure 12: Repeated inactivations of the primary somatosensory cortex.....	54
Figure 13: Reminders are needed for learning.....	55
Figure 14: From the whiskers to the cortex.....	62
Figure 15: Map and individual structure of barreloids in the thalamus.....	65
Figure 16: Thalamo-cortical projections in the paralemniscal and lemniscal pathways.....	67
Figure 17: Summary of the cerebral structures involved in processing whisker information...68	68
Figure 18: Neuronal selectivity for the whisking phase.....	74
Figure 19: Connections involved in phase and amplitude selectivity.....	76
Figure 20: Encoding radial position.....	78
Figure 21: Encoding of stimulus frequency.....	80
Figure 22: Whisker micromotions on sandpapers.....	82
Figure 23: High-acceleration events during contact with a sandpaper surface.....	84
Figure 24: Whisker resonance during surface contact.....	86
Figure 25: Neuronal responses to temporal series of whisker deflections.....	90
Figure 26: Tetrode implant.....	94
Figure 27: Set-up for recording in anesthetized rats.....	98
Figure 28: Tracking one whisker row.....	100
Figure 29: Whisker movement and "stick/slip" events during stimulation.....	103
Figure 30: Raster plots of slips, sticks, and spikes.....	105
Figure 31: Characterization of stick/slip event temporal patterns.....	107
Figure 32: Neuronal responses to stick and slip events.....	109
Figure 33: Spiking probability according to regular and irregular series.....	110
Figure 34: Effect of slip amplitude and inter-slip interval on spiking probability.....	112
Figure 35: Example recordings in a freely-behaving rat.....	117

